U.S. Department
of Transportation

**Federal Railroad
Administration**

TANK CAR FATIGUE CRACK GROWTH TEST

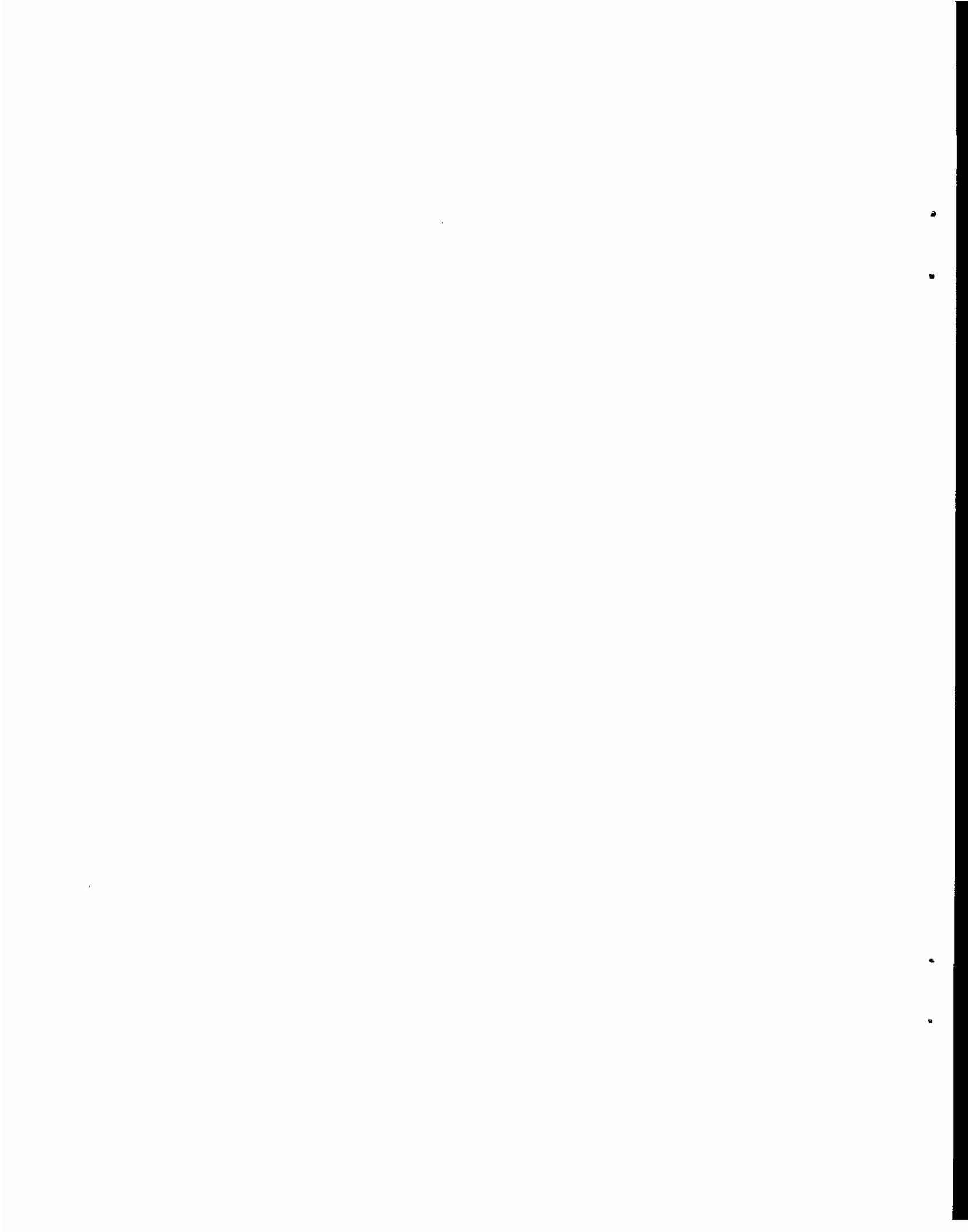**Office of Research and
Development
Washington D.C. 20590**

| 1. Report No.	2. Government Accession No.	3. Recipient's Catalog No.
DOT/FRA/ORD-93/10		

4. Title and Subtitle	5. Report Date
Tank Car Fatigue Crack Growth Test	March 1993
	6. Performing Organization Code

7. Author(s)	8. Performing Organization Report No.
David L. Cackovic, Britto Rajkumar, and Vinaya Sharma	

9. Performing Organization Name and Address	10. Work Unit No. (TRAIS)
Association of American Railroads Transportation Test Center P.O. Box 11130 Pueblo, CO 81001	
	11. Contract or Grant No.

12. Sponsoring Agency Name and Address	13. Type of Report or Period Covered
U.S. Department of Transportation Federal Railroad Administration Office of Research and Development 400 Seventh Street SW Washington, D.C. 20590	Test Report September 1989-December 1992
	14. Sponsoring Agency Code RDV 32

15. Supplementary Notes

16. Abstract

Under the Tank Car Fatigue Crack Growth Test program, the Association of American Railroads performed over-the-road tests, impact tests, perturbed track tests, quasi-static and cyclic Mini-shaker Unit vertical coupler loading tests, and a 300,000-mile accelerated-rate Simuloader fatigue test on a Department of Transportation 111A100W1 tank car. In addition, fractographic analysis of cracked tank car head pad samples obtained in the field and laboratory specimen crack growth tests were conducted.

It was determined that the critical region in fatigue of the tank car tested was the stub sill to tank-head reinforcing pad connection. The following conclusions were drawn during the course of the test program.
- The predominant factor in the cracking at the stub sill to tank shell connection was the vertical coupler loads.
- The Simuloader was able to re-create realistic load environment. One hour of Simuloader operation corresponded to 4,400 miles of revenue service.
- It was possible to monitor crack growth during the Simuloader testing of the tank car. The propagation of seven fatigue cracks was monitored.
- The fatigue load environment can be applied to any tank car on TTC's Simuloader, therefore allowing new stubsill designs to be tested.

17. Key Words	18. Distribution Statement
Stub sill, tank car, fatigue life, Simuloader, Mini-Shaker Unit, accelerated fatigue testing	This document is available through National Technical Information Service Springfield, VA 22161

19. Security Classification (of the report)	20. Security Classification (of this page)	21. No. of Pages	22. Price
Unclassified	Unclassified	79	

Form DOT F 1700.7 (8-72)

METRIC CONVERSION FACTORS
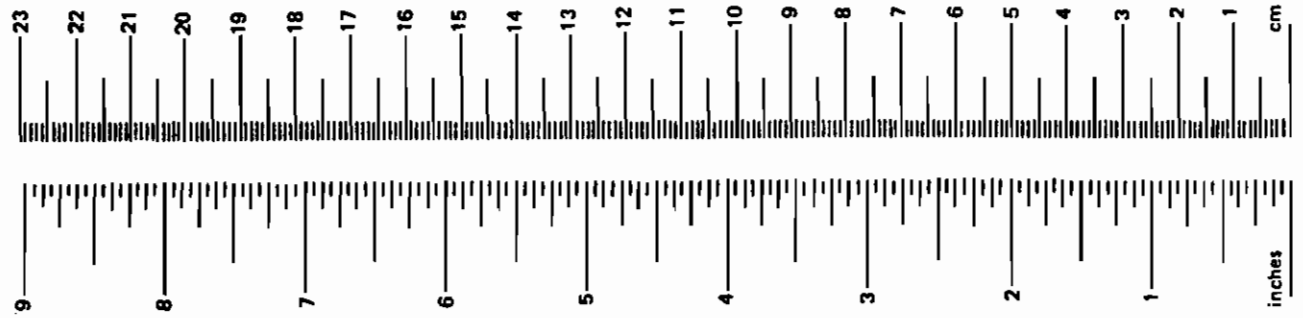
Approximate Conversions to Metric Measures

Symbol	When You Know	Multiply by	To Find	Symbol
	LENGTH			
in	inches	*2.50	centimeters	cm
ft	feet	30.00	centimeters	cm
yd	yards	0.90	meters	m
mi	miles	1.60	kilometers	km
	AREA			
in²	square inches	6.50	square centimeters	cm²
ft²	square feet	0.09	square meters	m²
yd²	square yards	0.80	square meters	m²
mi²	square miles	2.60	square kilometers	km²
	acres	0.40	hectares	ha
	MASS (weight)			
oz	ounces	28.00	grams	g
lb	pounds	0.45	kilograms	kg
	short tons (2000 lb)	0.90	tonnes	t
	VOLUME			
tsp	teaspoons	5.00	milliliters	ml
Tbsp	tablespoons	15.00	milliliters	ml
fl oz	fluid ounces	30.00	milliliters	ml
c	cups	0.24	liters	l
pt	pints	0.47	liters	l
qt	quarts	0.95	liters	l
gal	gallons	3.80	liters	l
ft³	cubic feet	0.03	cubic meters	m³
yd³	cubic yards	0.76	cubic meters	m³
	TEMPERATURE (exact)			
°F	Fahrenheit temperature	5/9 (after subtracting 32)	Celsius temperature	°C

* 1 in. = 2.54 cm (exactly)

Approximate Conversions from Metric Measures

Symbol	When You Know	Multiply by	To Find	Symbol
	LENGTH			
mm	millimeters	0.04	inches	in
cm	centimeters	0.40	inches	in
m	meters	3.30	feet	ft
m	meters	1.10	yards	yd
km	kilometers	0.60	miles	mi
	AREA			
cm²	square centim.	0.16	square inches	in²
m²	square meters	1.20	square yards	yd²
km²	square kilom.	0.40	square miles	mi²
ha	hectares (10,000 m²)	2.50	acres	
	MASS (weight)			
g	grams	0.035	ounces	oz
kg	kilograms	2.2	pounds	lb
t	tonnes (1000 kg)	1.1	short tons	
	VOLUME			
ml	milliliters	0.03	fluid ounces	fl oz
l	liters	2.10	pints	pt
l	liters	1.06	quarts	qt
l	liters	0.26	gallons	gal
m³	cubic meters	36.00	cubic feet	ft³
m³	cubic meters	1.30	cubic yards	yd³
	TEMPERATURE (exact)			
°C	Celsius temperature	9/5 (then add 32)	Fahrenheit temperature	°F

ACKNOWLEDGMENTS

LIST OF ABBREVIATIONS

FRA Federal Railroad Administration

DOT Department of Transportation

RSPA Research and Special Programs Administration

AAR Association of American Railroads

TTC Transportation Test Center

VNTSC Volpe National Transportation Systems Center

ATSF Atchison, Topeka & Santa Fe Railway or Santa Fe Railway

OTR Over-the-Road "test"

MSU Mini-Shaker Unit

RDL Rail Dynamics Laboratory

FEEST Freight Equipment Environmental Sampling Test

FAST Facility for Accelerated Service Testing

AE Acoustic Emission Testing

LTHD Locomotive Track Hazard Detection

s/s Samples per second

SPATE Stress Pattern Analysis through Thermal Emissions

KHN Knoop microhardness

HAZ Heat Affected Zone

VTU Vibration Test Unit

TIP Test Implementation Plan

SEM Scanning Electron Microscopy

EXECUTIVE SUMMARY

The Federal Railroad Administration (FRA) has been investigating incidences of fatigue cracking in tank cars. In this test project, the FRA has tasked the Association of American Railroads (AAR), Transportation Test Center (TTC), Pueblo, Colorado, to study and develop a test program related to fatigue crack growth in stub sill tank cars. The results of this task will assist the FRA in developing procedures and policies regarding the possible elimination of stub sill cracking or at the very least its curtailment to a safe acceptable level.

The FRA funded the Tank Car Fatigue Crack Growth test program at the Transportation Test Center (TTC), Pueblo, Colorado. Under the program, the AAR/TTC performed over-the-road (OTR) tests, impact tests, perturbed track tests, vertical coupler loading tests on the Mini-shaker Unit (MSU), and a 300,000-mile accelerated-rate fatigue test with a vibration machine called the Simuloader. In addition, fractographic analysis was performed on tank car head pad samples that developed cracks in revenue service. Laboratory specimen crack growth tests were also conducted.

A Trinity built 26,000 gallon capacity Department of Transportation (DOT) 111A100W1 car, owned by the Atchison, Topeka, and Santa Fe Railway Company (ATSF), was used as the test car. One end of the car was left in an as-built condition, and the other end was retrofitted with a head brace manufactured by Trinity.

The AAR/TTC performed OTR tests on the ATSF railroad to obtain the tank car load environmental data. Analysis of the results from the OTR testing revealed that the train slack action forces and bolster motions alone could not account for the significant strain levels measured during the OTR test at the interface between stub sill and tank shell. Subsequent discussions with the Fatigue Task Force Committee and other agencies concluded that the prime cause for the observed high strain levels leading to cracks in stub sill tank cars was related to vertical coupler loads caused by, among others, coupler height mismatch between cars and/or out-of-phase motions of couplers superimposed with train action forces. The results of the impact tests with various levels of coupler height mismatch, and the MSU quasi-static and cyclic vertical coupler load tests verified the above conclusion. The cyclic MSU vertical coupler load test was also key in the initiation of one crack at the stub sill to tank head reinforcing pad connection.

In addition, a comparative analysis of the coupler loads measured in the OTR test to those measured during the Freight Equipment Environmental Sampling Test (FEEST) showed that the FEEST loads were significantly more severe. The FEEST data were recorded over 23,000 loaded-car miles of revenue service. (See reference 19).

Accordingly, the AAR/TTC added a vertical coupler force actuator to the Simuloader and developed new Simuloader input profiles based on OTR test data adjusted to conform to AAR's FEEST vertical and longitudinal coupler force data. The input profile for the Simuloader maintained the phase relationships of various loads obtained during the OTR tests. This methodology accelerated the fatigue testing such that one hour of operation on the Simuloader was equivalent to 4,400 loaded-car miles of revenue service operation. Thus, it was possible to simulate 300,000 loaded-car miles of revenue service operation in less than 12 weeks of Simuloader testing.

The following conclusions were drawn from the Fatigue Crack Growth Test:

- The predominant factor in the service environment that contributes to high strain levels and subsequent cracking at the stub sill tank interface for tank cars pertains to the vertical coupler loads most likely caused by coupler height mismatch between cars and/or out-of-phase motions of couplers superimposed with train action forces.

- It was possible, at an accelerated rate, to re-create realistic load environment to facilitate fatigue testing (as found in the revenue service) for stub sill tank cars on the Simuloader.

- It was possible to initiate cracks and monitor crack growth during the Simuloader testing of the tank car. Seven fatigue cracks were monitored on the Simuloader during the simulation of 300,000 miles of revenue service. The first of these cracks, was initiated directly during cyclic vertical load tests conducted for this purpose. The remaining six cracks were initiated during testing on the Simuloader.

- The fatigue cracks generated during the Simuloader test were similar to cracks that developed in tank car head pads during revenue service operation -- samples of which were obtained and analyzed by TTC personnel. The largest crack increased in length to more than 4.5 inches after 160,000 simulated service miles. At some point, all the cracks quit increasing in length while continuing to increase in depth.

- The AAR is convinced that the fatigue load environment can be applied to any tank car on TTC's Simuloader in an accelerated fashion. Thus new stub sill retrofit designs can be tested within a period of six weeks to simulate 400,000 miles of loaded service environment.

The following recommendations are based on the findings from the Fatigue Crack Growth Test:

- This program showed, on a better than average car, that fatigue cracking at the stub sill to head pad connection of stub sill tank cars can occur. It is recommended that other typical cars, of similar and dissimilar design, be tested to increase the information base.

- Vertical coupler force was added only to one end of the Simuloader. It is recommended that this capability be added to the other end of the Simuloader for future testing of stub sill tank cars.

- The mechanism for which the vertical coupler loads are introduced into the stub sill; that is, how vertical loads enter the coupler joint and their transmission into the sill, is not understood. Such information would prove valuable to the future design of stub sill tanks and potential exists for better environmental replication through the Simuloader. AAR/TTC recommends a cooperative research and test program, utilizing dynamic modeling and testing to determine the mechanism.

- Vertical coupler loading should be taken into consideration during the design stage for new generation stub sill tank cars. The tank car designers should perform fatigue analysis of their stub sill designs by including vertical coupler loads in conjunction with other loading requirements. Existing designs should also be evaluated. Then the formulation of a periodic inspection for existing designs could begin.

Table of Contents

List of Tables

List of Figures

1.0 BACKGROUND/INTRODUCTION

The Federal Railroad Administration (FRA) has been investigating incidents of fatigue cracking in tank cars with stub sill construction (virtually all tank cars built since the 1950's, a total of about 162,000 cars) for several years.[1] These investigations have led to several observations concerning stub sill tank cars -- specifically in the area of welds of the stub sill to tank interface. One is that the stub sill design allows yard impact, and train-action buff and draft forces to be carried through the tank shell.

Previous FRA research projects addressed the problem of tank car attachments and residual stresses.[2,3] Based on these project results, it was determined that additional work was needed to analyze the issue of fatigue crack growth. Accordingly, the Association of American Railroads (AAR), Transportation Test Center (TTC), Pueblo, Colorado, was contracted by FRA to provide fatigue testing of a tank car on the Simuloader at the Rail Dynamics Laboratory (RDL) to simulate over-the-road (OTR) load environment at an accelerated rate. The results of the above task will assist the FRA in developing procedures and policies regarding the elimination of the stub sill cracking problem or its curtailment to a safe acceptable level.

The FRA awarded the Tank Car Fatigue Crack Growth Test contract in 1989. The project, which began in September, 1990, included the following main tasks:

- Planning and preparation of the Test Implementation Plan (TIP)
- Communications and coordination with the FRA, Volpe National Transportation Systems Center (VNTSC), AAR Fatigue Task Force, and the AAR Tank Car Committee
- OTR tests on the Atchison, Topeka, and Santa Fe Railway Company (ATSF) for collecting load environment data
- Load input profile preparation for TTC's Simuloader
- Accelerated-rate 300,000 mile fatigue tests on the loaded tank car with the Simuloader
- Fatigue analysis and crack growth rate determination

A 26,000 gallon capacity Department of Transportation (DOT) 111A100W1 car, manufactured by Trinity, Industries and owned by ATSF, was used as the test car under this program. The B-end of the test car was left in an as-built condition, and the A-end of the car was retrofitted with a head brace also manufactured by Trinity, Industries. Soon it was found that the as-built stub sill to head reinforcing pad connection on the B-end of the car was the most sensitive region in fatigue (hereafter termed "critical region").

OTR testing was completed in September 1990. Certain portions of the OTR test data showed significant strains in the critical region. Analysis of the data revealed that the train slack action forces and bolster motions alone could not account for the significant strain levels at the critical region measured during the OTR test. Subsequent discussions with the Fatigue Task Force Committee, and other agencies, concluded that the prime cause for the observed high strain levels leading to cracks in stub sill tank cars was probably related to vertical coupler loads caused by coupler height mismatch between cars and/or out-of-phase motions of couplers superimposed with train action forces.

Subsequently, in August 1991 the Tank Car Fatigue Crack Growth Test Program received a new direction from FRA by including the following supplemental support tasks.

- Impact tests at TTC to determine the effect of coupler height mismatch on loads induced in the critical region

- Dynamic perturbed track vertical coupler loading tests at TTC

- Quasi-static vertical coupler load tests at RDL on the Mini-shaker Unit (MSU)

- Cyclic vertical coupler load tests on the MSU

- Fractographic analysis of sill pad samples that developed cracks in revenue service

- Cyclic testing of tank car steel samples in a load frame to obtain fatigue crack growth properties at the University of Illinois, Urbana, Illinois

The impact tests with various levels of coupler height mismatch, and the quasi-static/cyclic vertical coupler load tests performed on the MSU readily produced high strain levels at the critical region similar to those measured during the OTR test. This confirmed that vertical coupler loads are the most dominant contributing factor for the observed fatigue intensive strains.

At this point, data collected from OTR tests were processed into Simuloader input profiles (fourth quarter 1990). The Simuloader uses a system of hydraulic actuators supported by hydraulic power sources, electronics, and computers to replicate vertical and lateral truck bolster displacements and longitudinal buff and draft loads measured during revenue service operation.

Preliminary exploratory Simuloader fatigue tests were performed in November 1991 to determine the effectiveness of the input profiles developed from the OTR test data. The ability to re-create the vertical coupler loading using the Simuloader was closely scrutinized. The criteria for evaluating the performance of the Simuloader were based on strain ranges and strain cycle counts from the strain gages located in the critical region of the tank car. Comparisons of critical-region strain gage ranges for the OTR, impact, MSU, and exploratory Simuloader tests showed that the Simuloader was unable to reproduce many of the OTR strain ranges due to limitations in vertical coupler loading; whereas, the MSU rig was able to do so.

For the above reasons, enhancing the Simuloader to include vertical coupler loading was discussed at a meeting December 10, 1991, between Oscar Orringer and Jeff Gordon of the VNTSC, Jose Pena and Gunars Spons of the FRA, and AAR representatives. At this meeting, it was agreed that the Simuloader be modified to include the vertical coupler loading capability. Thus, the capability to produce vertical coupler forces was added to the Simuloader by means of a vertically oriented actuator attached to the tank car's B-end stub sill.

The need to modify the Simuloader input profile development methods was also identified at the meeting. Discussions with the representatives of FRA and VNTSC concluded that the Simuloader input profiles should be adjusted to comply with AAR's Freight Equipment Environmental Sampling Test (FEEST) data published under "Road Environment Percent Occurrence Spectrum" of AAR's *Manual of Standards and Recommended Practices*, Section C - Part II, Chapter VII (1988), "Fatigue Design of New Freight Cars." Even though the data collected during the OTR test did not provide the complete spectrum of peak-to-peak longitudinal/vertical coupler loads, it did provide the phase relationships of various loads necessary to develop the Simuloader input profile.

The costs associated with the additional work of adding the vertically oriented actuator to one end of the Simuloader and enhancing the input profile were also addressed at the meeting. AAR recommended that funding for making hole drilling measurements and conducting impact tests, after the Simuloader test was 50 percent completed, be used to modify the Simuloader and develop the enhanced input profile. FRA agreed that the benefits lost by deleting these tasks were minimal compared to the benefit gained by enhancing input profile and adding the vertical coupler loading capability to the Simuloader.

Accordingly, the AAR developed a new Simuloader input profile generation process, called the "enhanced input profile development methodology," which incorporated the tank car coupler vertical and longitudinal forces published in the AAR *Manual of Standards and Recommended Practices*. The data used are representative of the severe environment recorded over approximately 23,000 loaded-car miles (as against the 1,160 loaded-car miles of tank car service recorded under this program). The new Simuloader input profile was generated using time history load data collected during the OTR test that was enhanced such that the OTR histogram data matched the FEEST histogram data for both longitudinal and vertical coupler forces. The phase relationships of various loads obtained during OTR test were retained.

4

After the successful implementation of vertical coupler loading arrangement for the Simuloader, the AAR performed the accelerated fatigue test with the new input profile at an accelerated test rate of 4,400 miles of revenue service load environment for each hour of operation on the Simuloader. Thus, it was possible to simulate 300,000 loaded-car miles of revenue service operation in less than 12 weeks of Simuloader testing.

1.1 KEY TECHNICAL PARTICIPANTS

Claire Orth and Jose Pena of the FRA were instrumental in the conduct of this test program. Britto Rajkumar and David Cackovic, AAR/TTC, performed the tasks required for the successful conduct of the test program. Dr. Vinaya Sharma, AAR/Chicago Technical Center, and AAR consultants Dr. Gerald Moyar and Samuel Halcomb helped in the planning and strategy of the test program, as well as in the interpretation of the results. Oscar Orringer and Jeff Gordon of VNTSC provided valuable suggestions for vertical loading arrangement of the Simuloader and for input profile generation conforming to FEEST data.

1.2 SIGNIFICANT SEQUENTIAL MILESTONES

Table 1 presents the description of significant milestones sequentially arranged, from the inception to the completion of the Fatigue Crack Growth Test Program for stub sill tank cars.

5

Table 1. Significant Milestones

Project Milestone	Date Achieved
Contract Award	9/29/89
Submit TIP	11/89
Receive Tank Car for Test	8/90
Prepare Tank Car for OTR Tests	8/90
Conduct OTR Tests	9/90
OTR Test Data Analysis	9/90 to 6/91
Submit Request for Supplemental Tests to FRA	11/90
Submit Proposal for Supplemental Tests to FRA	6/91
Supplemental Tests - Contract Award	8/91
Submit TIP for Supplemental Tests	9/91
Conduct Supplemental Tests	8/91 to 10/91
Supplemental Tests Data Analysis	8/91 to 12/91
Simuloader Test without Vertical Coupler Force (VCF)	10/91 to 2/92
Simuloader Test Data Analysis (without VCF)	11/90 - 5/91
VCF and SMU Input Development	12/91 - 2/92
Simuloader Test with VCF	2/92 - 4/92
Simuloader Test Data Analysis (with VCF)	2/92 - 5/92
Crack Growth (da/dn) Test	5/92 - 10/92

2.0 OBJECTIVES

The main objectives of the test program, as stated in the FRA original and supplemental Statements of Work, were:

1. To characterize the service stress environments on the tank car

2. To investigate crack growth rates at typical locations where cracks might form

3. To obtain dynamic measurements of buff load effects at the tank mid-span and near stub sill ends

4. To obtain crack growth rate parameters of sample tank car steels, perform yard impacts to determine the effect of coupler-height mismatches, characterize vertical coupler loads, and perform fractographic analysis of cracked sill pad specimens.

3.0 PREPARATORY TASKS, INFORMATION

3.1 COORDINATION WITH GOVERNMENT AND INDUSTRY

Throughout the implementation of this test program, considerable communications and coordination was required. Government organizations with significant input to the test program included the FRA and the VNTSC. Several planning meetings were held with these groups. In addition, presentations were made to groups representing industry including the AAR Tank Car Committee, the AAR Fatigue Task Force, and the Railway Progress Institute (RPI). Key meetings conducted during the program are listed in Table 2.

Table 2. Key Meetings with Government and Industry

Date and Group	Description of Agenda
4/24/90 FRA/TSC at TTC	Program Start Up Meeting - AAR test plans were discussed with Jose Pena and Gunars Spons, FRA, and Jeff Gordon, VNTSC.
7/18/90 Tank Car Comm. at Memphis, TN	Program plans presented, suggestions noted. Suggestion for acoustic emissions testing examined.

Table 2. Key Meetings with Government and Industry – continued.

Date and Group	Description of Agenda
8/15/90 AAR and Consultants	Meeting with AAR/TTC, AAR Chicago Technical Center, and consultants to inspect tank car and select strain measurement locations.
11/12/90 Fatigue Task Force at Washington, D.C.	Test and analytical procedures presented, suggestions noted, supplemental requirements developed for FRA consideration.
11/13/90 FRA at Washington, D.C.	Progress discussed, supplemental requirements discussed.
7/18/91 Tank Car Comm. at TTC	Tour of TTC, progress presented, Simuloader exhibited, acoustic emissions test conducted.
11/7/91 Fatigue Task Force at TTC	Progress presented, suggestions noted, Simuloader exhibited.
12/10/91 FRA/TSC at TTC	Discussion of Simuloader test results without vertical coupler loading. At this meeting it was agreed that a vertical coupler loading capability be added to one end of the Simuloader to increase the effectiveness of the Simuloader for reproducing the fatigue environment of stub sill tank cars. It was also decided to use load levels which are published in the AAR Fatigue Manual as a measure to supplement the OTR test data used for Simuloader testing. Specifically, the input longitudinal and vertical coupler loads will be scaled up, while the existing OTR test phase relationships will remain unchanged. This was done because the test loads, which contain the necessary phase relationships required to operate the Simuloader, were not as severe as the published FEEST design data. The FEEST data, in the form of histograms, is commonly used for fatigue life predictions of new car designs. Thus, the fatigue input loads used in the Simuloader testing is a hybrid version of the OTR test data.
4/9/92 RPI at TTC	Procedures, progress presented, suggestions noted, Simuloader exhibited.

3.2 TIP

A TIP for the original test program and the supplemental test program was prepared and submitted to FRA for approval. Each TIP included an introduction, lists of key personnel and responsibilities, test objectives and operations, instrumentation, data acquisition, data analysis, resource and safety requirements, and a test schedule.

3.3 TEST CAR

At the inception of the test program, the FRA, in its Statement of Work accompanying the request for proposal, did not explicitly describe which type of stub sill tank car should be tested. Therefore, AAR/TTC found a representative stub sill tank car for test -- a Trinity-built 26,000 gallon capacity DOT111A car, owned by the ATSF railroad and used for storing and hauling diesel fuel. The selected car was similar in design to cars which have developed cracks in the critical region in revenue service. The overall quality of welding in the test car was good.

The B-end of the car was left in the as-built condition. The A-end of the car was retrofitted with a head brace manufactured by Trinity that is designed to reduce the stresses in the critical region. TTC engineers witnessed the installation of the head brace. Figure 1 shows the test car. Figures 2 and 3 show the A- and B-ends of the car, and Figure 4 is an illustration depicting the critical region on the B-end of the car where cracks have been found in similar cars.

Figure 1. ATSF 98604 Stub Sill Tank Car
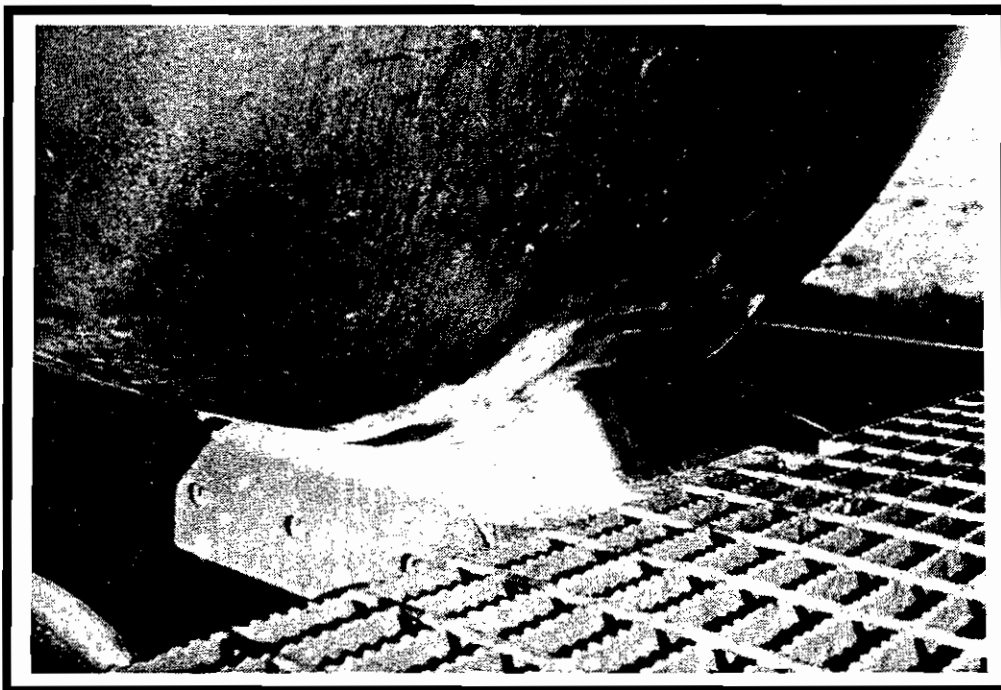
Figure 2. A-end of ATSF 98604 Stub Sill Tank Car

Figure 3. B-end of ATSF 98604 Stub Sill Tank Car

ATSF 98604
B-END
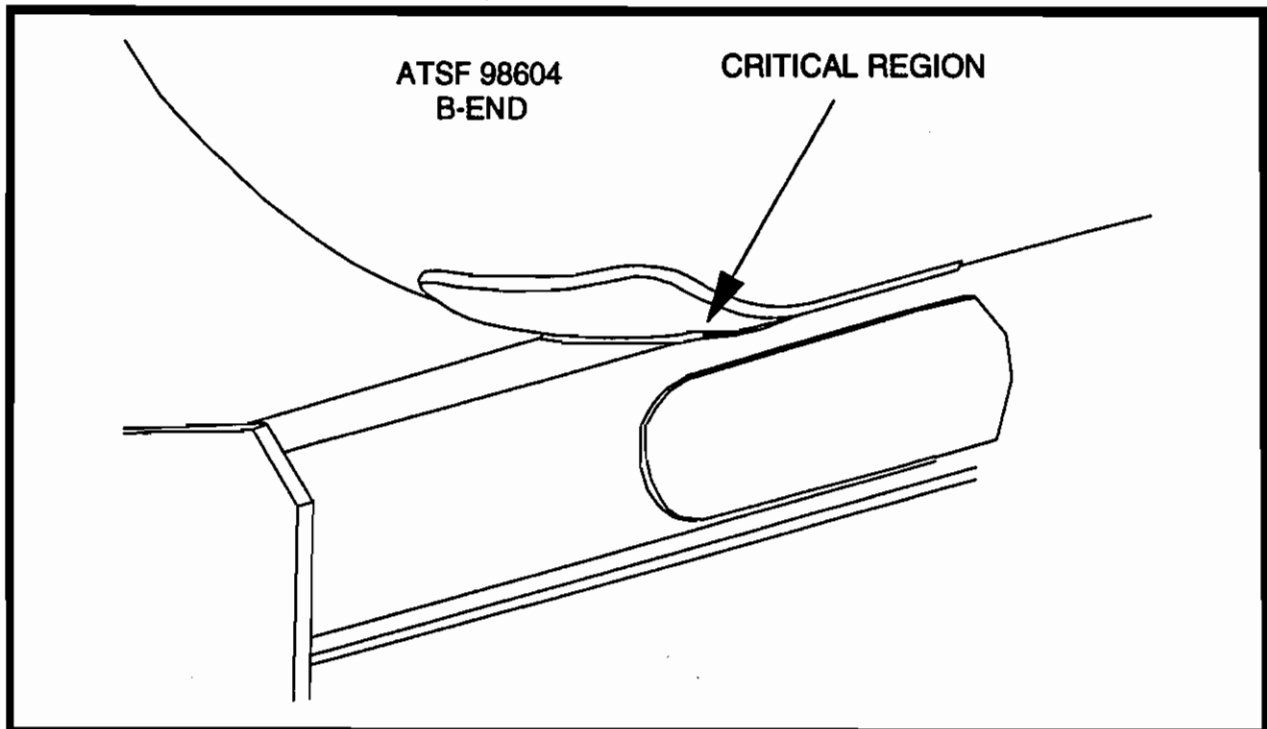
CRITICAL REGION

Figure 4. Critical Region Where Cracks Have Been Found in Similar Cars

11

The ATSF car, No. 98604, was inspected upon arrival for cracks or other defects. None was found, which may have been the result of the limited mileage (32,626 miles) on the car. The car was found to be clean upon arrival.

Regulations require the use of double-shelf couplers for tank cars which haul hazardous materials, including diesel fuel. However, the test required TTC's instrumented couplers, which are not of the double-shelf type. Therefore, the car was tested loaded with water. This caused another problem due to railroad weight restrictions. Diesel fuel has a specific gravity of less than 0.9; that is, its density is less than 90 percent of the density of water. Thus, the amount of water (23,141 gallons) required to load the car to its normal weight resulted a 12 percent outage condition as opposed to the more typical 2 percent outage condition when loaded to the same weight with diesel fuel (25,840 gallons). The test car's statistics are given in Table 3.

Table 3. Test Car Statistics

Category	Item
Classification	DOT 111A 100W1
Year Built	1980
Car number	ATSF 98604
Total mileage upon receipt	32,626
Average mileage per year	5,220
Capacity	26,367 gallons (full)
Draft Gear	M-901-E
Couplers	SE 60 CHT
Truck Type	Barber S-2-C
Side bearings as-received	Stucki 688 BR Resilient Constant Contact
Side bearings as-tested	Roller Side Bearings
Brake system	Rod-through style
Spring Group	D-5 (6 outer) D-6 (6 inner) D-6A (4 inner)
Snubbers	Stucki HS 7100
Weight on rail (maximum)	262,500
Light weight of car	69,500 pounds
Capacity	193,000 pounds
Typical load	Diesel Fuel
Load tested	Water
Outage tested	88%
Weight on rail (88% outage, water, as tested)	261,850
Length between strikers	58' 2 1/4 "
Length between truck centers	45' 10 1/4"
Length of truck wheel base	70 1/4"

3.4 ACOUSTIC EMISSIONS TESTING

During discussions with the AAR Tank Car Committee, TTC engineers found significant interest in tank car acoustic emissions (AE) testing. The AE method, as described in a procedures document by the Monsanto Company,[4] consists of subjecting railroad tank cars or intermodal tanks to predetermined loads or deflections and monitoring acoustic emission (transient stress waves) caused by stressed defects.

As a result of the interest in AE testing, Dr. Tim Fowler of Monsanto Company became involved with this program. He subsequently performed the AE pressurization and torsional loading tests on the tank car before the OTR test. The purpose of these tests was to evaluate the structural integrity of the tank car shell. The test showed no defects.

Later, after the OTR test, a demonstration of a new twist-bar AE test was performed on the stub sill tank car for the AAR Tank Car Committee at TTC. The purpose of this specific test is to expose defects in the critical region of the stub sill to tank car attachment area. The test results suggested possible but not conclusive defects.

4.0 OTR TEST

4.1 OTR TEST PROCEDURES

The OTR test was conducted to obtain the tank car load environment for the fatigue test on the Simuloader. Preparations for the OTR test were completed in August, 1990. The OTR test, performed on the ATSF railroad, was conducted September 19, 1990, through September 23, 1990. Analysis of the OTR test data was done between September 1990, and June 1991.

4.1.1 OTR Test Car Preparations

The test car was received at TTC through a link with the ATSF railroad in Avondale, Colorado. The car was equipped with constant contact side bearings when received at the TTC. The constant contact side bearings were removed and replaced with hard roller side bearings by TTC personnel prior to the OTR test. The car was loaded to 12 percent outage with water, weighed, then parked for instrumentation preparation.

4.1.2 OTR Test Instrumentation

The test car was instrumented for the OTR test in August 1990. The measurements included car body and truck responses, coupler forces, and truck bolster accelerations for Simuloader input profile development. The instrumentation method used for Simuloader input profile development was the Locomotive Track Hazard Detection system (LTHD).

Servo-accelerometers were used for the LTHD measurements. Piezo-resistive accelerometers were used to backup the LTHD measurements and for car body and coupler accelerations. Weldable strain gages were used for the strain measurements. Two couplers, instrumented with strain gages, were used to acquire coupler load data, and a tachometer was used to measure speed.

The AAR 112 instrumentation car was used to house the test personnel, digital and analog data acquisition systems, signal conditioners, and other associated equipment. Figure 5 displays the test and instrumentation cars used for the OTR test.
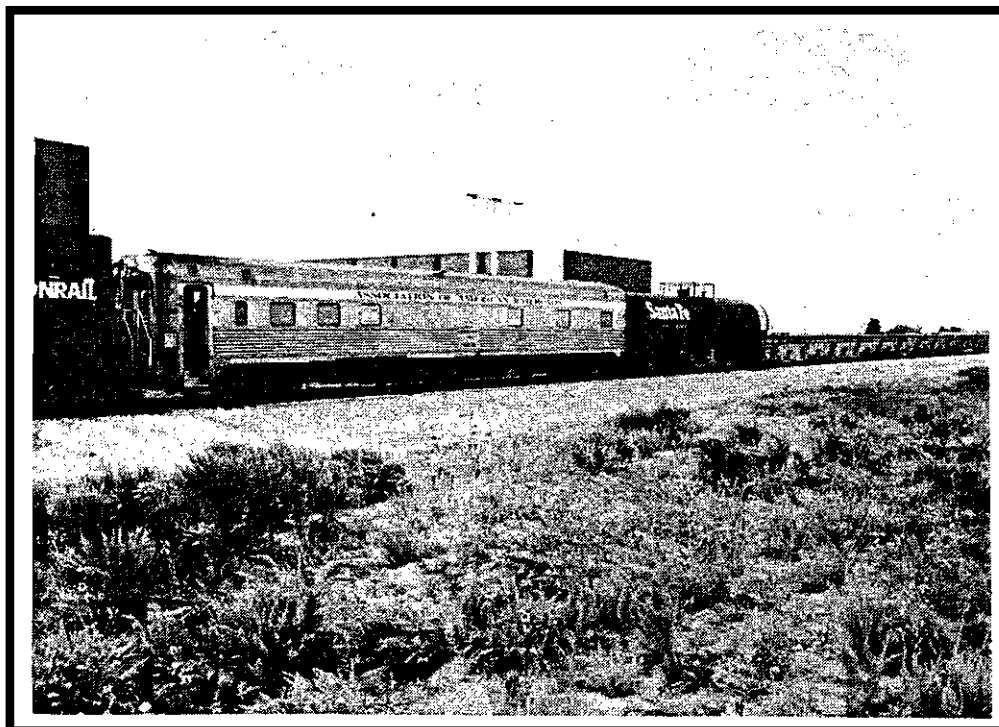
Figure 5. Test Car and AAR 112 Instrumentation Car

4.1.2.1 Measurement Definition -- LTHD Measurements

The LTHD system was designed to locate significant track geometry defects. The system can also be used to produce vertical and lateral space profiles describing wheel set motion. This equipment has been frequently used to obtain representative truck input profiles for the Vibration Test Unit (VTU) at TTC. For the OTR test, the LTHD system was used to produce vertical and lateral space profiles describing truck bolster motion. This adaptation of the LTHD system has been used successfully in previous test programs.

The LTHD method involves collecting lateral and vertical accelerations at each truck bolster (two vertical measurements and one lateral measurement per bolster). The accelerometers are located in boxes, which are attached to the ends of the truck bolsters. The boxes use a dense foam packing material to protect the accelerometers from high-frequency mechanical vibrations.

The acceleration signals are low-pass filtered and collected in digital form. Using software, the acceleration data are converted into the vertical and lateral displacements of the truck bolster. This conversion is done with a modified second-finite-difference double-integration routine, which corrects for angular and gravitational effects as well as for phase distortion and signal noise.

4.1.2.2 Measurement Definition -- Instrumented Couplers

The instrumented couplers measured the longitudinal forces due to buff and draft train action. These couplers utilize a two-active-arm wheatstone bridge strain gage circuit configured to negate localized stress variations and bending and twisting forces.

4.1.2.3 Measurement Definition -- Strain Gage Measurements

For the OTR test, 350-ohm strain gages were welded to the tank car at strategic locations to measure the strain responses.

4.1.2.4 Measurement Definition -- Test Car Speed

Spindle-driven, 60-pulse per revolution, axle mounted tachometers were used to measure train speed during the OTR test.

4.1.2.5 Measurement Definition -- Acceleration Measurements

Car body vertical, lateral, and longitudinal accelerations, along with coupler longitudinal accelerations, were acquired during the OTR test with piezo-resistive accelerometers.

4.1.2.6 Simuloader Input Profile Development Measurements

Table 4 defines the OTR test measurements, which were recorded to develop and evaluate the Simuloader input profile during the OTR test.

Table 4. Measurements for Simuloader Inputs

Name	Description and Location	Type	Range[a]
LLV1	LTHD Left Vertical Bolster Accel, B-end	Servo-Accel	±10 g's
LRV1	LTHD Right Vertical Bolster Accel, B-end	Servo-Accel	±10 g's
LLAT1	LTHD Lateral Bolster Accel, B-end	Servo-Accel	±10 g's
LLV2	LTHD Left Vertical Bolster Accel, A-end	Servo-Accel	±10 g's
LRV2	LTHD Right Vertical Bolster Accel, A-end	Servo-Accel	±10 g's
LLAT2	LTHD Lateral Bolster Accel, A-end	Servo-Accel	±10 g's
LV1	Left Vertical Bolster Accel, B-end	P-R Accel	±10 g's
RV1	Right Vertical Bolster Accel, B-end	P-R Accel	±10 g's
LAT1	Lateral Bolster Accel, B-end	P-R Accel	±10 g's
LV2	Left Vertical Bolster Accel, A-end	P-R Accel	±10 g's
RV2	Right Vertical Bolster Accel, A-end	P-R Accel	±10 g's
LAT2	Lateral Bolster Accel, A-end	P-R Accel	±10 g's[b]
CP1	A-end Coupler Force	Coupler	0-1000 kips
CP2	B-end Coupler Force	Coupler	0-1000 kips
AC1	A-end Coupler Longitudinal Accel	P-R Accel	±20 g's
AC2	B-end Coupler Longitudinal Accel	P-R Accel	±20 g's
SG01[c]	Stub Sill, B-end, in Front of Attachment Pad Connection	Strain-Gage	±500 $\mu\varepsilon$[d]
SG02[c]	Center of Truck Bolster, B-end , Parallel to Bolster	Strain-Gage	±200 $\mu\varepsilon$
SG03[c]	Car Body Bolster, B-end, Parallel to Bolster	Strain-Gage	±900 $\mu\varepsilon$
TSPD	Test Car Speed	Tachometer	0-100 mph
AZ1	Car Body Vert. Accel, B-end, Right Corner	P-R Accel	±10 g's
AY2	Car Body Long. Accel, B-end, Right Corner	P-R Accel	±10 g's
AX3	Car Body Lat. Accel, B-end, Right Corner	P-R Accel	±10 g's
DZ1	B-end Coupler Vertical Displacement, Relative to Sill	LVDT	±1"

[a] Ranges shown are initial values and may have been increased through the course of the test

[b] Ranges, defined for 10 volt system, not necessarily reflect expected values -- often hardware limited.

[c] Backup gages, for quick replacement in case of failure, were provided.

[d] $\mu\varepsilon$ denotes micro-strains

4.1.2.7 Strain Response Measurements

Table 5 lists the strain-response measurements that were recorded during the OTR test. The corresponding strain ranges are also listed.

Table 5. Strain Response Measurements

Name	Description	Type	Range
SG04	B-end, End Cap, Vertical Strain	Strain-Gage	±100 με
SG05	B-end, Sill-End Cap, Vertical Strain	Strain-Gage	±100 με
SG06	B-end, Sill-End Cap, Diagonal Strain	Strain-Gage	±100 με
SG07	B-end, Sill-End Cap, Lateral Strain	Strain-Gage	±500 με
SG08	B-end, Corner of Reinforcing Plate, Vertical Strain	Strain-Gage	±1000 με
SG09	B-end, Corner of Reinforcing Plate, Diagonal Strain	Strain-Gage	±200 με
SG10	B-end, Corner of Reinforcing Plate, Lateral Strain	Strain-Gage	±100 με
SG11	Mid-span Tank Underside Longitudinal Strain	Strain-Gage	±500 με
SG12	Mid-span Tank Underside Diagonal Strain	Strain-Gage	±100 με
SG13	Mid-span Tank Underside Lateral Strain	Strain-Gage	±100 με
SG14	A-end, End Cap, Vertical Strain	Strain-Gage	±100 με
SG15	A-end, Sill-End Cap, Vertical Strain	Strain-Gage	±100 με
SG16	A-end, Sill-End Cap, Diagonal Strain	Strain-Gage	±100 με
SG17	A-end, Sill-End Cap, Lateral Strain	Strain-Gage	±100 με
SG18	A-end, Corner of Reinforcing Plate, Vertical Strain	Strain-Gage	±100 με
SG19	A-end, Corner of Reinforcing Plate, Diagonal Strain	Strain-Gage	±100 με
SG20	A-end, Corner of Reinforcing Plate, Lateral Strain	Strain-Gage	±100 με

4.1.2.8 OTR Test Data Collection

Forty-four digital, 23 analog, and 14 strip chart recordings were made. Below are descriptions of the digital, analog, and strip chart data recording devices used during the OTR test. Table 6 lists the data acquisition requirements met for each measurement channel.

DIGITAL DATA ACQUISITION

Two Hewlett Packard (HP) computers were used to collect and analyze the OTR test data. The data was sampled at 256 samples per second (s/s), low-pass filtered at 30 Hz, and stored in 15-minute packets on an optical disk storage device. The LTHD measurements were also low-pass filtered by frequency device filters, which are integral to the LTHD system.

ANALOG DATA ACQUISITION

Two Kiowa 650A 14 channel analog recorders, operated at a tape speed of 1.19 cm/s, were used to record selected data.

STRIP CHART RECORDERS

Two eight-channel strip chart recorders were used to perform real-time monitoring of key measurements. The chart speed was 5 mm/sec.

Table 6. Data Recording Requirements for OTR Test

No.	Name	Digital Record	Analog Record	Chart Record	Comment
1	LLV1	X X (twice)	X	X	For LTHD channels 1-6, digital recordings were made before and after the LTHD filtering process. The analog recordings were made of the unfiltered data only. The chart recordings were of the filtered data.
2	LRV1	X X	X	X	" " " "
3	LLAT1	X X	X	X	" " " "
4	LLV2	X X	X	X	" " " "
5	LRV2	X X	X	X	" " " "
6	LLAT2	X X	X	X	" " " "

Table 6. Data Recording Requirements for OTR Test -- continued

Date and Group		Description of Agenda			
No.	Name	Digital Record	Analog Record	Chart Record	Comment
7	CP1	X	X	X	Coupler force
8	CP2	X	X	X	Coupler force
9	LV1		X		Backup to LTHD measurement
10	RV1		X		Backup to LTHD measurement
11	LAT1		X		Backup to LTHD measurement
12	LV2		X		Backup to LTHD measurement
13	RV2		X		Backup to LTHD measurement
14	LAT2		X		Backup to LTHD measurement
15	AC1	X	X		Coupler acceleration
16	AC2	X	X		Coupler acceleration
17	SG01	X	X	X	Strain measurement
18	SG02	X	X	X	Strain measurement
19	SG03	X	X	X	Strain measurement
20	SP1	X	X		Test car speed
21-23	AZ1 - AX3	X			Car body accelerations
24	DZ1	X			Coupler vertical displacement
25	LTLV1	X	X	X	AAR additional measurement
26	LTRV1	X	X	X	AAR additional measurement
27	LTLAT1	X	X	X	AAR additional measurement
28-44	SG04 - SG20	X			Strain measurements

4.1.2.9 Instrumentation Documentation

Sketches and photographs of the OTR test measurements were taken. Appendix A includes drawings of the key response strain gage instrumentation locations.

4.1.3 <u>Pre-test Checkouts and Calibrations</u>

On September 5 and 6, 1990, pre-test instrumentation checkouts and strategic gage calibrations were performed. The checkout tests conducted are listed in Table 7. These tests were conducted in a perturbed track test zone on the TTC's Precision Test Track (PTT), which is highlighted in the TTC map shown in Figure 6.

The pre-test strategic gage calibrations performed are listed in Table 8.

Table 7. Checkout Tests Performed

Checkout Test	Description
Twist-and-roll	Twist-and-roll tests at 10, 15, 20, and 25 mph over old 800-foot, 20 bump section on PTT. Twist-and-roll tests at 10, 15, 20, and 25 mph over new 400-foot, 10 bump section on PTT.
Bounce	Bounce tests at 30, 40, 50, 60, and 70 mph over bounce test section on PTT.
Switching	Switching operations at 0.5, 1, 1.5, and 2 mph.
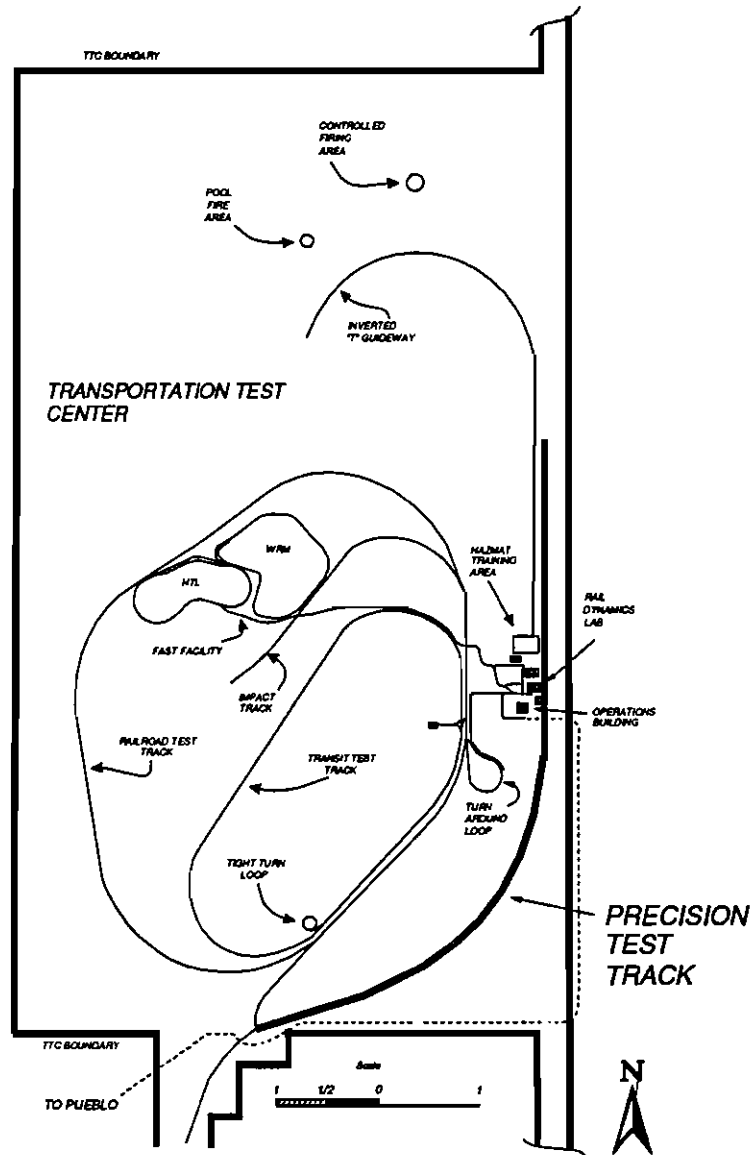
Figure 6. PTT

Table 8. Pre-test Strategic Gage Calibrations

Calibration	Description
Truck bolster SG02	Load cell placed in front and rear of center bowl, car body jacked up and down to relieve and apply load -- main gage circuit
Truck bolster SG02'	Load cell placed in front and rear of center bowl, car body jacked up and down to relieve and apply load -- backup gage circuit
Stub Sill SG01	Lifting of coupler to induce upward vertical coupler load

4.1.4 OTR Test Route

The OTR test was conducted on the ATSF railroad. The route taken was Pueblo - Albuquerque - Los Angeles. Test data were acquired during the outgoing trip on a local-freight type train typically used for tank car service. Data reduction and analysis were performed during the return trip.

Figure 7 displays the test route.

- ATSF: PUEBLO - ALBUQUERQUE - LOS ANGELES
- 1160 MILES

PUEBLO

LOS ANGELES

ALBUQUERQUE
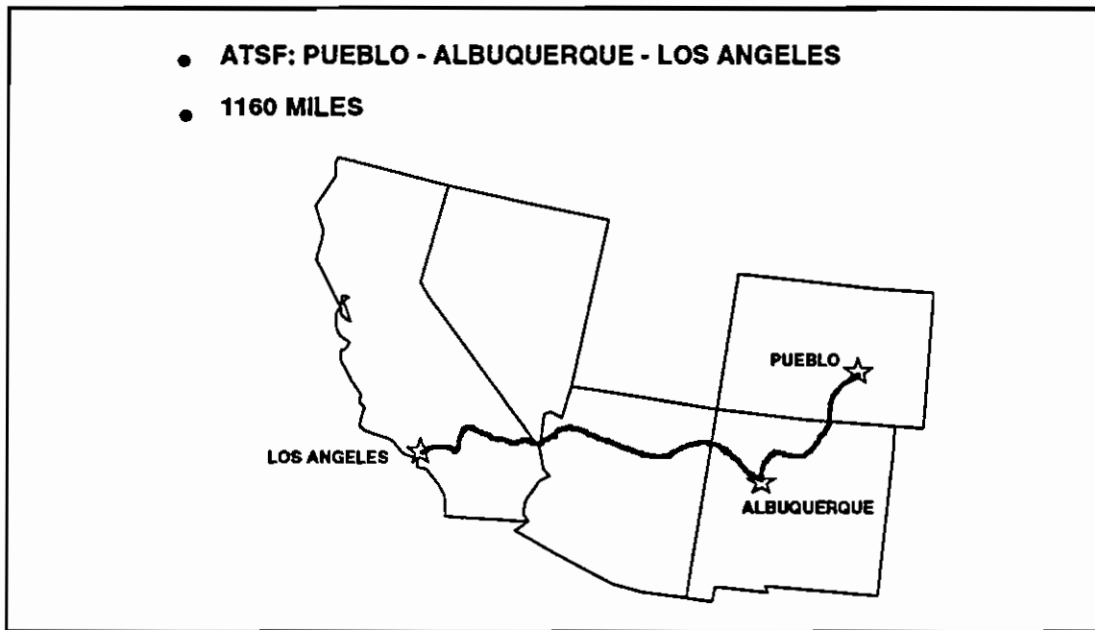
Figure 7. OTR Test Route

4.1.5 OTR Test Logistics and Documentation

A run log was recorded during the OTR test conducted in September 1990. The log documented the time, date, digital run number, optical disk number, automatic location detector number, test car location with mile posts, and analog tape footage. A comment line was also included. This log facilitated easy data retrieval and analysis at a later date.

One ATSF Research and Test employee accompanied TTC's test team on the OTR test. Initially it was planned to position the test and instrumentation cars in the rear two-thirds of the train consist with loaded cars in front and in back of the test car. During the course of the OTR test, however, it was not always possible to position the test car in the desired location. The trains were typical through-freight consists. Table 9 shows the test consist makeup for the OTR test.

Table 9. Test Consist Makeup for OTR Test, September, 1990

Start Destination	Stop Destination	Description
La Junta, CO	Albuquerque, NM	Test car 42 in a 77 car train. Leading 41 cars were loaded and totaled 3593 tons, 35 empty trailing cars totaled 1083 tons.
Albuquerque, NM	Barstow, CA	Test car 46 in a 68 car train. Leading 45 cars totaled 5207 tons (2700 foot length), 35 trailing cars totaled 1083 tons (4579 feet cumulative length).
Barstow, CA	Los Angeles, CA	Makeup similar to Albuquerque to Barstow consist.

Mile posts were noted for each 15-minute data file stored by the digital data acquisition system. Key OTR test locations, mile posts, and the date and time traversing these locations are listed in Table 10.

Table 10. Selected OTR Test Logistics, September, 1990

Date	Time	Nearest Mile Post noted	Description
9/19	13:45	603	Checkout runs between Avondale and La Junta, CO
9/19	18:28	555	Depart La Junta Station
9/19	22:24	651	Raton, NM
9/20	06:46	651	Depart Raton
9/20	14:06	831	Lamy, NM
9/20	16:00	831	Depart Lamy
9/20	17:46	901	Albuquerque, NM
9/21	1:03	1	Depart Albuquerque
9/21	10:50	283	Winslow, AZ
9/21	19:16	283	Depart Winslow
9/22	3:30	522	Griffith, AZ
9/22	6:39	522	Depart Griffith
9/22	15:16	743	Barstow, CA
9/23	2:58	1	Depart Barstow
9/23	5:37	76	San Bernardino, CA -- End of Test

4.1.6 OTR Test Data Analysis

Initially, a significant strain threshold for the gages in the critical region was defined as 150 microstrains. Through the course of the test, 157 fifteen-minute duration data files of digital information were stored. For each file, statistics of the car body response strain data were computed. If a critical-region strain gage showed strain ranges below the 150 microstrain value, the run was discarded. Statistics, at 50-second intervals, were then computed for the remaining 15-minute data files. If a critical-region strain gage showed strain ranges below the 150 microstrain value, the 50-second interval was discarded.

The resulting fifteen 50-second OTR test data files were processed with the following operations.

(1) The 15-minute runs with strain data greater than the threshold level were transferred to TTC's VAX 11/780 computer

(2) The 50-second sections found to contain high level strains were then appended into one 750-second condensed OTR file with TTC's Common Format Analysis System (CFAS). The output of this operation was used for input profile development.

4.2 OTR TEST RESULTS

4.2.1 Pre-test Checkouts and Calibrations

The results from the checkout tests on perturbed track were used to select strain ranges for recording. It was desired to carefully select strain ranges in order to have proper resolution for low-level signals, while ensuring that the highest level signals did not saturate the 10-volt data acquisition system. Despite this precaution, several of the 20 strain gages recorded during the OTR test over-ranged the data acquisition system regardless. This was because the checkout twist-and-roll, bounce, and switching tests did not excite the dynamic vertical coupler loads which were encountered during the OTR test. However, the data lost was minimal.

Results of the pre-test strategic gage calibrations performed are listed in Table 11.

Table 11. Results of Pre-test Strategic Gage Calibrations

Calibration	Result
Truck bolster SG02	Average -- 0.86 $\mu\varepsilon$ per kip bolster load
Truck bolster SG02'	Average -- 1.02 $\mu\varepsilon$ per kip bolster load
Stub Sill SG01	Average -- 8.18 $\mu\varepsilon$ per kip upward vertical coupler load

4.2.2 Determination of Threshold Value for Condensation of Test Data

The threshold strain value for input profile data condensation was defined for critical-region strain gages SG08, SG09, and SG10, and longitudinal mid-span strain gage SG11. Strain thresholds for the critical-region strain gage locations monitored during the OTR test, used to condense the data to include only "significant" fatigue events, were selected as described in the following excerpts from a letter (November 3, 1990) by Dr. Moyar.

> Part of the "investigation of crack growth rate at typical locations" we are charged with has to do with identification of loading conditions and crack sizes for which no measurable cyclic propagation is expected. This is the so called "threshold" ΔK. The corresponding limit or property is $\Delta Ktho$. The data selected

for pearlitic tank car steels by both TSC[5] and Battelle[6] is taken from Rolfe and Barsom.[7] If it is appropriate for application to propagation of cracks in the heat affected zone (HAZ) of our tank car head reinforcement plate the value of

$$\Delta K_{tho} = 7.0[KSI\sqrt{inch}]$$

by definition (for 0 mean stress)

$$\Delta K_{tho} = G(a)\sqrt{a}\,\Delta S$$

where: ΔS is the nominal stress range [KSI]

a is the crack depth [in.]

$G(a)$ Is a function of crack geometry and size

If there is a mean stress in the cycle

$$\Delta K_{tho} = (1 - R)\Delta K_{tho}$$

where R is the ratio of min. to max. stress in the cycle.

The geometry factor selected by the TSC consultants has the form

$$G(a) = 1.12 M_k \sqrt{\Pi/Q}$$

where M_k is taken as 1.05 and Q is taken as 2.0 to represent an elliptically shaped crack having a semi-minor axis, a (depth of crack). With these values the threshold stress intensity factor becomes

$$\Delta K_{tho} = 1.474\sqrt{a}\,\Delta S$$

We can further relate nominal micro strain range $\Delta\varepsilon$ to the stress range by means of the simple elastic uniaxial relation

$$\Delta S = 0.03\Delta\varepsilon$$

Therefore, the threshold strain range in terms of the crack size and threshold stress intensity property is

$$\Delta\varepsilon(\mu inches) = \frac{158}{\sqrt{a}}$$

If we specify a crack as deep as the head pad is thick (5/8"), then the threshold strain range is **200 microinches.** ...should allow for some uncertainty in strain gradient and bi-axiality effects in extrapolating single element strain gage data. Therefore, **a practical threshold of about 150 microstrain range for actual strain gage data would certainly be a conservative limit to use in eliminating insignificant data periods.**

4.2.3 OTR Test Data Condensation Results

Using the threshold described in Section 4.2.2 for the critical-region strain gages, critical time slices of the OTR test data representing the 15 significant events described in Table 12 were identified. These data were appended into one 750 second file with 50-second segments.

Table 12. Critical Time Slices of OTR Test Data

Event No.	15-Minute Storage File	Date, Approx. Time, Nearest Milepost of 50-Second Time Slice in 15-minute File Where Event Occurred
1	TANK_RN021	9/20/90, 8:40, milepost 692, between Raton, NM and Las Vegas, NM
2	TANK_RN023	9/20/90, 9:26, milepost 714, between Raton, NM and Las Vegas, NM
3	TANK_RN025	9/20/90, 9:45, milepost 724, between Raton, NM and Las Vegas, NM
4	TANK_RN037	9/20/90, 12:55, milepost 810, between Las Vegas, NM and Lamy, NM
5	TANK_RN037	9/20/90, 12:55, milepost 810, between Las Vegas, NM and Lamy, NM
6	TANK_RN044	9/20/90, 16:25, milepost 849, between Lamy, NM and Albuquerque, NM
7	TANK_RN046	9/20/90, 16:55, milepost 870, between Lamy, NM and Albuquerque, NM
8	TANK_RN047	9/20/90, 17:11, milepost 882, between Lamy, NM and Albuquerque, NM
9	TANK_RN048	9/20/90, 17:25, milepost 892, between Lamy, NM and Albuquerque, NM
10	TANK_RN048	9/20/90, 17:25, milepost 892, between Lamy, NM and Albuquerque, NM
11	TANK_RN048	9/20/90, 17:25, milepost 892, between Lamy, NM and Albuquerque, NM
12	TANK_RN048	9/20/90, 17:25, milepost 892, between Lamy, NM and Albuquerque, NM
13	TANK_RN048	9/20/90, 17:25, milepost 892, between Lamy, NM and Albuquerque, NM
14	TANK_RN048	9/20/90, 17:25, milepost 892, between Lamy, NM and Albuquerque, NM
15	TANK_RN049	9/20/90, 17:33, milepost 901, between Lamy, NM and Albuquerque, NM

4.2.4 OTR Test Significant Response Analysis

Time histories of condensed OTR test channels LCF, SG01, SG02, SG03, SG08, SG09, SG10, and SG11 are shown in Figures 8-11. The histories are categorized as either Type 1 or Type 2 responses. A Type 1 response was defined as a single event, such as a run-in of the train consist. A Type 2 response was more difficult to define. It is likely that this response was the result of a combination of dynamic brake train handling and track input due to a high frequency of crossings as the consist approached Albuquerque. It was this response which included significant frequent vertical coupler loads.

Figure 8. Response Type 1 -- LCF, SG01, SG02, and SG03
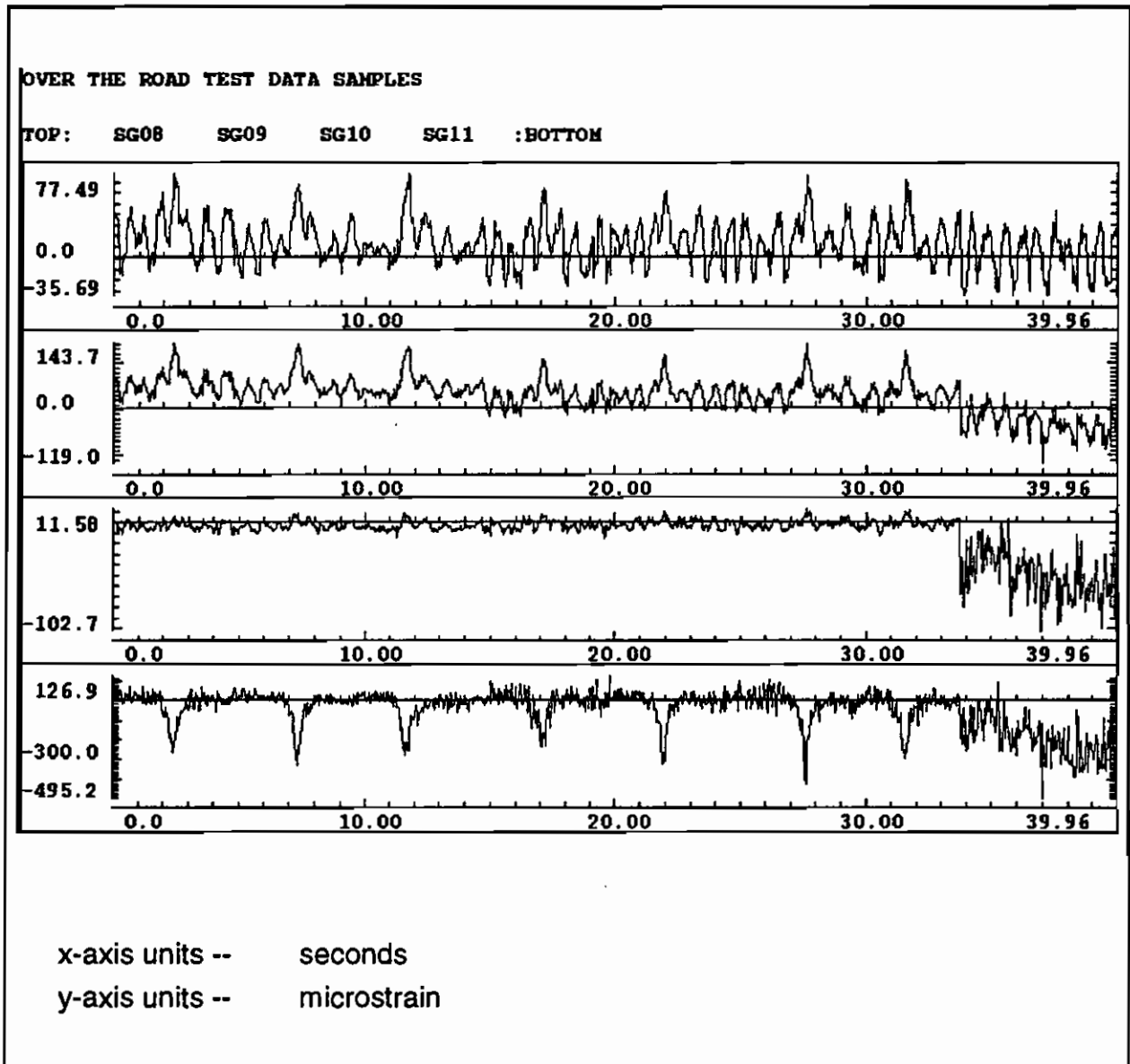
Figure 9. Response Type 1 -- SG08, SG09, SG10, and SG11
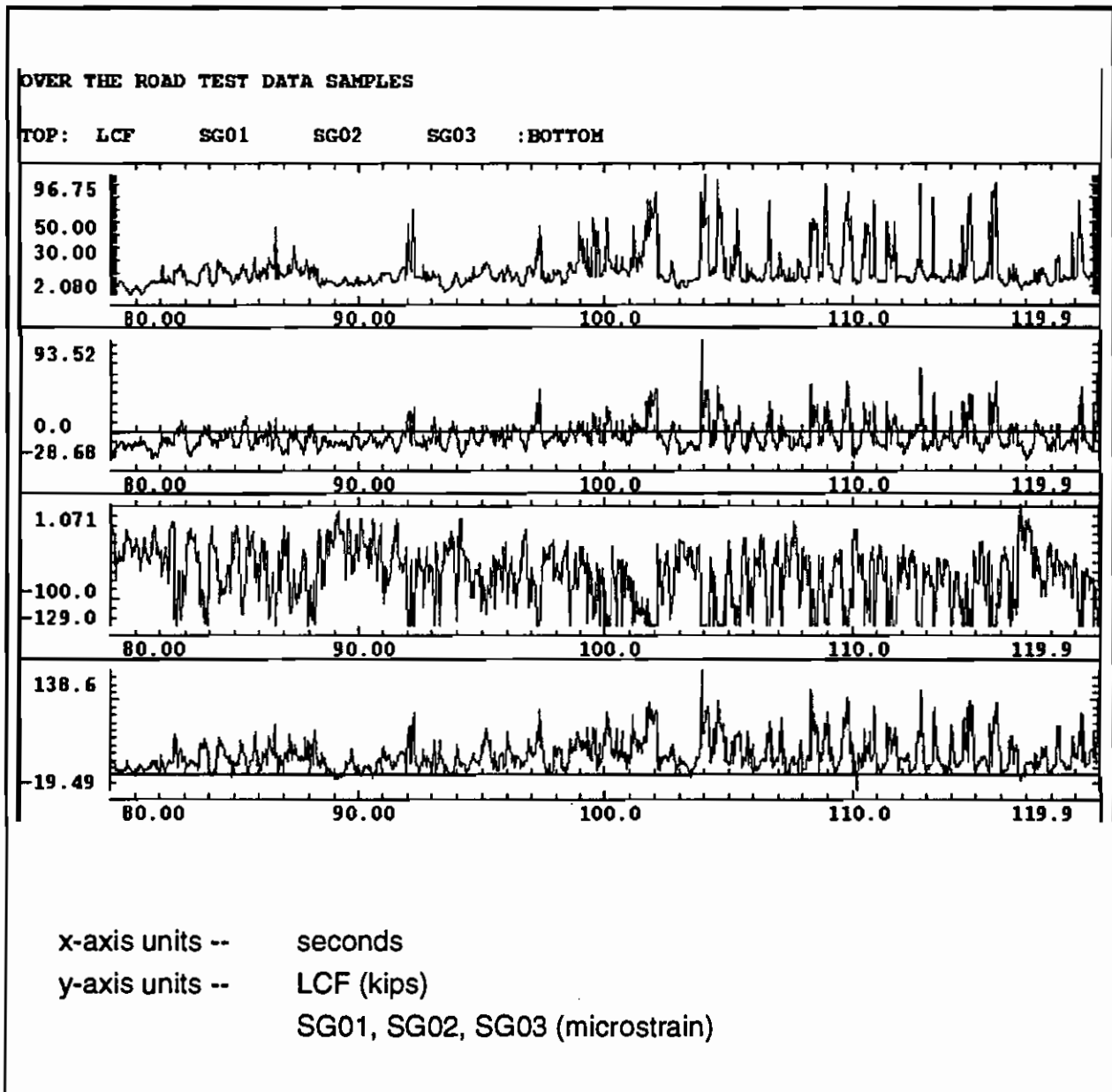
Figure 10. Response Type 2 — LCF, SG01, SG02, and SG03

OVER THE ROAD TEST DATA SAMPLES

TOP: SG08   SG09   SG10   SG11   :BOTTOM

x-axis units --   seconds
y-axis units --   microstrain
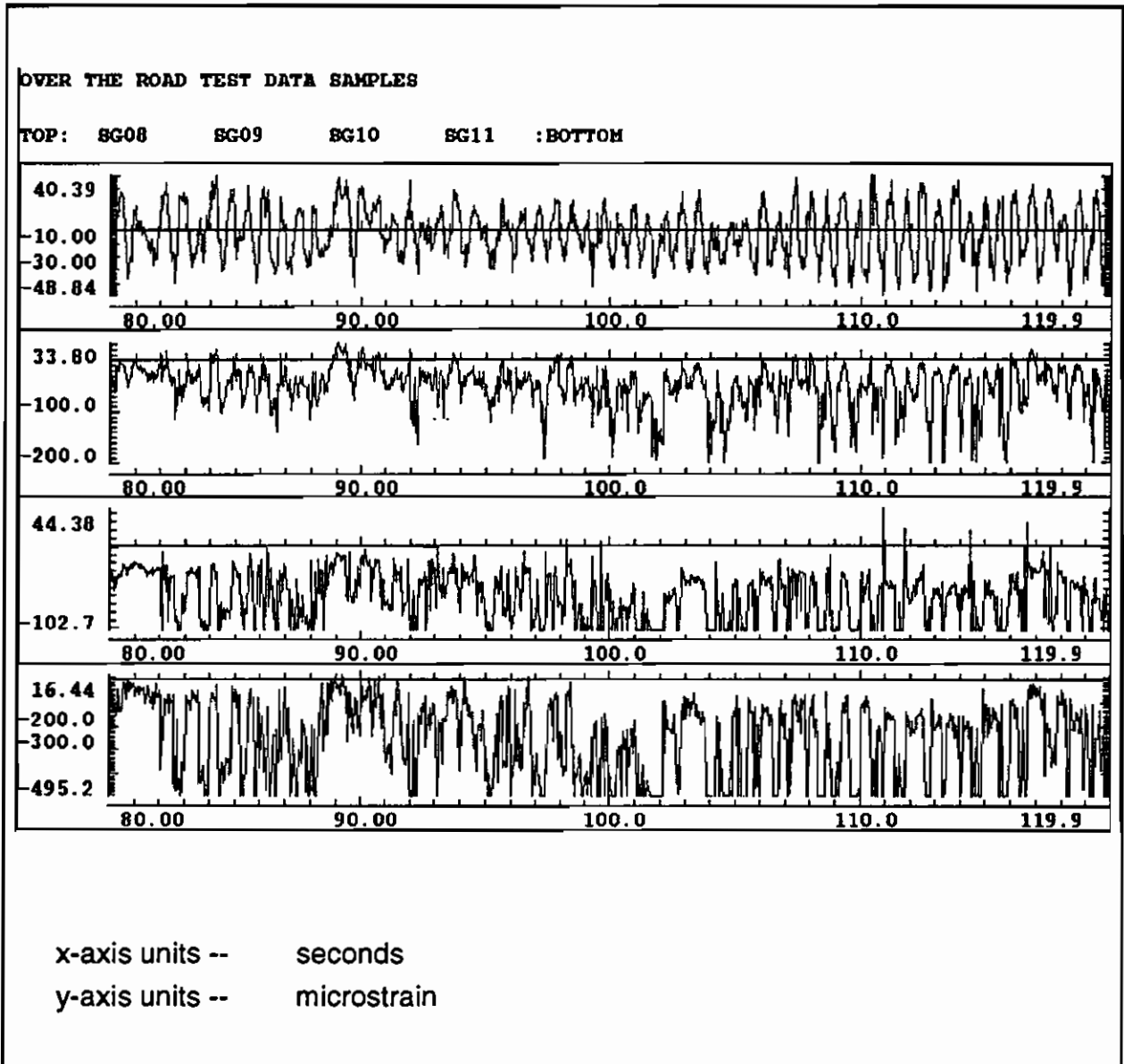
Figure 11. Response Type 2 -- SG08, SG09, SG10, and SG11

4.2.5 Head Brace Retrofit Strain Responses – OTR Test

The tank car tested was modified at the A-end with a head brace retrofit. Strain gages, installed on this end at locations which matched the gage locations at the critical region at the B-end of the tank car, showed that the strain levels experienced at these locations were reduced appreciably with the head brace retrofit.

4.3 OTR TEST CONCLUSIONS

The OTR test resulted in approximately 750 seconds of significant fatigue causing events. The significant responses were defined as Type 1 and Type 2, which corresponded to single events and random repetitive events.

Type 1 responses were caused by train run-ins, while Type 2 responses were the result of a combination of dynamic brake train handling and track input, due to a high frequency of crossings as the consist approached Albuquerque. It was this response that included significant frequent vertical coupler loads.

A comparison of the response measurements in the critical region of the B-end of the car (original stub sill and head pad configuration) to those on the A-end of the car (modified end) showed that, at least for the measurements designed to characterize the original end, the modified end experienced significantly lower strain levels.

5.0 SUPPLEMENTAL TESTS ADDITIONAL MEASUREMENTS

Supplemental tests, added to investigate vertical coupler loading, did not require all of the measurements from the OTR test, but required additional measurements not recorded during the OTR test. Table 13 lists the measurements from the OTR test, which were required specifically for OTR test environmental replication and were inappropriate for the supplemental tests.

33

Table 13. Test Measurements not Recorded - Supplemental Tests

Measurement	Description
LTLV1	LTHD Left Vertical Keeper Plate Accel, B-end
LTRV1	LTHD Right Vertical Keeper Plate Accel, B-end
LTLAT1	LTHD Lateral Keeper Plate Accel, B-end
LLV1	LTHD Left Vertical Bolster Accel, B-end
LRV1	LTHD Right Vertical Bolster Accel, B-end
LLAT1	LTHD Lateral Bolster Accel, B-end
LLV2	LTHD Left Vertical Bolster Accel, A-end
LRV2	LTHD Right Vertical Bolster Accel, A-end
LLAT2	LTHD Lateral Bolster Accel, A-end
LV1	Left Vertical Bolster Accel, B-end
RV1	Right Vertical Bolster Accel, B-end
LAT1	Lateral Bolster Accel, B-end
LV2	Left Vertical Bolster Accel, A-end
RV2	Right Vertical Bolster Accel, A-end
LAT2	Lateral Bolster Accel, A-end
CP1	A-end Coupler Force
AC1	A-end Coupler Longitudinal Accel
AC2	B-end Coupler Longitudinal Accel
SG02	Center of Truck Bolster, B-end , Parallel to Bolster
SP1	Test Car Speed

Table 14 lists additional measurements added for the supplemental tests. Appendix B contains sketches of several of the additional strain-gage locations. TTC's data van, shown in Figure 12, was used to house the instrumentation hardware and computer systems for the supplemental tests. The computer and signal conditioner systems used in the OTR test were transferred from the AAR 112 car to the data van.

Table 14. Additional Test Measurements

Name	Description and Location	Type	Est. Range
SG21	B-End, Draft Sill, Bottom Right S_C	Strain-Gage	±2000 µε
SG22	B-End, Draft Sill, Bottom Left	Strain-Gage	±2000 µε
SG23	B-End, Draft Sill, Side Right S_C	Strain-Gage	±2000 µε
SG24	B-End, Draft Sill, Side Left	Strain-Gage	±2000 µε
SG25	B-End Inside Head Pad Right Corner Vertical Strain S_C	Strain-Gage	±4000 µε
SG26	B-End Inside Head Pad Right Corner Diagonal Strain S_C	Strain-Gage	±4000 µε
SG27	B-End Inside Head Pad Right Corner Lateral Strain	Strain-Gage	±2000 µε
SG28	B-End Head Pad Left Corner Vertical Strain	Strain-Gage	±4000 µε
SG29	B-End Head Pad Left Corner Diagonal Strain	Strain-Gage	±4000 µε
SG30	B-End Head Pad Left Corner Lateral Strain	Strain-Gage	±2000 µε
SG31	B-End Inside Head Pad Left Corner Vertical Strain	Strain-Gage	±4000 µε
SG32	B-End Inside Head Pad Left Corner Diagonal Strain	Strain-Gage	±4000 µε
SG33	B-End Inside Head Pad Left Corner Lateral Strain	Strain-Gage	± µε
SG34	B-end sill top long. Strain, left	Strain-Gage	±2000 µε
SG35	B-end sill bottom long. Strain, left (not recorded for Simuloader tests)	Strain-Gage	±2000 µε
SG36	B-end sill bottom long. Strain, rt. (not recorded for Simuloader tests)	Strain-Gage	±2000 µε
SG37	B-end cradle pad, web/sill corner, longitudinal strain	Strain-Gage	±2000 µε
SG38	B-end cradle pad, web/sill corner, diagonal strain	Strain-Gage	±2000 µε
SG39	B-end cradle pad, web/sill corner, lateral strain	Strain-Gage	±2000 µε
SG40	Tank underside long. Strain, 3-inch from SG11 S_C	Strain-Gage	±1300 µε
SG41	B-end cradle pad, head pad/sill corner, longitudinal strain	Strain-Gage	±2000 µε
SG42	B-end cradle pad, head pad/sill corner, diagonal strain	Strain-Gage	±2000 µε
SG43	B-end cradle pad, head pad/sill corner, lateral strain	Strain-Gage	±2000 µε
SG44	A-end retrofit vertical strain	Strain-Gage	±2000 µε
AZ4	Car body vert. accel, A-end, left corner	P-R Accel	±10 g's

Figure 12. Data Van

6.0 SUPPLEMENTAL IMPACT TESTS

6.1 SUPPLEMENTAL IMPACT TEST PROCEDURES

The supplemental impact tests were conducted to evaluate the effect of yard impacts and coupler height mismatch. The following subsections describe the impact test procedures. The impact tests were conducted on August 30, September 4, and September 5, 1991. Impact tests at the mid-point of the Simuloader tests were not performed.

6.1.1 Impact Tests – Instrumentation and Documentation

The measurements for the impact tests, including the measurements repeated from the OTR test and the additional measurements added for the supplemental tests, were low-pass filtered at 120 Hz, and sampled at 1024 s/s using an HP based data acquisition system. The instrumented couplers were also low-pass filtered at 600 Hz and recorded at 5000 s/s with another HP-based system. Sixteen channels were displayed on a strip-chart recorder.

Photographs of the test car and of all the measurement transducers were taken. Video of the impacts was recorded.

6.1.2 Impact Tests -- Track Facility

The impacts were conducted on the Impact Track. The Impact Track has as slight grade well suited for impact tests and is located near the Facility for Accelerated Service Testing Facility (FAST) at TTC. The Impact Track is highlighted in the TTC map shown in Figure 13.
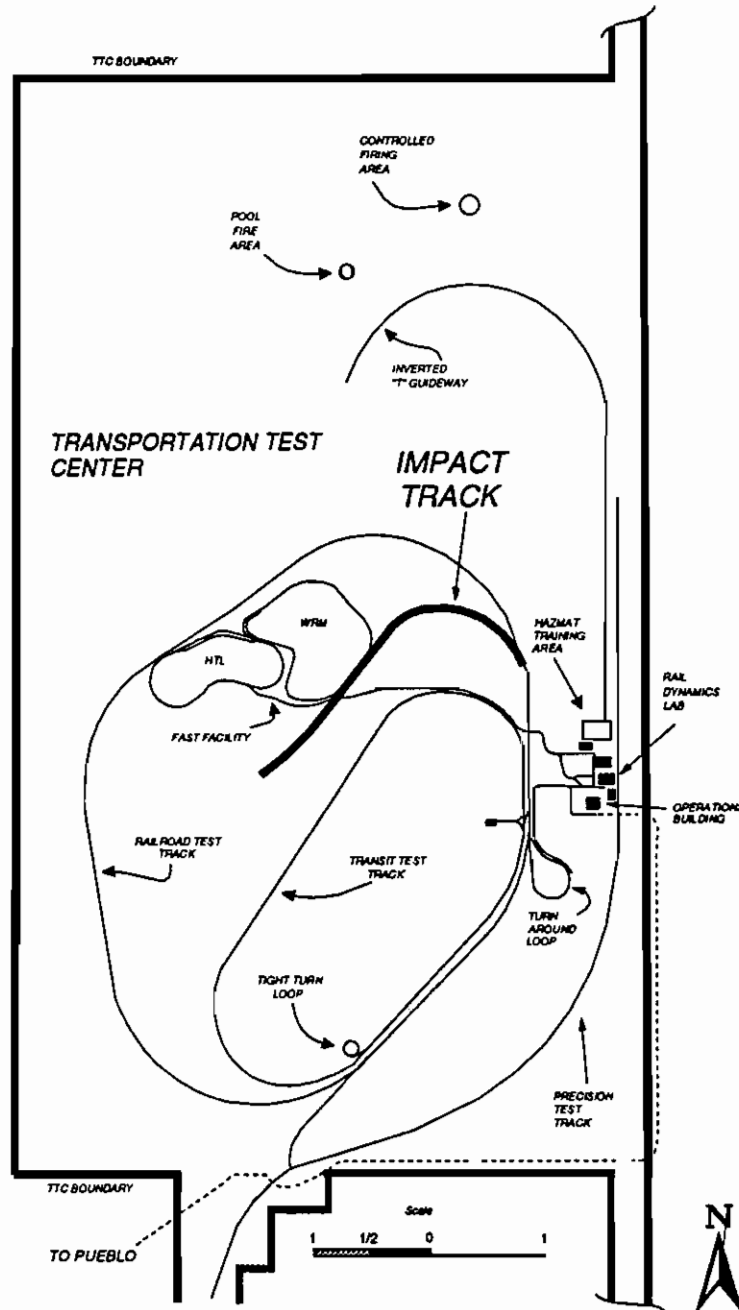
Figure 13. Impact Track

6.1.3 Impact Test

A fully loaded 70-ton capacity hopper car, EL 33716, used as the hammer car was impacted into the tank car. The hammer car weighed 193,750 pounds. The tank car, tested at 12 percent and 2 percent outage loads, was impacted at the B-end. Three loaded cars, with handbrakes set, completed the anvil string. The anvil string was placed several feet behind in order to catch the tank car after impact.

Three tank car coupler height positions (centered, high, and low) were tested, as shown in Figure 14. Figure 15 shows the hopper car being impacted into the tank car and three anvil cars.

COUPLER SHIM - CONCEPT

COUPLER ANGLE

COUPLER CONFIGURATIONS	
CENTER	THIN SHIMS, ONE ABOVE, ONE BELOW COUPLER, 1/4" THICK (EACH)
UP	THICK SHIM, BELOW COUPLER, 1/4" THICK (EACH)
DOWN	THICK SHIM, ABOVE COUPLER, 1/2" THICK
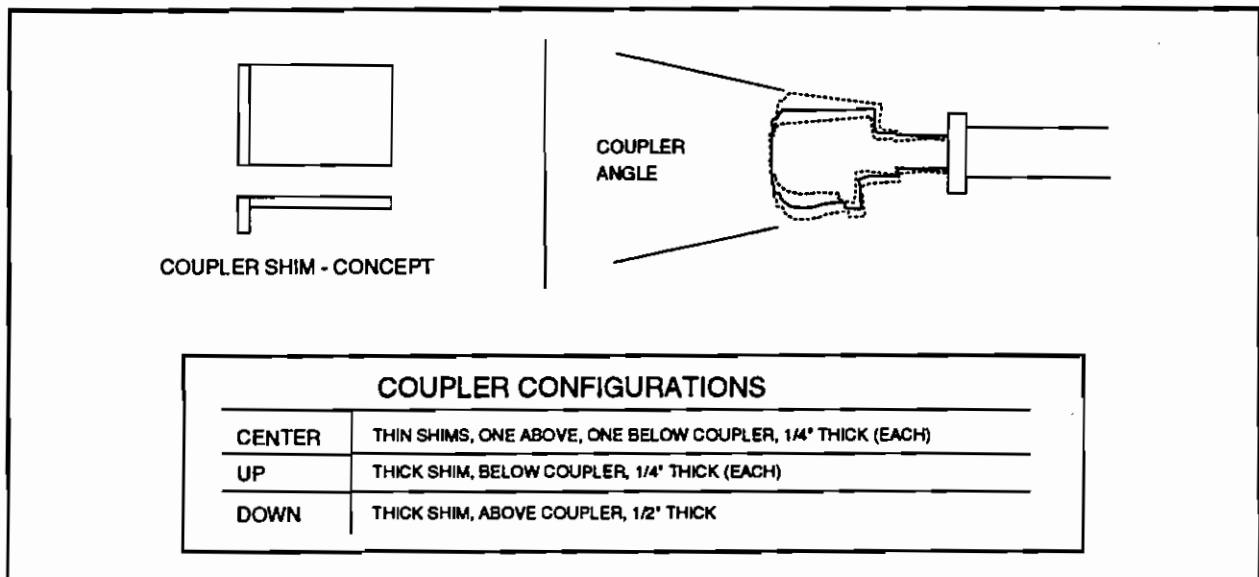
Figure 14. Coupler Height Adjustments (Angle)

TANK CAR IMPACT TESTS

TANK CAR
B-END   A-END

HAMMER CAR
LOADED 70-TON HOPPER

ANVIL CARS - LOADED 70-TON HOPPERS
WITH HANDBRAKES SET
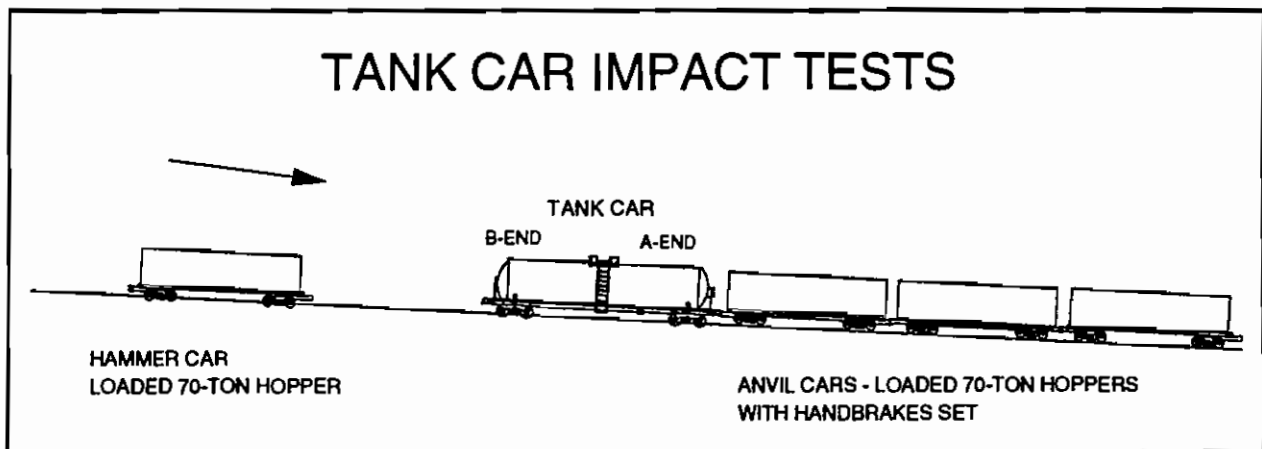
Figure 15. Impact Test

The impact tests were conducted on August 30, September 4, and September 5, 1991. Table 15 is a test matrix for the impact tests.

Table 15. Impact Test Matrix

Run(s)	Speed	Configuration
1-9	1 mph to 9 mph, 1 mph steps, 88 percent load	Centered
10-12	2 mph to 6 mph, 2 mph steps, 88 percent load	Centered
13-14	7 mph, 88 percent load	Down
15	7 mph, 88 percent load	Down
16-18	2 mph to 6 mph, 2 mph steps, 88 percent load	Up
19-20	7 mph, 88 percent load	Up
21-28	1 mph to 8 mph, 1 mph steps, 88 percent load, repeats	Centered
29-30	4 and 6 mph, A-end uncoupled from anvil cars, 88 percent load	n/a
31-33	4, 6, and 7 mph, 98 percent load	Centered
34-36	4, 6, and 7 mph, 98 percent load	Down
37-41	4, 6, 7, 8, and 9 mph, 98 percent load	Up
42-43	8 and 9 mph, 98 percent load	Down

6.1.4 Impact Test Data Analysis

The impact test data were reduced to the form of statistics and time histories to determine the characteristic strains due to the impact loads. The effects of coupler height mismatch were also analyzed.

6.2 SUPPLEMENTAL IMPACT TEST RESULTS

6.2.1 Impact Tests – Statistical Results

The impact tests were conducted to document the characteristic stresses due to impact loads, and the effect of coupler height mismatch. This is particularly of interest in the critical region of the B-end of the car. Thus, B-end strain gage rosettes SG08 - SG10 (rosette 1), SG25-SG27 (rosette 2), SG28-SG30 (rosette 3), and SG31-SG33 (rosette 4), located as shown in Figures 16, 17, and 18, are the most often analyzed measurements. It was found that the symmetrically located rosettes on each side gave similar results. Therefore, in this section results from strain gage rosettes 1 and 2 are presented along with longitudinal coupler force and mid-span longitudinal strain (SG11).
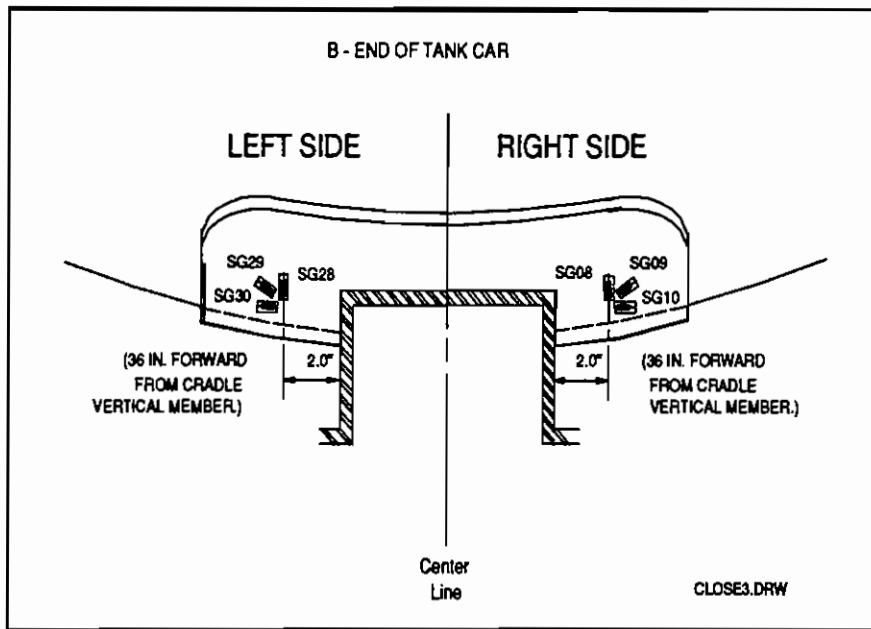
Figure 16. Critical Region Strain Measurements -- View 1
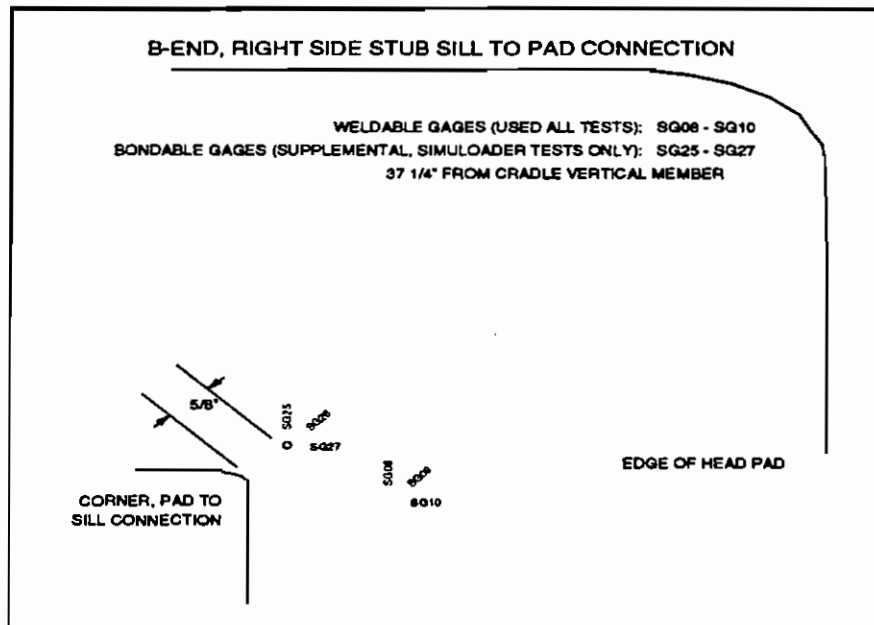
Figure 17. Critical Region Strain Measurements -- View 2

Figure 18. Critical Region Strain Measurements -- View 3
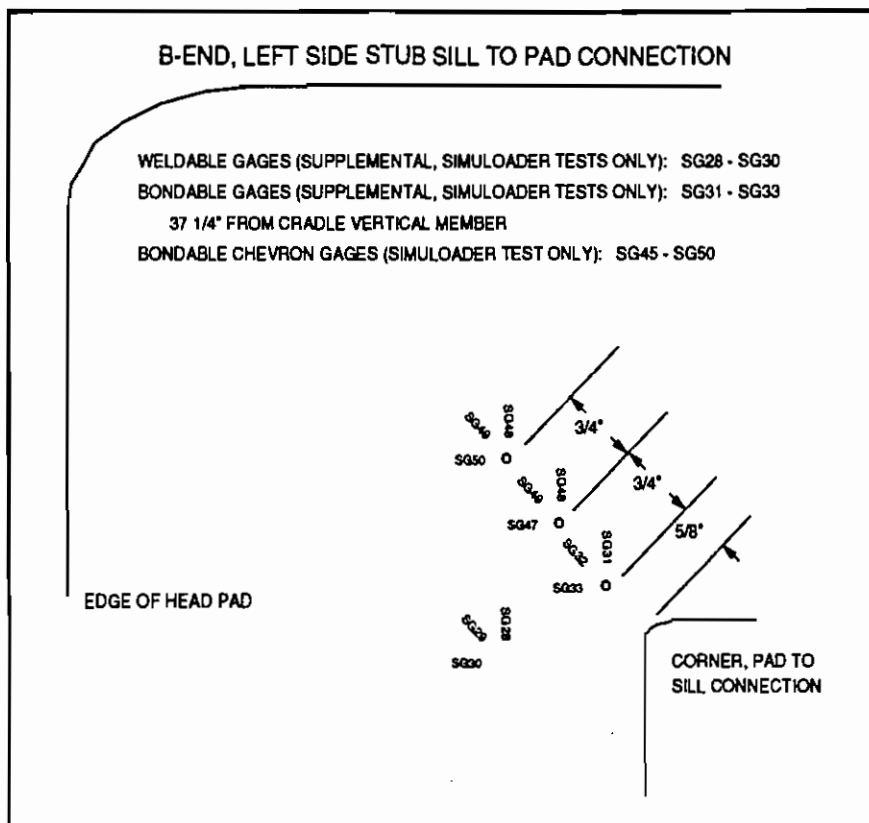
Figures 19 through 28 are graphs showing the statistical results for the 12 percent outage impact tests. Impacts on the tank car filled to a 2 percent outage configuration gave similar results. Figure 19 displays the maximum longitudinal coupler force measured for each impact. This figure shows only a slight variation in the force measurement for the coupler centered, up, and down test configurations. Figure 20 displays the maximum compression strain for the mid-span longitudinally oriented strain gage, SG11. Again, only slight variation was found for the three coupler positions.

TO43 IMPACTS
88%, B-End Impacted
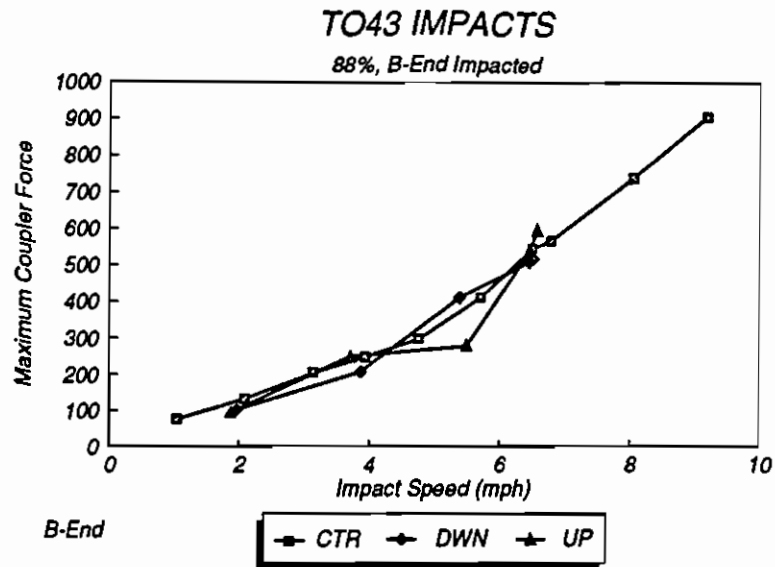
Figure 19. Longitudinal Coupler Force Measurement -- Impact Tests

TO43 IMPACTS
88%, B-End Impacted
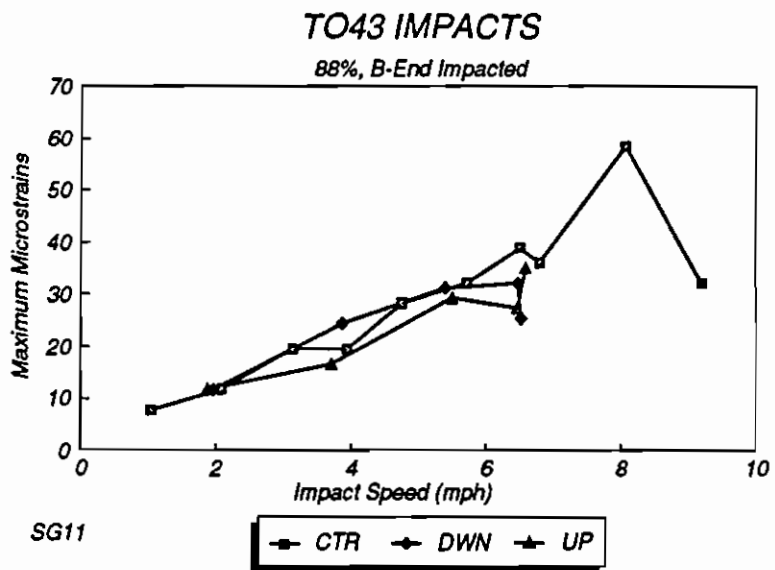
Figure 20. SG11 Strain Gage Response -- Impact Tests

Figures 21 through 27 display the maximum tensile strains for the stub sill longitudinally oriented strain gage SG01, critical-region gages SG08-SG10 (rosette 1), and SG25-SG27 (rosette 2). With the exception of SG09 which shows little variation, each gage exhibits a pronounced increase in strain for the coupler "up" test configuration. The close correlation of SG01 with the critical-region gages points to downward bending (vertical coupler loading) of the sill as the cause -- thus, coupler up position on the tank car induced

42

an angle in the coupler which resulted in the loading of the rear draft lugs with a downward force component. The maximum compressive strains for the strain gages, an example of which is shown in Figure 28 (SG08), were less in magnitude and showed little correlation to coupler position on impact.
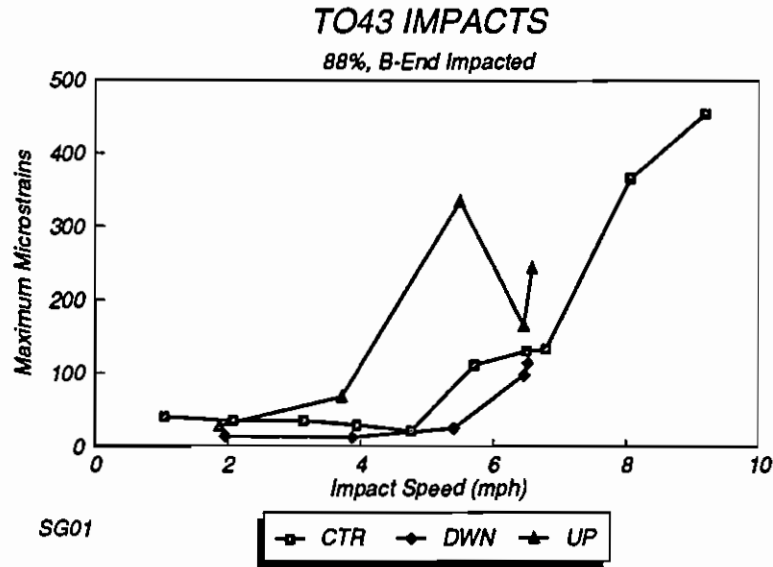
Figure 21. SG01 Tensile Strain Response -- Impact Tests
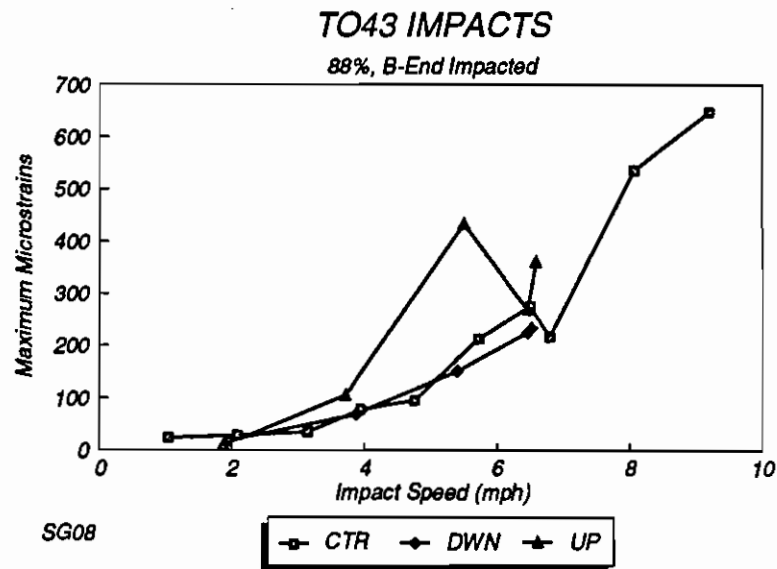
Figure 22. SG08 Tensile Strain Response -- Impact Tests
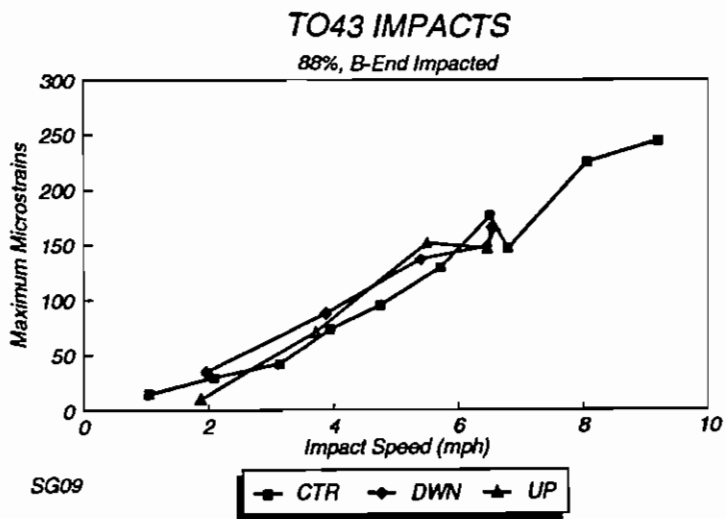
Figure 23. SG09 Tensile Strain Response -- Impact Tests
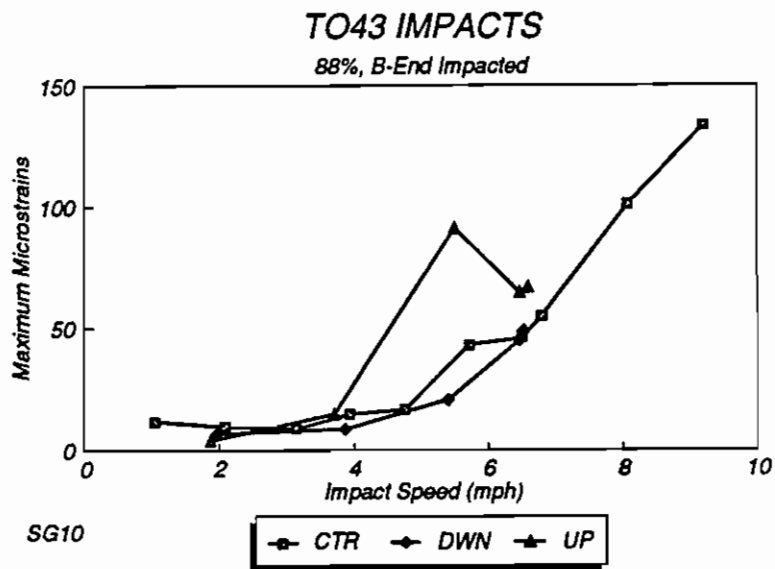
Figure 24. SG10 Tensile Strain Response -- Impact Tests

44

TO43 IMPACTS
88%, B-End Impacted

SG25

CTR *DWN* *UP*
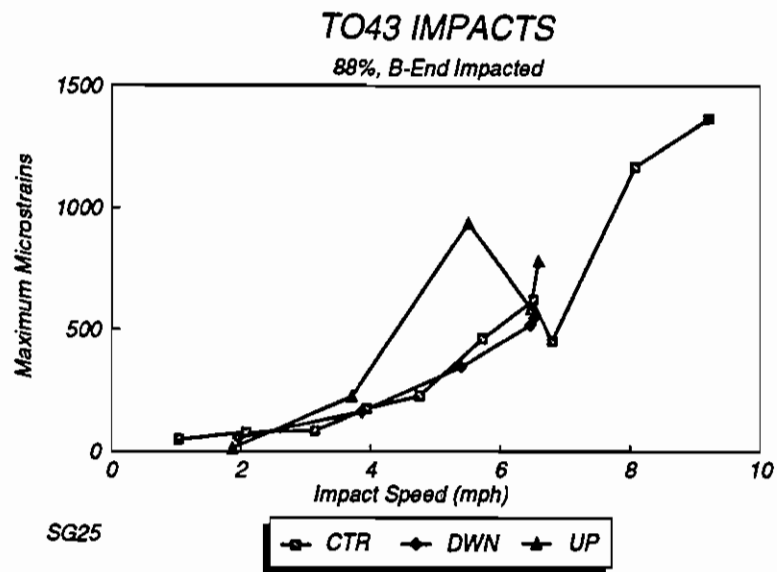
Figure 25. SG25 Tensile Strain Response -- Impact Tests

TO43 IMPACTS
88%, B-End Impacted

SG26

CTR *DWN* *UP*
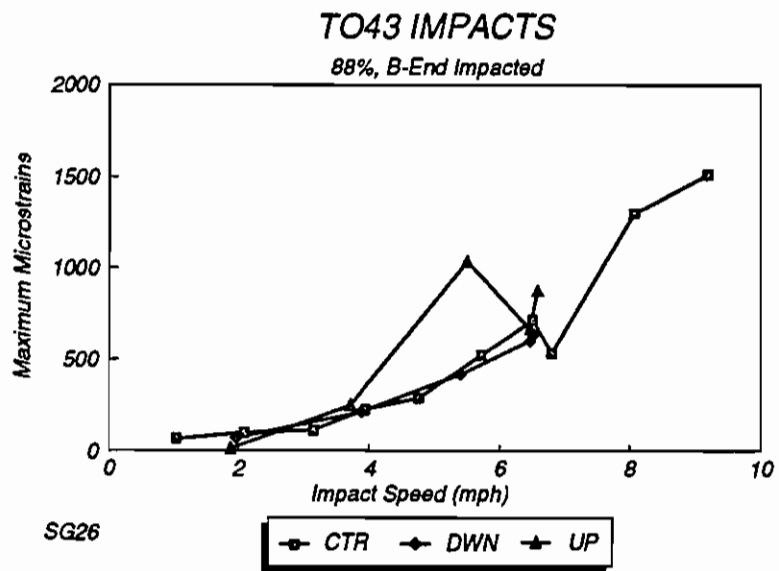
Figure 26. SG26 Tensile Strain Response -- Impact Tests
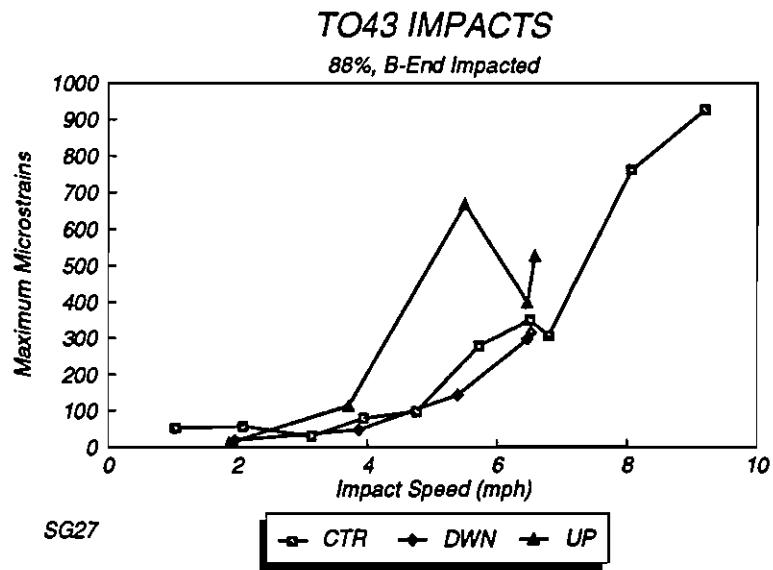
Figure 27. SG27 Tensile Strain Response -- Impact Tests
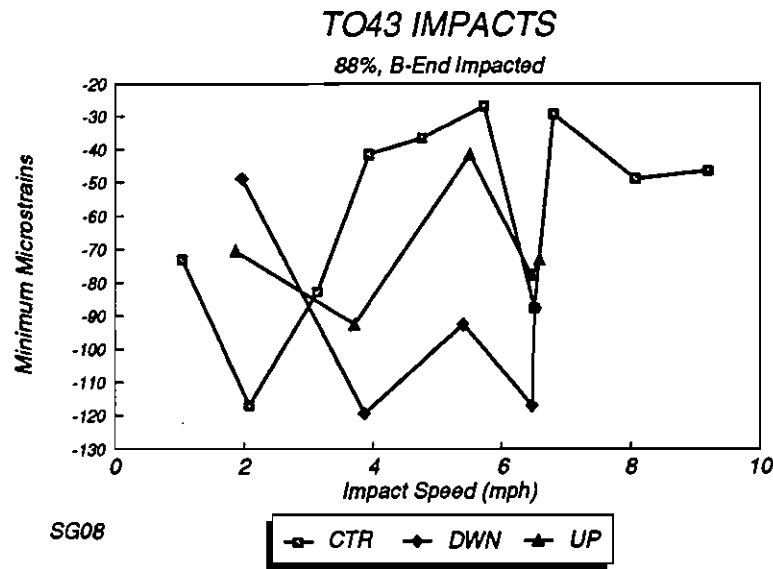
Figure 28. SG08 Compressive Strain Response -- Impact Tests

Table 16 summarizes the results for the various 12 percent outage impact test configurations for impact speeds at approximately 6.5 mph. The maximum stress was calculated with the following equation.

$$\sigma_{max} = \frac{E(\varepsilon_1 + \varepsilon_3)}{2(1-\mu)} + \frac{E}{\sqrt{2}(1+\mu)}[(\varepsilon_1 - \varepsilon_2)^2 + (\varepsilon_2 - \varepsilon_3)^2]^{1/2}$$

where: E = Young's modulus

            μ = Poisson's ratio

Table 16. Impact Test Result Summary, Tests at Approx. 6.5 mph

Configuration, Run	Speed (mph)	Coupler Force (kips)	Max. Stress Computed from Rosette 2 — Max (ksi)
12% Outage, Coupler Centered, Average of Runs 7, 15, and 27	6.67	520	20.8
12% Outage, Coupler Up, Average of Runs 19 and 20	6.55	565	29.7
12% Outage, Coupler Down, Average of Runs 13 and 14	6.5	515	23.3

It was clear from the data that the coupler-up configuration, underlined in the table, results in the largest stresses in the critical region.

6.2.2 Impact Tests -- Time Histories

Figures 29-32 contain selected time histories of the impact test which support the conclusions of the graphic and tabulated data in the previous section. Coupler longitudinal forces and strain gage results (SG25, SG26, and SG27) of impact runs 15, 20, and 14 are shown.

47

Figure 29. 6.5 mph Impact Test Time Histories -- LCF
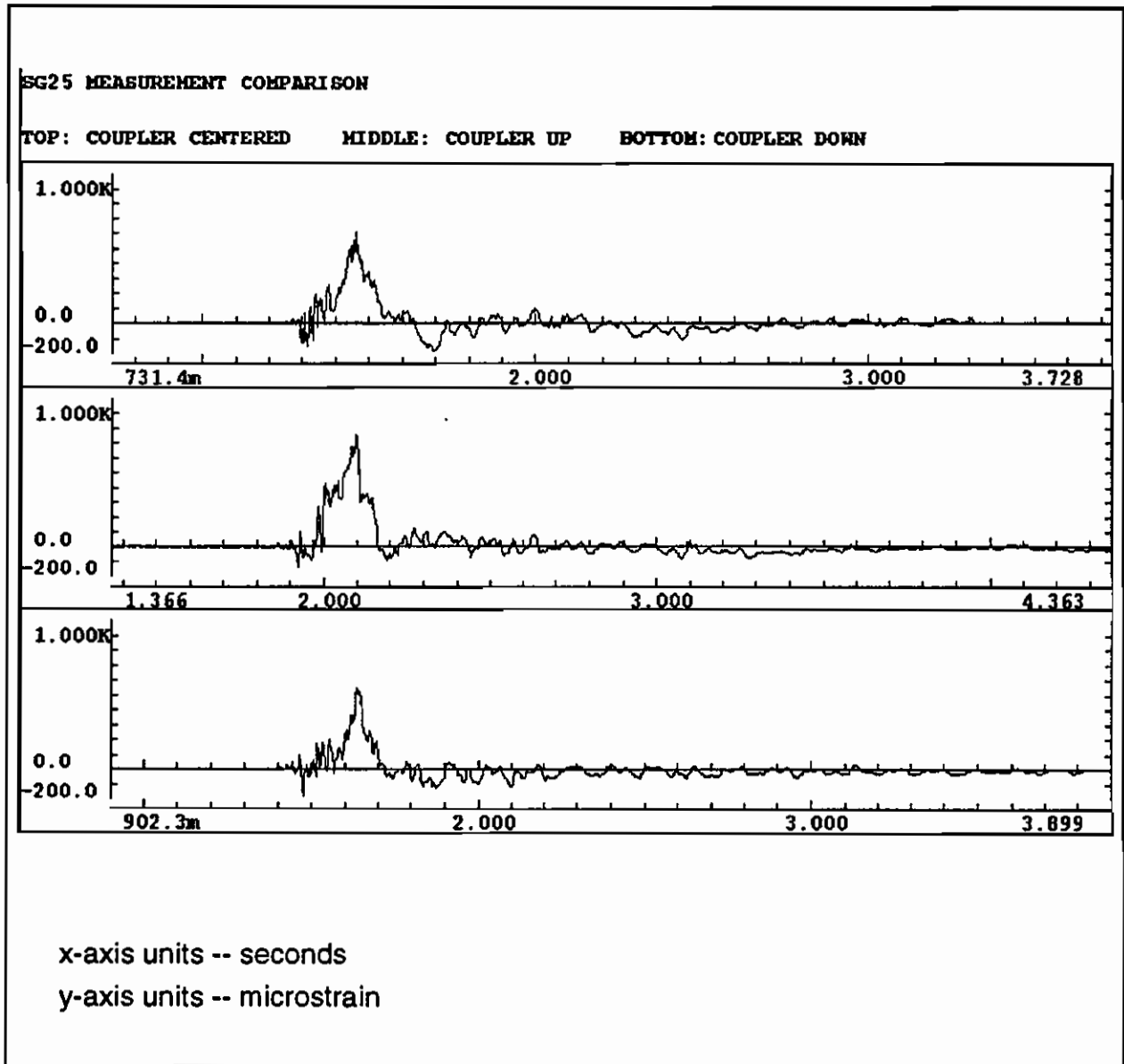
Figure 30. 6.5 mph Impact Test Time Histories -- SG25

49

SG26 MEASUREMENT COMPARISON

TOP: COUPLER CENTERED   MIDDLE: COUPLER UP   BOTTOM: COUPLER DOWN

x-axis units -- seconds

y-axis units -- microstrain
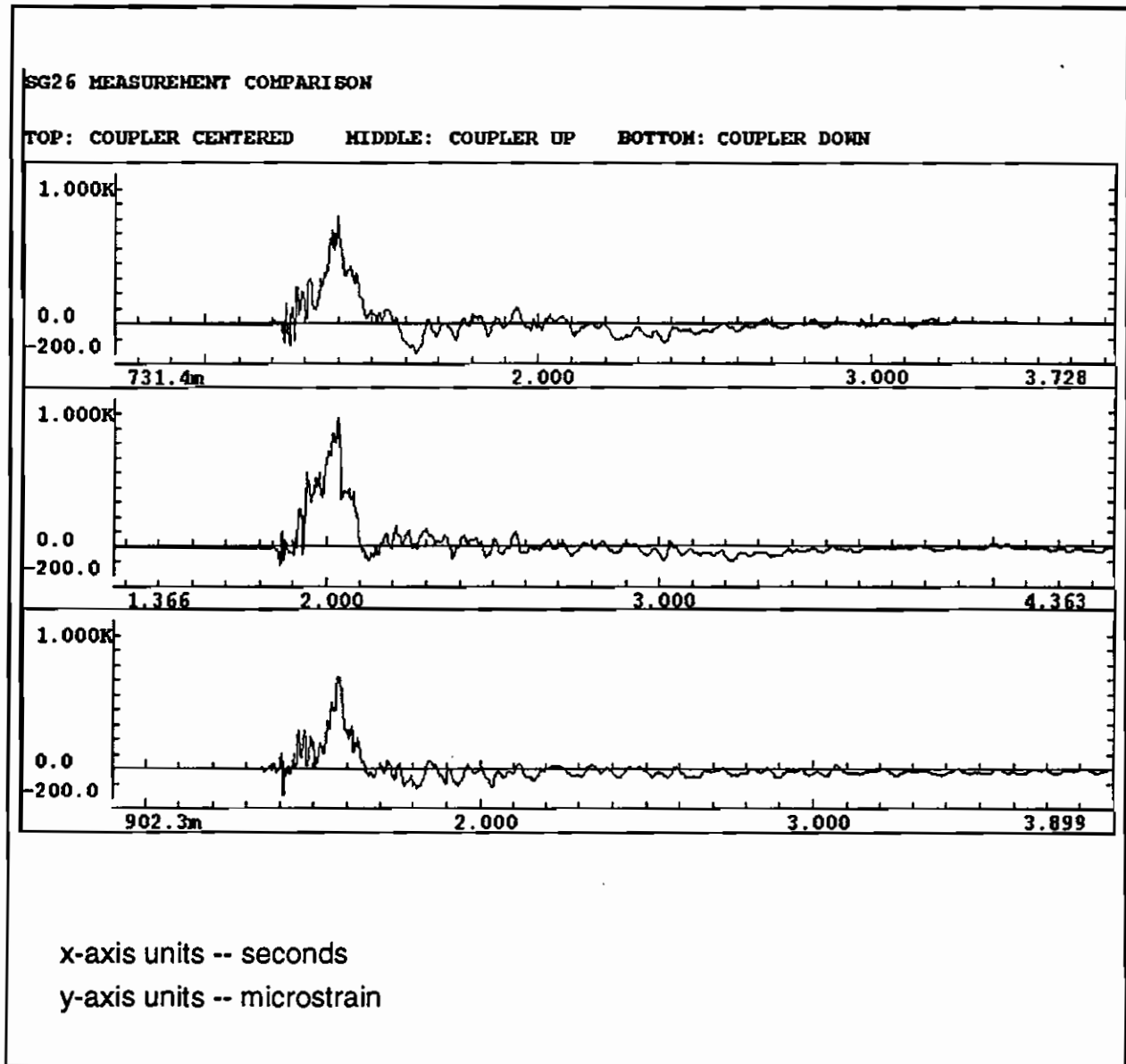
Figure 31. 6.5 mph Impact Test Time Histories -- SG26
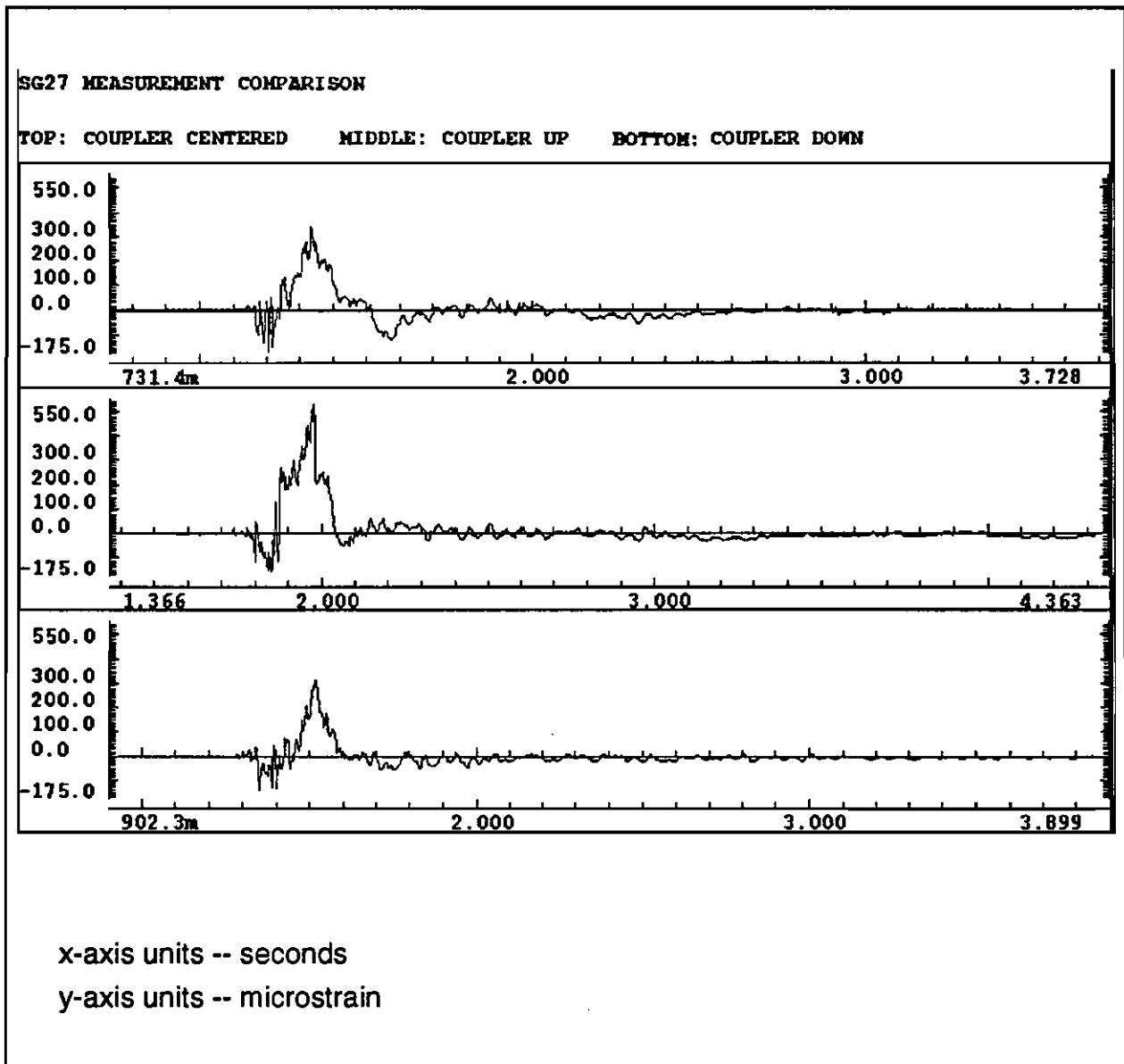
Figure 32. 6.5 mph Impact Test Time Histories -- SG27

6.2.3 Impact Tests -- Hypothesis

The tabulated data and time histories both showed that the coupler shimmed up test configuration resulted in the largest tensile strains in the critical-region strain gages. A hypothesis that may explain this and the vertical coupler load phenomenon, developed by Moyar,[8] is presented in Section 12.1 in support of development of the vertical coupler force Simuloader input profiles.

6.3 SUPPLEMENTAL IMPACT TEST CONCLUSIONS

The graphic displays of statistical results, statistical tabulations, and time histories all point to the coupler up test configuration as causing the largest stresses in the critical region when impacted.

7.0 SUPPLEMENTAL PERTURBED TRACK TESTS

7.1 SUPPLEMENTAL PERTURBED TRACK TEST PROCEDURES

The perturbed track tests were conducted to investigate the effect of pitch and bounce and twist and roll perturbed track zones combined with controlled buff and draft loads. It was hoped that responses similar to those obtained during the OTR test would be obtained. The following subsections describe the supplemental perturbed track test procedures.

7.1.1 Perturbed Track Test Instrumentation

All of the measurements recorded for the supplemental impact tests were recorded during the perturbed track tests. The data van was mounted on a flatcar. The HP 330 computer was used to sample the data at 256 s/s. The measurements were low-pass filtered at 30 Hz. Sixteen channels were displayed on a strip-chart recorder.

Photographs of the test car and consist were taken.

7.1.2 Perturbed Track Tests -- Track Facility

The perturbed track tests were conducted on the pitch and bounce and twist and roll test zones of the PTT depicted in Figure 33.

PITCH AND BOUNCE	TWIST AND ROLL
PARALLEL JOINTED RAIL	STAGGERED JOINTED RAIL
3/4 IN.	3/4 IN.
39 FT.	39 FT.
400 FT. TANGENT	400 FT. TANGENT
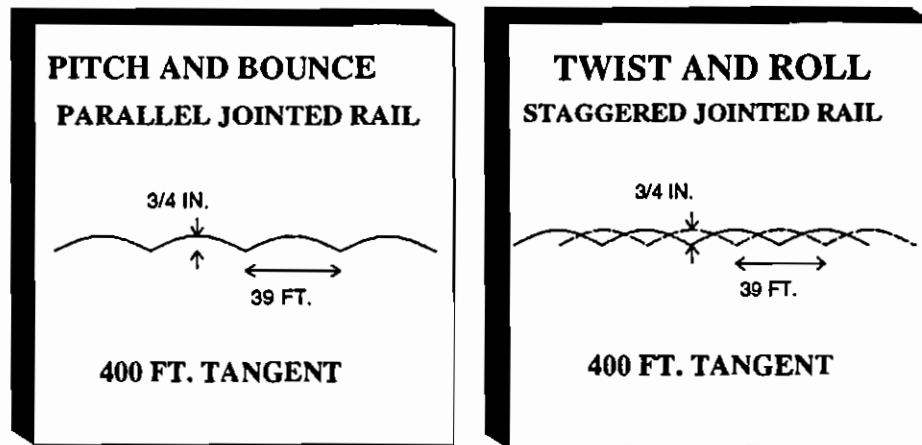
Figure 33. Perturbed Track Test Zones

7.1.3 Perturbed Track Test

The perturbed track tests were performed with two braking configurations. The first configuration, the buff (compression) configuration, was conducted with the consist braked as shown in Figure 34. The locomotive engineer accelerated the consist to test speed. As the locomotive entered the test zone, the engineer applied dynamic brakes. This created a "run-in" of the 10 trailing buffer cars, while the test car was operated over normal track, and while excited by the twist and roll and pitch and bounce perturbed-track zones.
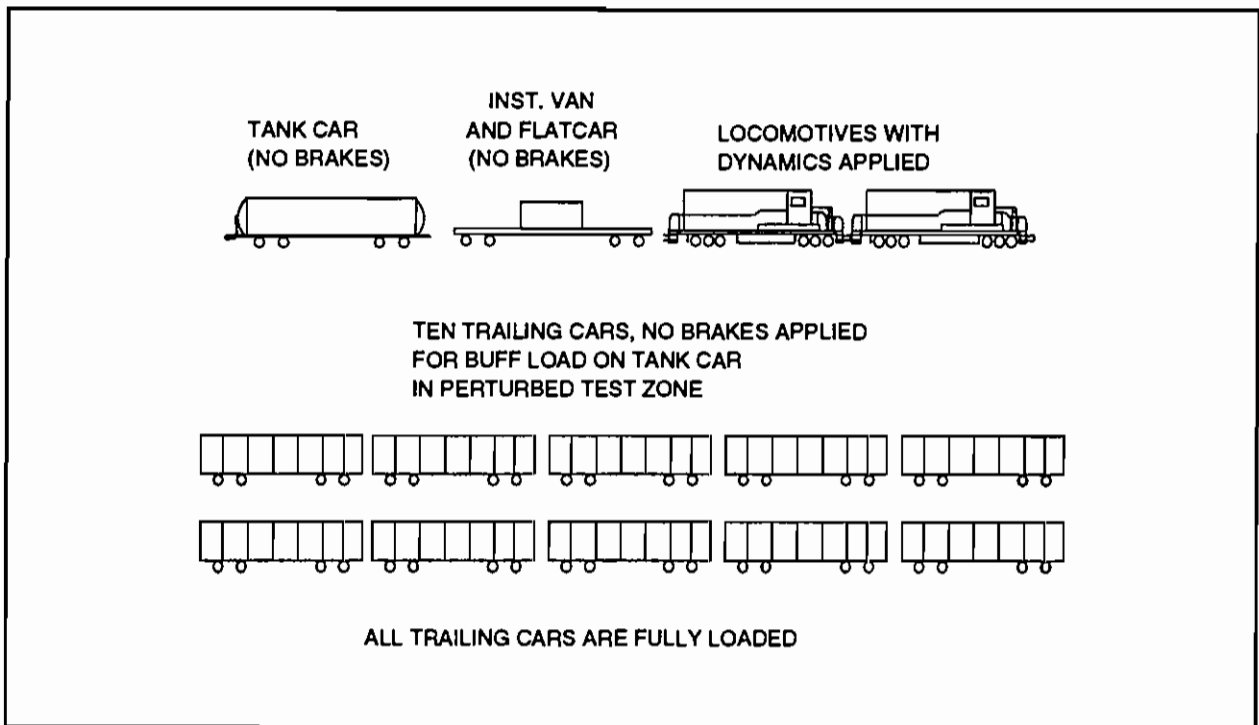
Figure 34. Buff Test Consist

The second configuration, the draft (tension) configuration, was performed with the consist braked as shown in Figure 35. The locomotive engineer accelerated the train to test speed. As the locomotive entered the test zone, the engineer applied the air brakes of the trailing 10 buffer cars. This created draft forces in the tank car, while it was operated over normal and perturbed track.
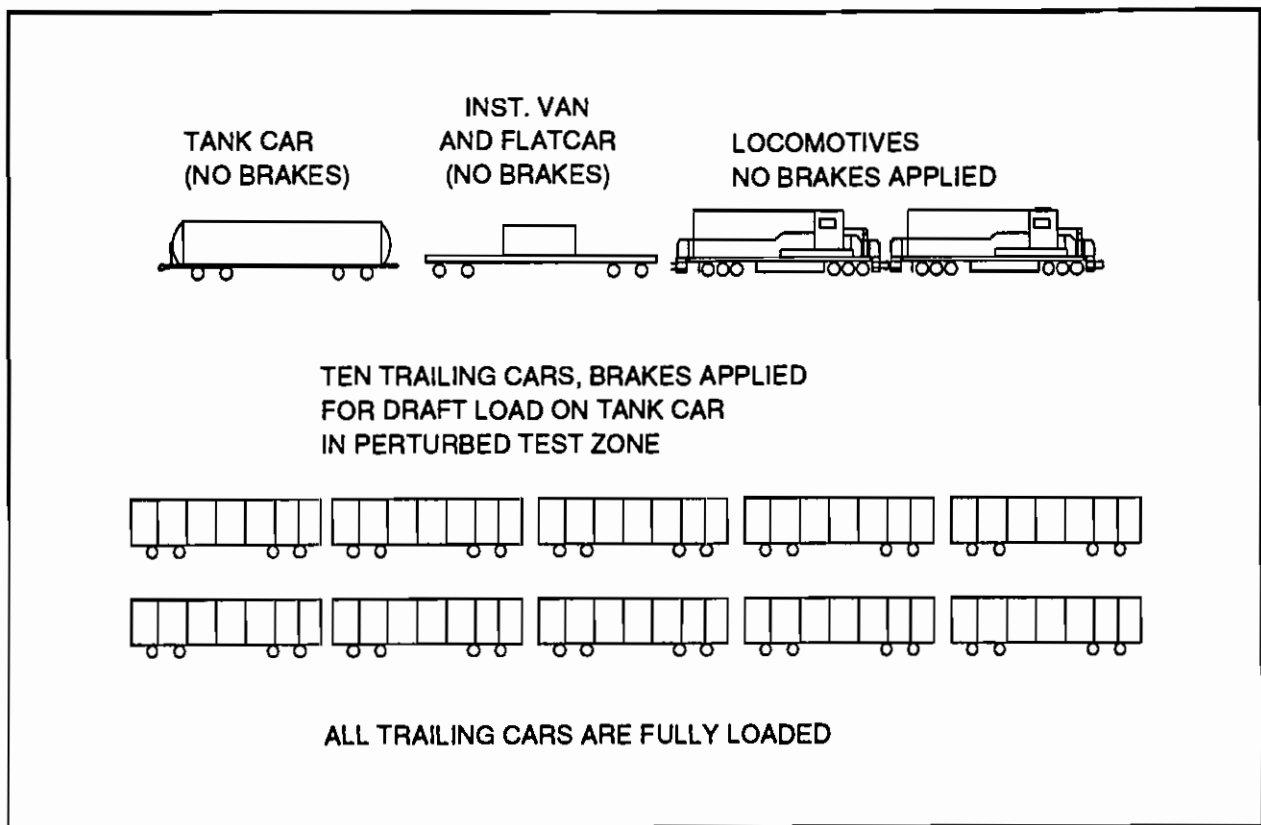
Figure 35. Draft Test Consist

Buff configuration and draft configuration test runs over perturbed track were conducted as shown in Table 17.

Table 17. Perturbed Track Test Runs

Test Zone	Test Speeds
Pitch and Bounce	20, 25, 30, 35, 40 and 50 mph
Twist and roll	12, 14, 16, 18, and 20 mph
Nominal Track	15, 25, 30, and 50 mph

7.1.4 Perturbed Track Test Data Analysis

The data were reduced to the form of statistics and time histories to determine the characteristic strains due to the combinations of buff and draft with the excitation due to the perturbations.

7.2 SUPPLEMENTAL PERTURBED TRACK TEST RESULTS

The perturbed track test responses were found not to be similar to those obtained during the OTR test; thus, the goal was not obtained. However, the test results were useful for sensitivity information required for preliminary (pre-Simuloader test) fatigue analysis. The following subsections describe the supplemental perturbed track test results.

7.2.1 Perturbed Track Test Results

It was found during analysis of the perturbed track test data that the buff and draft simulation configurations were extremely difficult to obtain successfully. Thus, only results from selected runs with meaningful responses are given.

Strain measurements SG08, SG09, and SG10, recorded during the OTR test, showed that the perturbed track tests never excited the complex modes of vibration experienced during the OTR test. Therefore, data from these gages showed low levels of response during the perturbed track tests. Thus, data are shown for critical-region strain gages SG25, SG26, and SG27 (rosette 2), and SG31, SG32, and SG33 (rosette 4), which were added for the supplemental tests. These gages, as shown previously in Figures 16 through 18, are closer to the weld corner of the head pad to sill connection. Thus, the gages in rosettes 2 and 4 are more sensitive than gages SG08 through SG10.

Table 18 is a tabulation of significant buff and draft test results for strain gages SG25, SG26, SG27, SG31, SG32, and SG33.

Table 18.   Perturbed Track Test Results

Run	Speed (mph)	LCF (kips)	Maximum Strain (με)			Maximum Strain (με)			Buff or Draft T+R or P+B
			SG27	SG26	SG25	SG33	SG32	SG31	
55D	18-20	+95	-249	-279	-100	-219	-265	-99	Draft T+R
62B	30-40	-66	200	209	155	159	199	114	Buff P+B
63	50	+79	-197	-216	-74	-180	-223	-68	Draft P+B

7.2.1.1 Longitudinal Coupler Force Sensitivity Information

From the average strain values of all of the perturbed track tests, principal stresses due to longitudinal coupler loads were extrapolated to be:

$$100 \text{ kips draft} = -10.4 \text{ ksi}$$
$$100 \text{ kips buff } = +12.0 \text{ ksi}$$

7.3 SUPPLEMENTAL PERTURBED TRACK TEST CONCLUSIONS

Producing significant buff and draft loads while traversing twist and roll and pitch and bounce perturbed track was not easily achieved. In addition, when this was accomplished, the second goal of reproducing the severe and complex modes of vibration experienced during the OTR test was not achieved.

However, useful values of principal stress due to longitudinal coupler loads were obtained. These values were useful for fatigue life estimation before more reliable data were available from quasi-static Simuloader calibration tests. It should be noted that these calibration values are somewhat higher than the Simuloader squeeze data (described later), which may indicate that the combined buff/draft loads and perturbed track input did increase the stress in the critical region.

8.0 SUPPLEMENTAL VERTICAL COUPLER LOADING MSU TESTS

8.1 SUPPLEMENTAL VERTICAL COUPLER LOADING TEST PROCEDURES

The quasi-static MSU vertical coupler loading test, performed October 3, 1991, was conducted to characterize the effect of vertical coupler loads on the stub sill longitudinal strain gage (SG01) and head pad to stub sill intersection and to determine the loads for the cyclic MSU test.

The purpose of the cyclic MSU vertical coupler loading test, performed October 7-10, 1991, was to load the stub sill-to-tank connection repeatedly to allow comparative fatigue analysis to be conducted and to instigate crack initiation.

The B-end of the tank car, the end with the unmodified stub sill to tank connection, was tested with the MSU. The following subsections describe the supplemental vertical coupler loading test procedures.

8.1.1 Vertical Coupler Loading Tests – MSU Facility

The B-end of the tank car was tested with the MSU. The MSU is a hydraulic shaker system, which consists of two actuators and a controller. This system subjects railcars to vertical and lateral quasi-static and dynamic loads. TTC fabricated a loading fixture that allowed the loads from the MSU to be input into the coupler. Figure 36 shows the MSU, loading fixture, and test car.
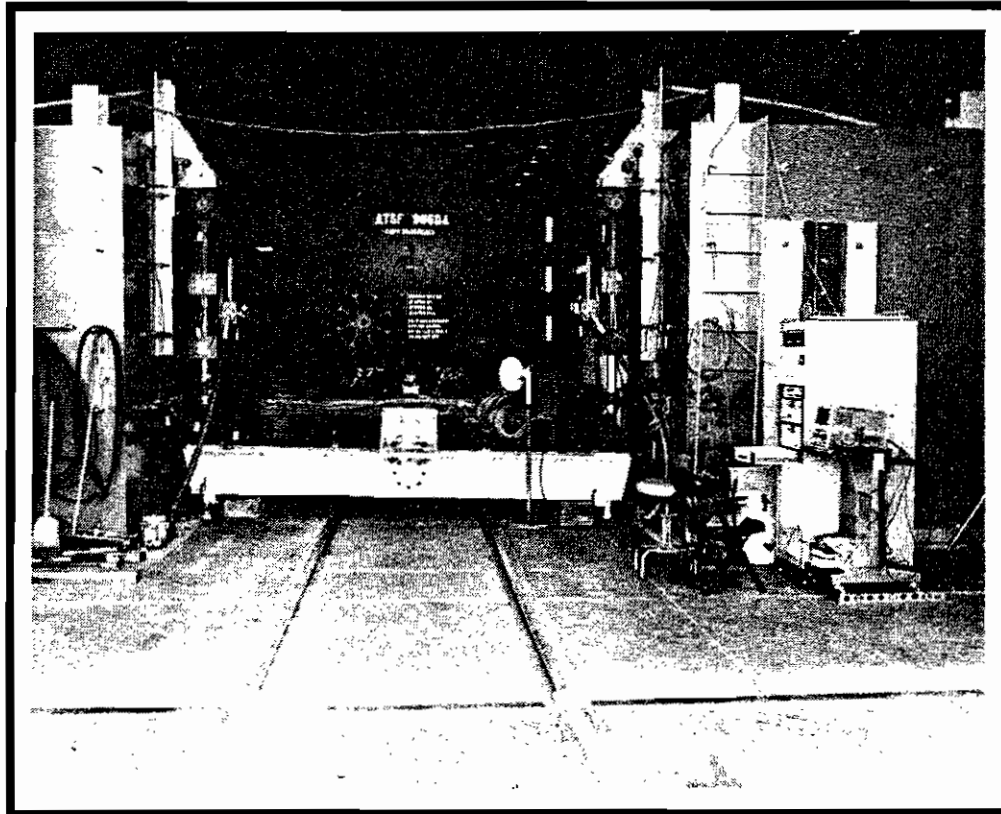
Figure 36. MSU, Coupler to MSU Loading Fixture, and Test Car

8.1.2 Vertical Coupler Loading Tests – Instrumentation Preparations

The measurements recorded for the perturbed track tests were also recorded during the MSU tests. Two actuator displacements and two actuator load cell signals were also recorded. The data van used for the perturbed track tests was also used for collecting the MSU test measurements. The test data were sampled at 256 s/s and low-pass filtered at 30 Hz.

8.1.3 Vertical Coupler Loading Tests -- Quasi-static MSU Test

The MSU Quasi-static Test was done before the cyclic testing. This test required all measurements to be recorded while applying the loads vertically in phase at 5 kip steps. Analysis of the quasi-static test data was performed in order to determine the loads for the cyclic test and to determine vertical coupler load versus stress sensitivities for fatigue analysis. Table 19 lists, in sequence, the static MSU vertical coupler loads applied to the B-end of the stub sill tank car. Test data was recorded in 5-second bursts at each static load.

Table 19. Quasi-static MSU Tests

Quasi-Static MSU Test Description
Zero values -- coupler positioned as to not load the sill vertically nor laterally
10 kips vertically downward (evenly distributed through each actuator)
20, 30, 40, and 50 kips applied vertically downward (evenly distributed through each actuator)
Zero values -- coupler positioned as to not load the sill vertically nor laterally
20, 30, 40, and 50 kips applied vertically upward (evenly distributed through each actuator)

8.1.3.1 Vertical Coupler Loading Tests -- Quasi-Static MSU Test Data Analysis

Statistics from the MSU quasi-static test were used to determine the sensitivity of the critical region to vertical coupler load and to select the vertical coupler force operating range for the cyclic vertical coupler force MSU test.

8.1.4 Vertical Coupler Loading Tests -- Cyclic MSU Test

Based on the MSU Quasi-static test results, an operating range of 10 kips downward to 30 kips downward was selected for the cyclic MSU test. The cyclic MSU tests were conducted for 260,500 cycles with this load range, as shown in Table 20.

Table 20. Cyclic MSU Tests

Date	Cyclic MSU Test Description
10/7/91	5 Hz, 10 kip downward force to 30 kip downward force load range -- 34,000 cumulative cycles
10/8/91	5 Hz, 10 kip downward force to 30 kip downward force load range -- 73,500 cycles for day, 107,500 cumulative cycles
10/9/91	5 Hz, 10 kip downward force to 30 kip downward force load range -- 83,100 cycles for day, 190,600 cumulative cycles
10/10/91	5 Hz, 10 kip downward force to 30 kip downward force load range -- 69,900 cycles for day, 260,500 cumulative cycles

While conducting the cyclic MSU vertical coupler load test, it was critical to carefully monitor for crack initiation and growth. Strain gages and dye penetrant examination materials were used for this task. Strain gages, specifically gages SG08, SG28, rosette SG25-27, and rosette SG31-33, were monitored with a strip-chart recorder. The cyclic output from these gages was closely monitored for deviations, which could indicate cracking. At regular intervals, dye penetrant examinations of the critical region were also done.

8.1.4.1 Vertical Coupler Loading Tests -- Cyclic MSU Test Data Analysis

Stress ranges were computed from statistics recorded during the cyclic MSU test. These data were useful in monitoring the repeatability of the input loads, thus improving the consistency of the operation. Fatigue analysis was also done to predict when cracks might appear.

8.2 SUPPLEMENTAL VERTICAL COUPLER LOADING TEST RESULTS

8.2.1 Quasi-Static Vertical Coupler Loading Tests

8.2.1.1 Quasi-Static Vertical Coupler Loading Tests -- SG01 Calibration

The most important result of the quasi-static MSU test was the calibration of SG01 to vertical coupler load. Figure 37 displays the calibration data. A linear regression was also performed. The results of this analysis, used to develop the vertical coupler force input profile for the Simuloader, are described in Section 12.1.2.

Similar analysis was done on gages SG21, SG22, SG23, and SG24. These gages showed similar characteristics as the SG01 calibration.

SG01 CALIBRATION FOR VERTICAL COUPLER LOADS

Calibration Data	
Load (kips)	microStrain
-50	818
-40	663
-30	502
-20	353
-10	199
10	-115
20	-250
30	-400
40	-559
50	-709
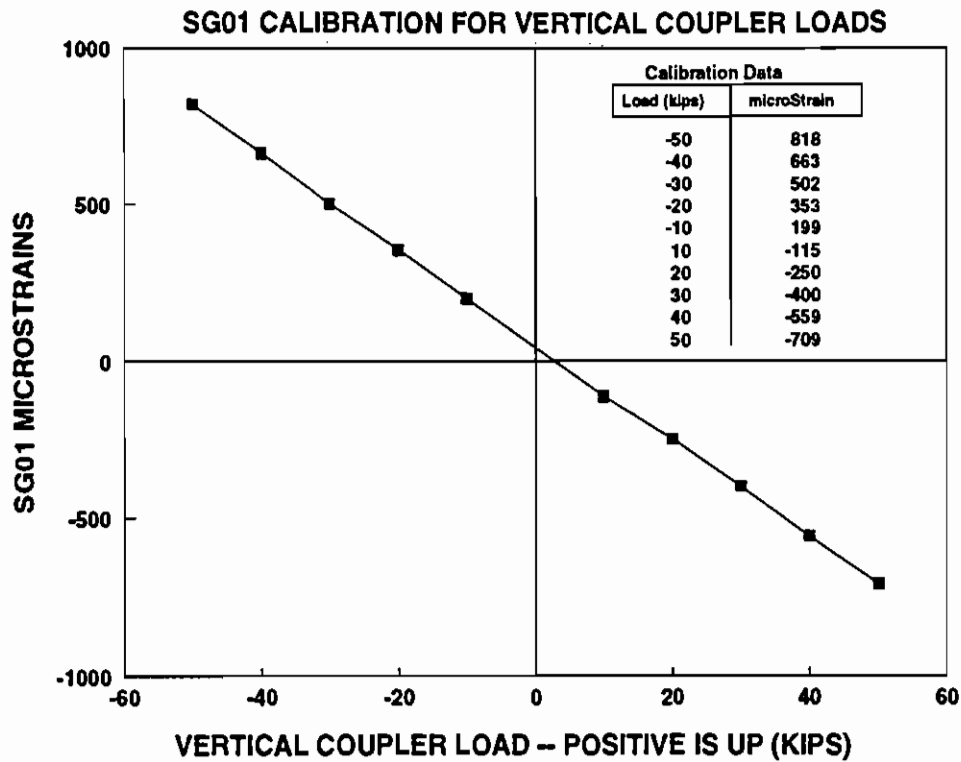
Figure 37. SG01 Calibration to Vertical Coupler Load

8.2.1.2 Quasi-Static Vertical Coupler Loading Tests -- Statistical Results

Results from the static MSU test were also used to determine the head-pad strains corresponding to vertical coupler loads. Fatigue analysis, using these data and a model of a weld detail similar to the sill to pad connection, was done to determine the force input and number of load cycles for the cyclic MSU test. Table 21 is a tabulation of quasi-static MSU test maximum stress results for selected key strain gage rosettes.

Table 21.   Static MSU Test Results – Key Rosette Maximum Stress

Load (kips)	Rosette 1[1] Maximum Stress	Rosette 2[2] Maximum Stress	Rosette 3[3] Maximum Stress	Rosette 4[4] Maximum Stress	Load Dir
-10	5.64 ksi	11.6 ksi	4.01 ksi	13.2 ksi	Down
-20	11.1 ksi	22.5 ksi	7.32 ksi	21.7 ksi	Down
-30	16.6 ksi	34.8 ksi	10.8 ksi	30.2 ksi	Down
-40	22.9 ksi	47.2 ksi	14.0 ksi	43.0 ksi	Down
10	-3.58 ksi	-5.63 ksi	-3.94 ksi	-6.17 ksi	Up
20	-7.66 ksi	-12.7 ksi	-13.0 ksi	-13.2 ksi	Up
30	-11.7 ksi	-20.0 ksi	-21.9 ksi	-20.7 ksi	Up
40	-15.8 ksi	-26.7 ksi	-24.8 ksi	-26.5 ksi	Up

[1] Rosette 1 -- Critical region strain gages SG08, SG09, and SG10
[2] Rosette 2 -- Critical region strain gages SG25, SG26, and SG27
[3] Rosette 3 -- Critical region strain gages SG28, SG29, and SG30
[4] Rosette 4 -- Critical region strain gages SG31, SG32, and SG33

8.2.1.3 Vertical Coupler Load Sensitivity Information for Fatigue Analysis

From the computed stress values of the quasi-static MSU tests for rosettes 2 and 4, critical region principal stresses due to vertical coupler loads were found to be:

> 30 kips vertical downward coupler force = 32.5 ksi
> 30 kips vertical upward coupler force = -20.35 ksi

The more conservative value, 32.5 ksi/30 kips, was used for fatigue life estimation until more reliable data were available from quasi-static Simuloader calibration tests.

8.2.2 Cyclic Vertical Coupler Loading Tests

The purpose of the cyclic MSU test was to load the stub sill-to-tank connection repeatedly to allow comparative fatigue analysis to be conducted and to instigate the beginning of crack initiation.

8.2.2.1 Fatigue Analysis for Selection of Cyclic Vertical Coupler Loads

To initiate cracking in the critical region, it was decided to apply 10 to 30 kip downward vertical coupler load cycles to the stub sill, thus applying the equivalent of 12.4 to 32.5 ksi to the critical region (using the more conservative rosette 2 and 4 sensitivities).

A modified Goodman diagram (MGD), selected from the AAR *Manual of Standards and Recommended Practices*,[9] was used to facilitate fatigue analysis of the critical region under the selected loading conditions. This method allows parameters required for fatigue life computation to be extrapolated from empirically obtained data for certain structural details under different loadings. Thus, fatigue parameters from "unknown" real world structural details can be estimated, allowing fatigue life computation to be done. Figure 38 shows the MGD chosen to represent the stub sill to head pad connection, and Figure 39 displays the idealized MGD curve.
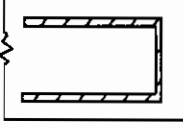
NO.	DESCRIPTION OF MEMBER	MEMBER DETAILS	NOM. YIELD STRESS (ksi)	Y-INTERCEPT OF M.G.D.(ksi)		MGD SLOPE (m)	S-N SLOPE (k)
				2×10^{6} (b)	10×10^{6} (b')		
3.1.5.1	Continuous welded I-Beam with square end cover plates, welded all around -flexural loading.		50	6.3	5.4	1.0	0.31

Figure 38. MGD Chosen for Stub Sill to Head Pad Connection
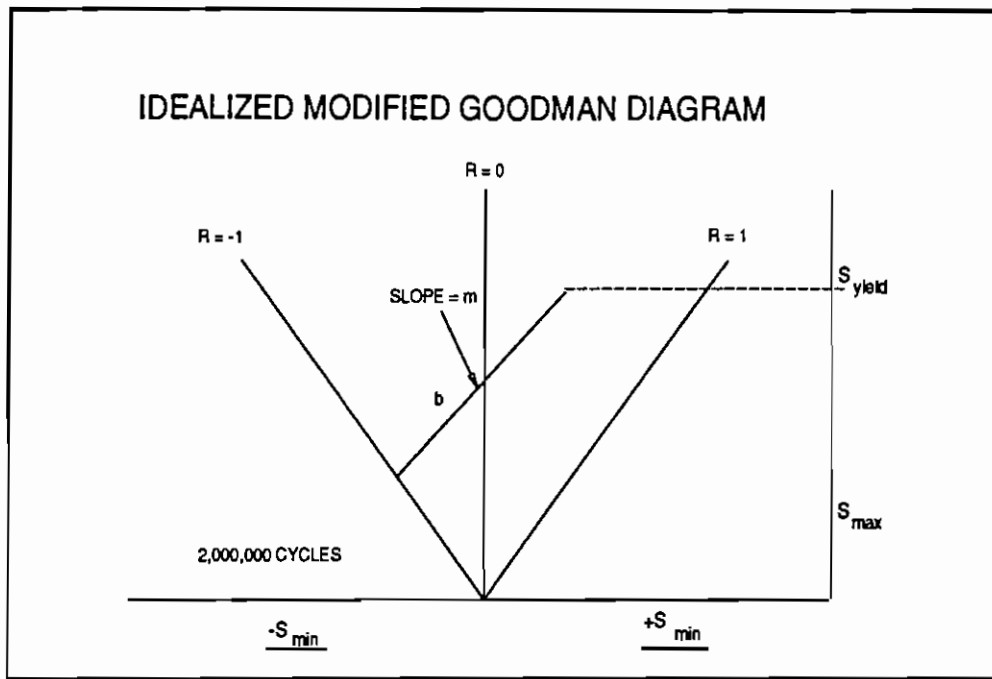
Figure 39. Idealized MGD Curve

Computed fatigue life predicts the life of a structure from new condition to when cracks initiate. Thus, in the case of the cyclic vertical coupler loading, the computed fatigue life was useful in determining the number of cycles until a crack might be found using non-destructive evaluation techniques. The computation method requires an iterative technique for random loadings. However, for the single loading environment of the cyclic MSU test, the computation was very simple.

For steels, the computation is as follows:

$$N = \frac{2,000,000}{\left(\dfrac{\sigma}{\sigma_e}\right)^{\frac{1}{k}}}$$

where

$$\sigma_e = \frac{b}{1 - mR}$$

and: σ is the maximum stress range [ksi]

  k slope of S-N diagram

  R is the ratio of minimum and maximum stress

  b, m are MGD parameters

Thus, for the MGD chosen (Figure 38), the fatigue life calculation for the -10 to -30 kip cyclic vertical coupler load is computed as follows:

$$N = \frac{2,000,000}{\left(\frac{\frac{32.5}{6.3}}{\left[1-(1)\left(\frac{12.4}{32.5}\right)\right]}\right)^{\frac{1}{31}}} = 47,390 cycles$$

This value is for 90 percent survival, i.e., it is probable that 90 percent of all samples tested with these loads would survive 47,390 cycles. Similarly, it was computed that 50 percent of all samples tested in this manner would survive 150,236 cycles. This was done by multiplying the MGD value of b (6.3 for 90 percent survival) by a factor of 1.43 (50 percent survival).[10]

8.2.2.2 Cyclic Vertical Coupler Load Test Results

It was imperative to monitor the critical region during the cyclic vertical coupler load test. The purpose of this test was to initiate cracking of the connection, not totally fatigue the joint to the point where critical crack lengths were obtained. The goal was to begin the Simuloader fatigue test with small cracks initiated to allow crack growth to be monitored during the Simuloader test.

After approximately 90,500 cycles a very fine small crack was observed on the right side, weld-toe corner of the stub sill to head pad connection. It was decided to further propagate this crack to the point where it might be observed in the field. Thus, an additional 170,000 cycles were run for a total of 260,500 cycles. No other cracks were observed during the cyclic MSU test. The final crack length was found to be 3 27/32 inches along the weld toe. Actual crack depth was unknown, but it was noted that the crack was extremely fine and it was assumed, based on NDE experience, to be very shallow.

Figure 40 shows the critical region where the crack was observed during the MSU test.
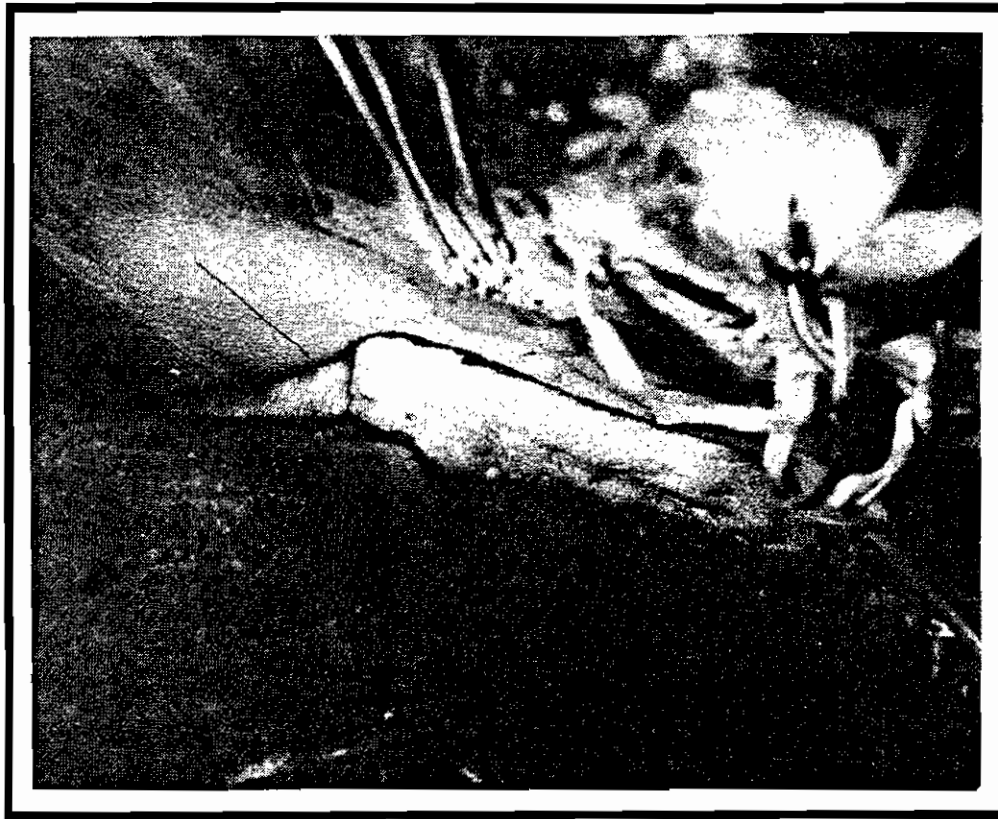
Figure 40. Location of Crack -- Cyclic MSU Test

Real-time load input monitoring was done with strip-chart recorders and the rosette 2 and 4 strain gage outputs. Large excursions of peak-to-peak strain levels were noted. This allowed continuous monitoring of the accuracy of the MSU input loads. In addition, stress ranges for the input loads were calculated using critical-region rosettes 1 through 4. Figure 41 shows the stress range for the cyclic MSU test at various points in the test. As pointed out, it is clearly evident from this figure that the increased sensitivity of the gages was located closer to the connection weld toe.
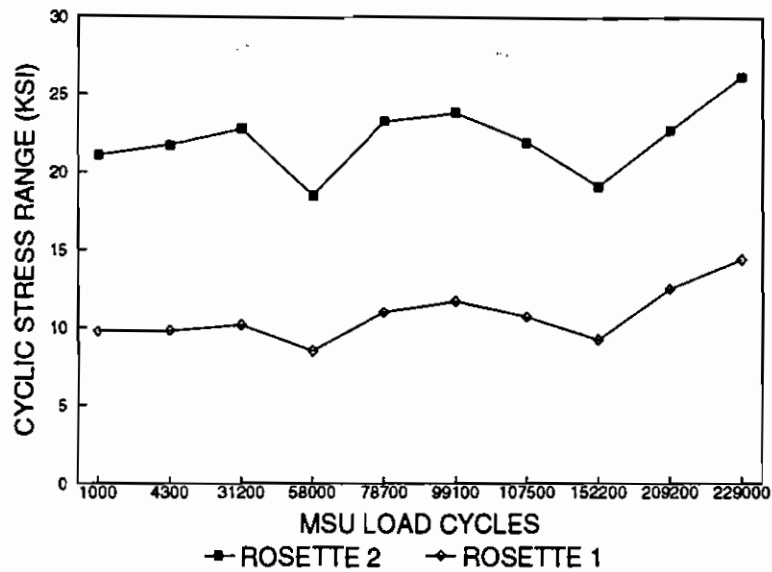
Figure 41. Cyclic MSU Test Input Stress Ranges

8.3 <u>SUPPLEMENTAL VERTICAL COUPLER LOADING TEST CONCLUSIONS</u>

QUASI-STATIC VERTICAL COUPLER LOADING TESTS

Results from the quasi-static MSU vertical coupler loading test, performed to character-ize the effect of vertical coupler loads and to determine the loads for the cyclic MSU test, showed the importance of this load mechanism to the fatigue of the stub sill to head pad connection. Thus, when Simuloader testing commenced, it was understood that the Simuloader's ability (or lack of) to apply vertical coupler force was paramount, which subsequently led to the addition of a vertical coupler load actuator system to the Simu-loader.

Calibration data from the quasi-static MSU vertical coupler load test allowed an appropriate vertical coupler force signal to be synthesized from OTR test strain mea-surement SG01. Similarly, critical-region strain gage data allowed fatigue analysis to be performed to determine the force input and number of cycles for the cyclic MSU vertical coupler loading test. It should be noted that the critical-region strain gage sensitivity value used for fatigue analysis is somewhat higher than the value obtained from the Simuloader vertical coupler load calibration data (described later), which may indicate that the two-actuator MSU method of inputting the vertical coupler load was slightly uneven.

In addition to meeting the goal of loading the stub sill-to-tank connection repeatedly to allow comparative fatigue analysis to be conducted and initiating crack growth, the cyclic MSU vertical coupler loading test showed good correlation between actual and predicted results. Predictions of approximately 47,000 to 150,000 cycles to crack initiation compared favorably to the 90,000 cycles required to initiate a crack.

9.0 SUPPLEMENTAL FRACTOGRAPHIC ANALYSIS

9.1 SUPPLEMENTAL FRACTOGRAPHIC ANALYSIS PROCEDURES

The supplemental fractographic analysis was done to investigate the crack initiation location and mechanism. Two samples of head pads that had developed cracks in revenue service, obtained from a chemical company, were analyzed to evaluate the type of fracture, crack origin location, crack propagation mode, and crack propagation rate. The following subsections describe the supplemental fractographic analysis procedures.

9.1.1 Head Pad Samples

Four low-pressure tank car head pads, one low-pressure tank car cradle pad, and five high-pressure tank car head pads were received. Each pad was fabricated from American Society of Testing Material (ASTM) A515 steel, which is a low-carbon steel with a relatively high ductile to brittle transition temperature. Two of the head pad samples were analyzed. Details of the two samples tested are given below.

- Sample 408046, B-end head pad
  Two pieces, 13-inch and 15-inch cracks

- Sample 408121, B-end head pad
  Three pieces, 24-inch crack

9.1.2 Fractographic Analysis Techniques

The procedures and results described below are from an internal document written by a TTC metallurgical specialist.[11]

VISUAL EXAMINATION

Each head pad was visually inspected for cracks, defects, and anomalies. The cracks were then visually examined from the backside of the head pads -- the surface that was welded to the tank car.

SECTIONING

Both head pad samples required sectioning to expose the fracture surfaces for stereographic examination. It was determined that the smaller of the two cracks in head pad 408046 would be sectioned as it was tighter and not entirely exposed to the elements. The larger of the two cracks appeared to be heavily oxidized and looked to have serious mechanical damage on the fracture surface. Thus, head pad 408121 was sectioned to reduce the size of the fracture surface for stereographic examination.

STEREOGRAPHIC EXAMINATION

Stereographic examinations were performed to find chevron markings and crack propagation bands on the fracture surface.

SCANNING ELECTRON MICROSCOPY EXAMINATION

Sample 408121 was chosen for scanning electron microscopy (SEM) examination because it appeared to have a cleaner surface free of oxidation and mechanical damage. Before SEM examination, the sample was ultrasonically cleaned to remove any debris from sectioning and handling.

MICROEXAMINATION

Studies of the head pad material microstructure were conducted at the crack origin to determine the condition of the plate material. A perpendicular cut was made through the crack origin of sample 408121 using a slow speed diamond wafer cut-off saw. A 0.035-inch diamond waffer blade was used to preserve any artifacts that might be present at the crack origin. After the sample was cut into two pieces, both were highly polished with diamond paste and alumina compound for metallographic examination. The polished sections were then etched in a 2 percent solution of nitric acid and methanol.

MICROHARDNESS TEST

Knoop microhardness (KHN) measurements were taken on the polished surface of the sample used for microstructure analysis.

9.2 SUPPLEMENTAL FRACTOGRAPHIC ANALYSIS RESULTS

The results described below are of fractographic analysis procedures performed on head pads 408046 B-end and 408121 B-end.

VISUAL EXAMINATION

Each head pad contained long cracks running perpendicular to the longitudinal axis of the pads. These cracks can be clearly distinguished in Figures 42 and 43. Sample 408046 was cracked in two places, one measured 13 inches and the other measured 15 inches. Sample 408121 contained a single crack, which ran across the entire width of the head pad (approximately 24 inches).

Figure 42. Crack Orientation in Relation to Head Pad -- Sample 408046
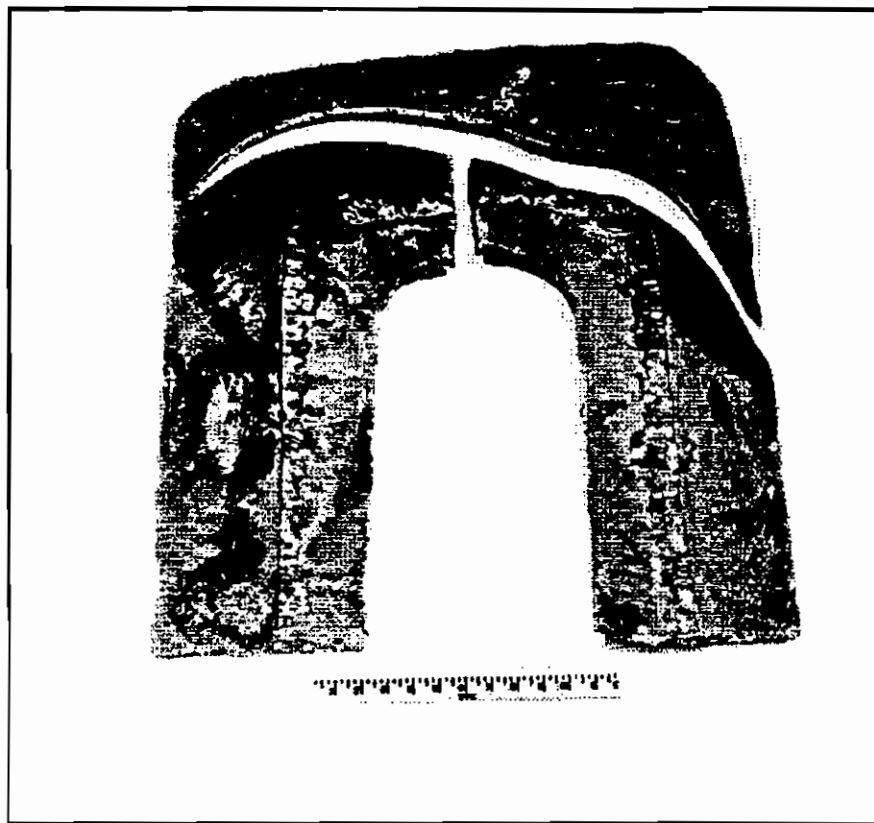
Figure 43. Crack Orientation in Relation to Head Pad -- Sample 408121

The cracks were then visually examined from the backside of the head pads which was the surface that was welded to the tank car. The head pads were removed from the tank car bodies by scarfing with a oxyacetylene flame. The scarfing operation produced a rough surface and probably added to the oxidation on the fracture surface of the cracks. When examining the cracks from this vantage point, it was clearly visible that each crack path intersected the corner of the welds at the point where the weld turned from the longitudinal to the lateral direction. This was observed in both sample head pads.

It was concluded from the visual examination that the cracks were possibly associated with the welds and would require sectioning for additional examination to determine the crack origin and the mode of fracture.

SECTIONING

Both samples required sectioning to expose the fracture surfaces for stereographic examination. Head pad 408121 required additional sectioning to reduce the size of the fracture surface for stereographic examination.

STEREOGRAPHIC EXAMINATION

Stereographic examinations were performed to find chevron markings and crack propagation bands on the fracture surface. After stereographic examination, it was determined from chevron markings and crack propagation bands on the fracture surface that the cracks on both samples did indeed originate near the edge of the welded sections. Figures 44 and 45 show signs of chevrons and propagation bands emanating from the crack origin in the welded sample from head pad 408121. Similar results were found on sample 408046.
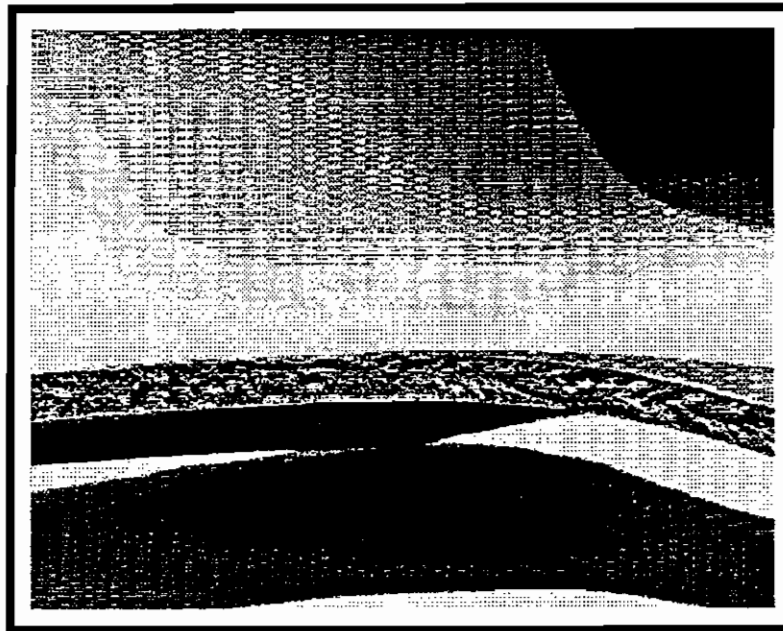
Figure 44. Appearance of Fracture Surface Showing Chevrons and Close-up Crack Initiation -- Sample 408121
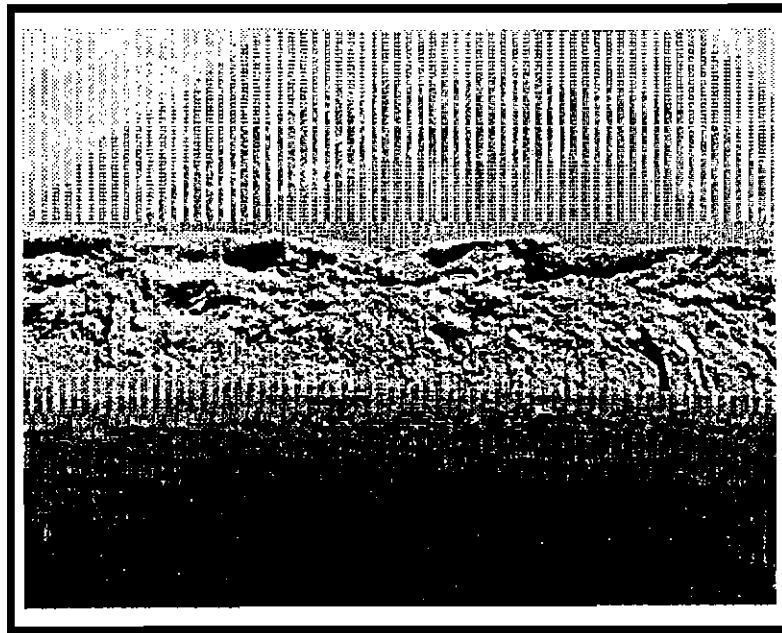
Figure 45. Appearance of Fracture Surface Showing Chevrons and Close-up Crack Initiation (View 2) -- Sample 408121

SCANNING ELECTRON MICROSCOPY EXAMINATION

Sample 408121 was chosen for SEM examination because it appeared to have a cleaner surface free of oxidation and mechanical damage. Before SEM examination, the sample was ultrasonically cleaned to remove any debris from sectioning and handling.

After the SEM examination, it was apparent that the fracture surface of sample 408121 was layered with corrosive products hindering a detailed study of the surface topography. During the SEM examination, localized areas of cleavage were detected indicating that the fracture was naturally brittle. Studies near the crack origin did not reveal anything because it was covered completely with oxidation. SEM studies were not attempted on sample 408046 because its fracture surface contained more rust than sample 408121.

MICROEXAMINATION

Studies of the head pad material microstructure were conducted at the crack origin to determine the condition of the plate material.

After etching the two pieces it was apparent that the area near the crack origin did not resemble that of the original base metal. Figure 46 shows a discolored HAZ at the

73

crack origin. The discolored area is approximately one inch from the welded area, which attached the head pad to the tank car. Microexamination shows the original microstructure of the head pad was altered at the point of crack origin.
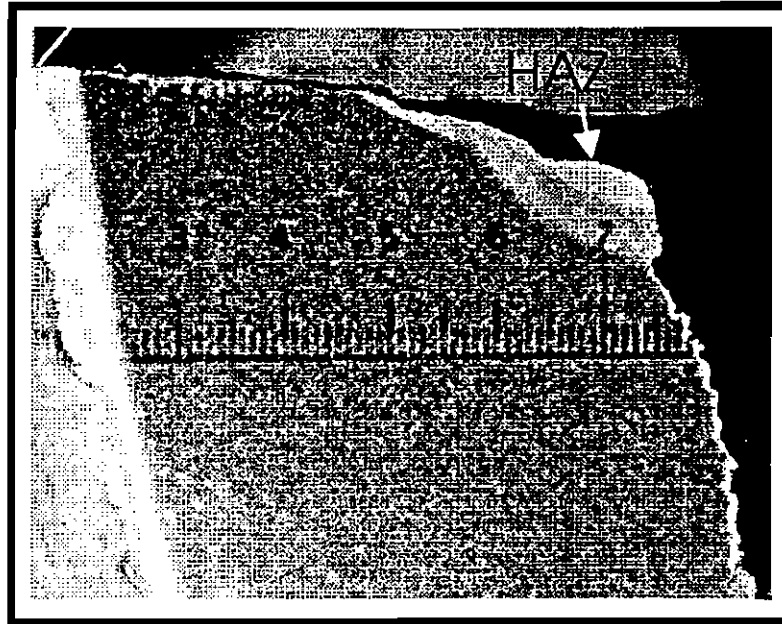
Figure 46. Heat Affected Zone at Crack Initiation Site -- Sample 408121

The composite micrograph in Figure 47 shows the phase changes that occurred as a result of the localized high heat input. When viewing the micrograph from the top to bottom, one can differentiate these phases that occurred as a result of the heat input. At the very top of the micrograph, a columnar grain structure formed indicating the base material was liquified then solidified into a columnar orientation. A close-up view of the columnar structure can be seen in Figure 48. Directly underneath the columnar grains is a narrow zone of lath martensite (Figure 49). Lath martensite is a form of martensite that forms in low carbon material and is usually not as hard as the more common plate martensite. The micrograph in Figure 50 represents the original microstructure of the base material. The percent of free ferrite in sample 408121 indicates the carbon percent to be in the area of 0.25 percent for the head pad base material.
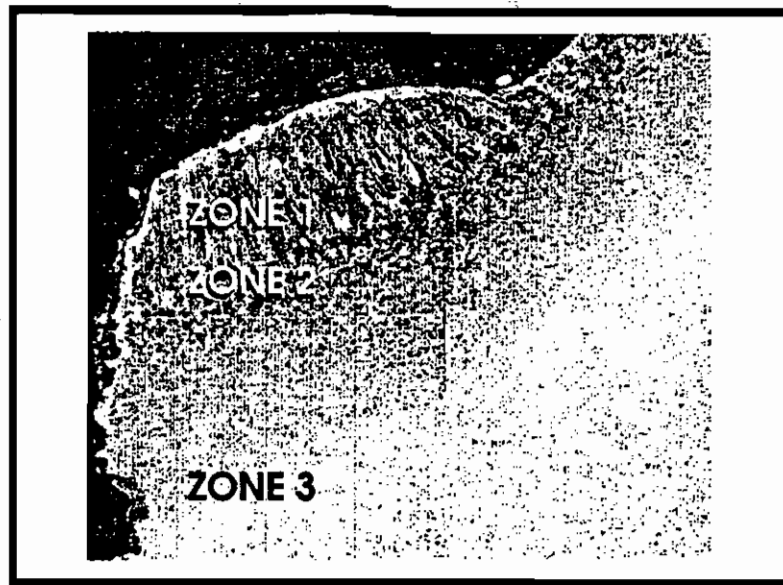
Figure 47. Microstructure at Crack Origin Showing Multiple Phases --
Sample 408121

Figure 48. Zone 1 Close-up View -- Sample 408121
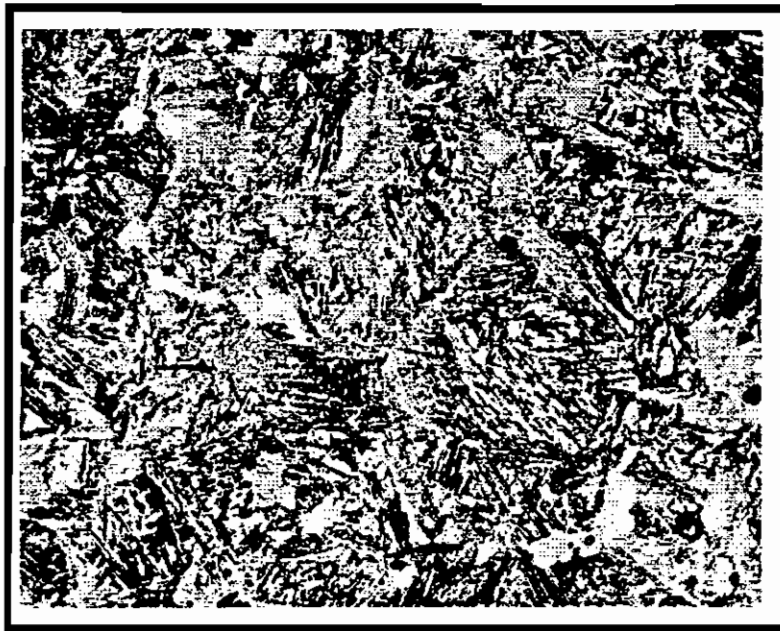
Figure 49. Zone 2 Close-up View -- Sample 408121
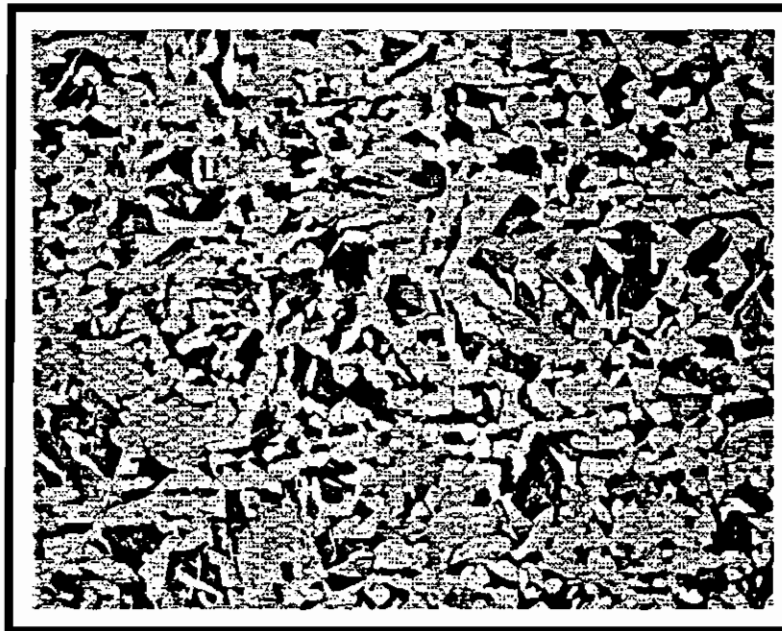
Figure 50. Base Material Close-up View -- Sample 408121

KHN measurements were taken on the polished surface of the sample used for micro-structure analysis. Figure 51 illustrates the microhardness traverses taken on sample 408121. The hardness traverses were taken across the different phases in the steel sample starting at the HAZ from the top at the columnar structure down into the original base material. The first three measurements indicate the columnar structure to be sufficiently hard with reading of KHN 365-340. When examining the micrograph in Figure 49, the structure displays very little proeutectoid ferrite, which would explain the higher than normal readings. In the martensitic zone, the KHN reads 460 — normal for this type of structure. The readings gradually decrease as they near the base material. The normal readings for the base material are probably KHN 220-230.
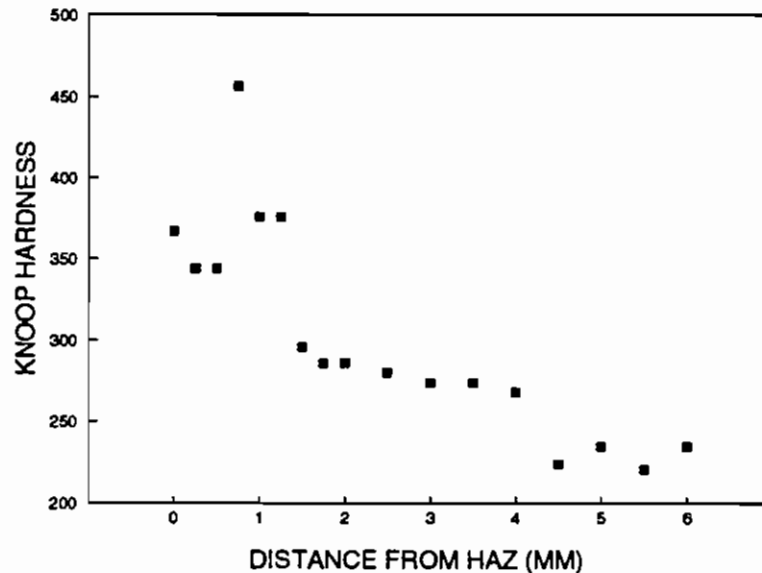
Figure 51. Knoop Microhardness Plot — Sample 408121

9.3 SUPPLEMENTAL FRACTOGRAPHIC ANALYSIS CONCLUSIONS

The localized area at the HAZ where the crack originated may have been caused from an arc strike to commence welding of the head pad. Because the arc strike was of sufficient

distance from the head pad welding area where temperatures were higher, localized phase transformations occurred because of the faster cooling rate, thus altering the base structure of the head pad.

10.0 SUPPLEMENTAL CRACK GROWTH (da/dn) TESTS

Supplemental da/dn tests were conducted on tank car steel samples to obtain crack-growth equations. The equations, meant to augment the results from the full-scale testing, may be used to indicate the characteristic rate of growth given proper application.

10.1 SUPPLEMENTAL DA/DN TEST PROCEDURES

Tests on three tank car steel specimens were performed at the University of Illinois, Materials Engineering Research Laboratory (MERL) facility utilizing a servo-hydraulic test system. The testing was conducted in accordance with ASTM E647; "A Standard Method for Constant Load Amplitude Fatigue Crack Growth Rates above 10^{-8} m/cycle."

10.1.1 Da/dn Test Methodology

The parameters determined from the da/dn tests allow the incremental rate of cracking in the stable middle stress intensity factor (ΔK) range to be estimated according to the crack growth equation:

$$\frac{da}{dn} = \frac{C(\Delta K)^n}{(1-R)}$$

where: $\frac{da}{dn}$ = incremental crack growth

R = ratio of min. to max. cyclic stress
C = material property parameter to be determined
n = material property parameter to be determined
ΔK = stress intensity factor -- function of stress range, crack length, and crack shape and boundary geometry

The value for ΔK used for prediction of crack growth rate for the ASTM E647 testing was given as:

$$\Delta K = \frac{\Delta P}{B\sqrt{W}} \frac{(2+\alpha)}{(1-\alpha)^{3/2}} (0.886 + 4.64\alpha - 13.32\alpha^2 + 14.72\alpha^3 - 5.6\alpha^4)$$

where: ΔP = load range, maximum minus minimum

          B = specimen thickness

          W = distance parallel to crack between applied load and end

                of specimen (i.e., W = 63.5 mm less 12.85 mm in Figure 53)

          α = crack length a divided by W

10.1.2 Da/dn Test Fixture

A load-frame test machine, similar to that shown in Figure 52, was used by the University of Illinois to test the steel samples.
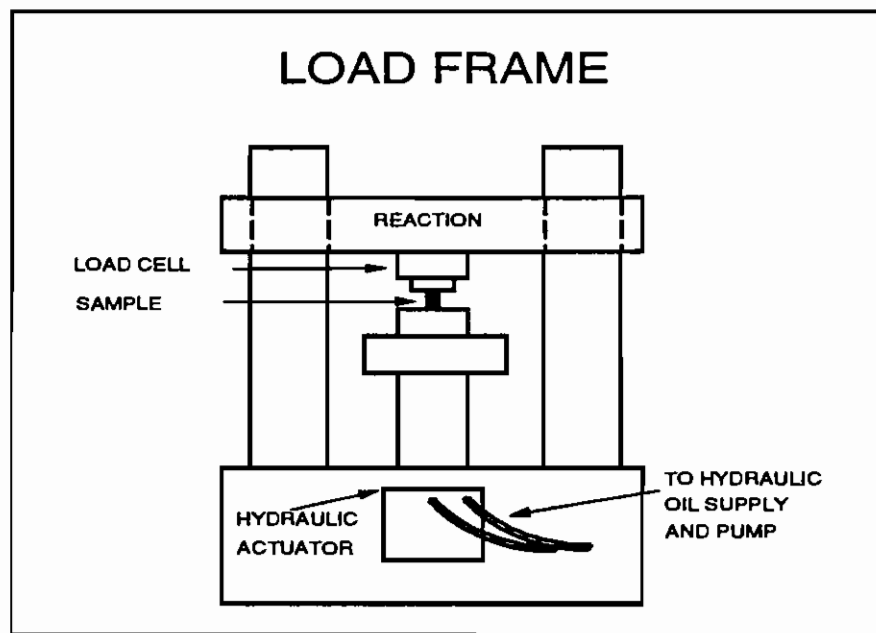
Figure 52. Da/dn Crack Growth Test Fixture at University of Illinois

10.1.3 Da/dn Test Specimen

The samples were from a 12 x 12 inch sample of A515 steel with the chemistry listed in Table 22. The published specification for A515 steel shows maximum allowable carbon (.35) and manganese (.90) content levels higher than were contained in the sample tested.

The test samples were machined to the dimensions shown in Figure 53.

Table 22. Da/dn Test Sample Chemistry

C	M_n	P	S	S_i	C_u	N_i	C_r	M_o	V	T_i	A_i	B	C_o	N
.27	.79	.027	.009	.174	.011	.02	.04	.006	.002				.001	
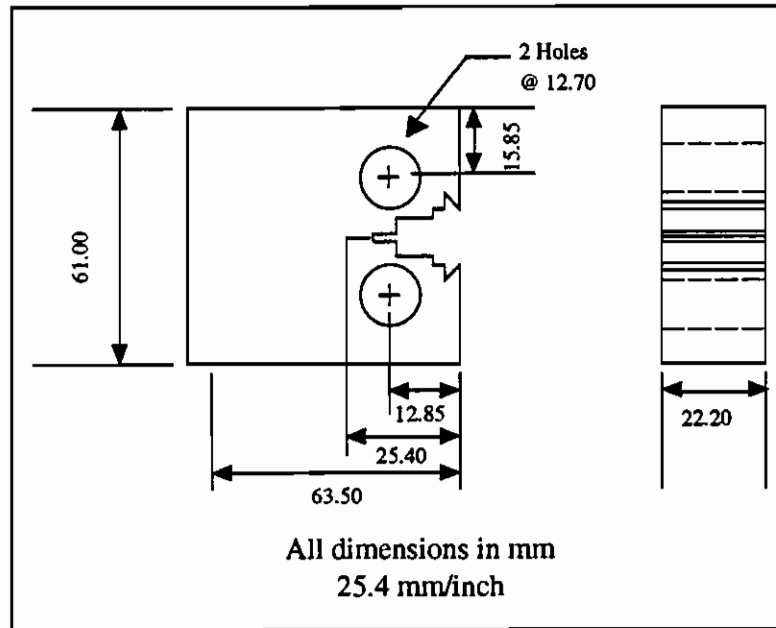
Figure 53. Da/dn Crack Growth Test Machined Test Specimen

10.1.4 Da/dn Crack Growth Test Input Loads

The tests were conducted in the stable ΔK regime. Two of the samples were tested with R-ratios of -1 and 0.1. The procedure was to determine the stable ΔK regime with a careful approach with loads below the regime, then complete the test within the stable regime. The R=0.1 stress ratio, representing R=0, eliminated the need to change direction of the actuator system at or near zero load levels. Tests with the R-ratio of -1, with load crossings through zero, were not found to be troublesome.

The third sample was tested with random loads that were to correspond to the stress levels experienced by the critical region of the tank car when subjected to the Simuloader input load spectra for vertical coupler loads.

The random loads, obtained from the FEEST test program, were converted to stress levels with a sensitivity rate of -22.75 ksi per 25 kips vertical coupler load (vertical upward positive). This sensitivity, obtained from strain gage data at the critical region, may include stress concentration effects. Thus, the value for sensitivity, though the best available and used for fatigue analysis throughout this test program, may be conservative. Therefore, in addition to the elimination of insignificant loads below 10 kips peak-to-peak, loads corresponding to stresses above 36 ksi, after the sensitivity value was applied, were also dropped.

The procedure for utilizing the random loads included the initial correlation of the maximum desired stress value to an input load. It was also important to ensure that the selected value allow testing to be conducted within the stable growth regime. Therefore, an input load of 25 kN (5,618 lbf) was correlated to the maximum stress value of 36 ksi in the input load history.

Figures 54 and 55 show the FEEST random loads simulated and a section of the randomized stress cycles obtained from combining the sensitivity data and the FEEST data.
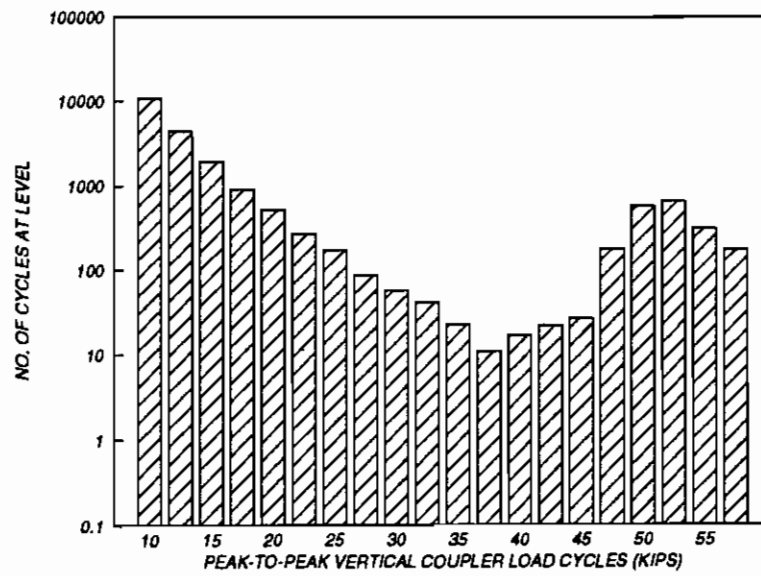
Figure 54. Random Loads for Third Test Specimen
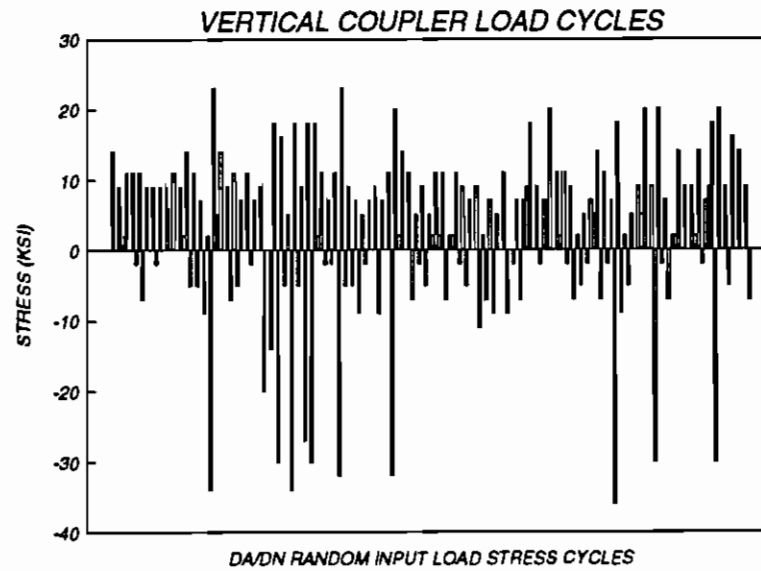
Figure 55. Example, Random Loads for Third Test Specimen

82

10.2 SUPPLEMENTAL DA/DN TEST RESULTS

The resultant da/dn crack growth equations for the R=-1, R=0.1, and random loads are given below along with graphs showing test data.

10.2.1 R=-1 Test Results

Figure 56 displays a da/dn versus ΔK data summary for the R=-1 constant amplitude loading test. The "knee" of this figure corresponds to when the stable ΔK regime was obtained. Thus, the curve fit for the crack growth equation was done for data above the knee. Figure 57 shows the crack length versus number of load cycles for the R=-1 test configuration.
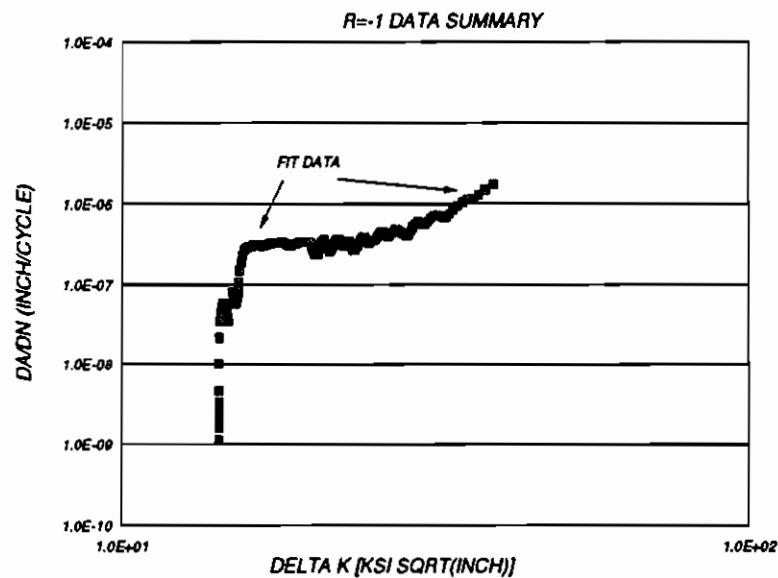
Figure 56. Da/dn Versus ΔK, R=-1 Test Configuration
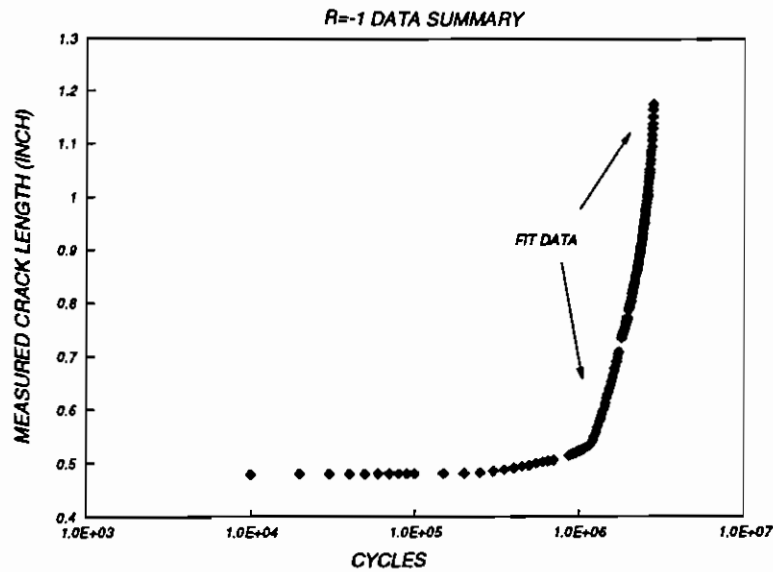
Figure 57. Crack Length Versus Number of Load Cycles, R=-1

The crack growth equation for the R=-1 tests and fit to the stable crack growth region is given below. The coefficient of determination for the curve fit (R^2) was 0.94133. A perfect curve fit would give a value of 1.0 for R^2.

$$\frac{da}{dn} = (5.549E - 10)(\Delta K)^{3.0063}$$

10.2.2 R=0.1 Test Results

Figure 58 displays a da/dn versus ΔK data summary for the R=0.1 constant amplitude loading test. The "knee" of this figure corresponds to when the stable ΔK regime was obtained. Thus, the curve fit for the crack growth equation was done for data above the knee. Figure 59 shows the crack length versus number of load cycles for the R=0.1 test configuration.
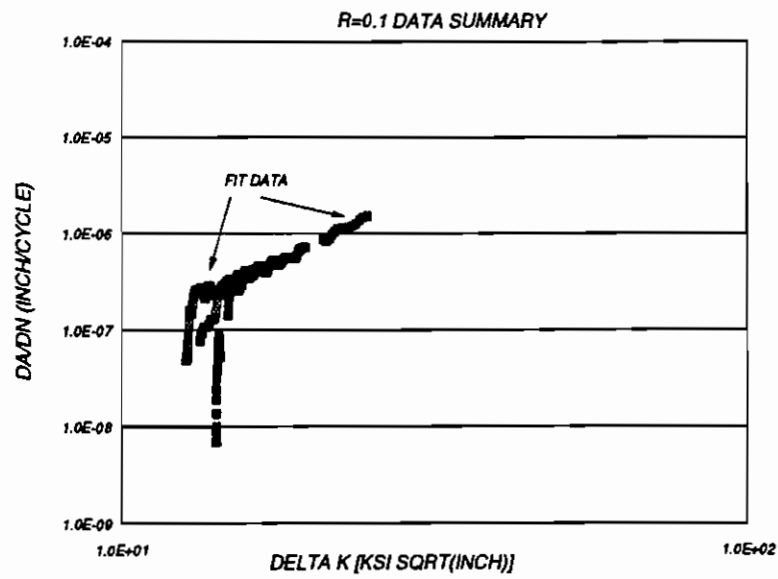
Figure 58. Da/dn Versus ΔK, R=0.1 Test Configuration
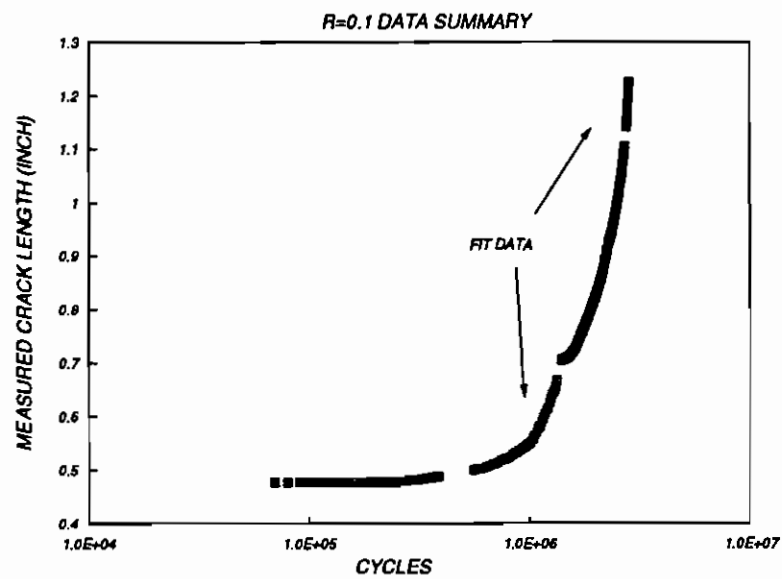
Figure 59. Crack Length Versus Number of Load Cycles, R=0.1

The crack growth equation for the R=0.1 tests is given below. The coefficient of determination for the curve fit (R^2) was 0.98345.

$$\frac{da}{dn} = (4.1064E - 09)(\Delta K)^{3.144}$$

10.2.3 Load Environment Test Results

The input loading block, representing the AAR FEEST data with the modifications described in Section 10.1.4, required 279 repetitions to propagate the crack to a point where a rapid increase in the rate of crack growth was attained. If a correlation of the test sample with the given loads to the FEEST data and a real tank car can be made, this would correspond to approximately 6.4 million miles. However, as will be seen later, crack growth on the tank car progressed at a much faster rate. Thus, it is assumed that the relationship derived to match the FEEST vertical coupler loads to head pad stresses and subsequent input loads on the test sample was not realistic.

Figure 60 shows the variable amplitude crack growth versus input loading block.
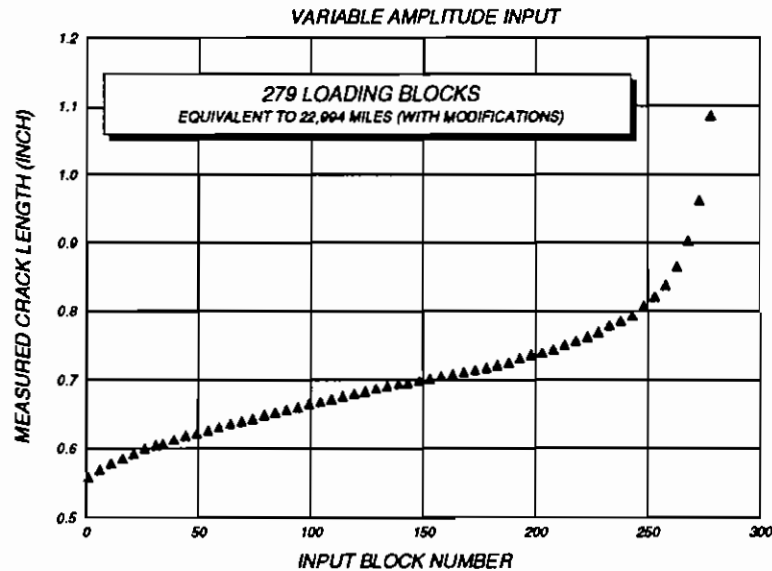
Figure 60. Crack Length Versus Number of Loading Blocks, Variable Load Inputs

10.3 SUPPLEMENTAL DA/DN TEST CONCLUSIONS

The crack growth equations, developed for the tank car steel samples for stress ratios of R=-1 and R=0.1 (R=0), can be used for various crack profiles to indicate crack growth rate under a given load. With the crack growth equations developed and the given steel material, with appropriate representations of crack geometry available in references 12, 13, and 14, and with an input load history, head pad crack growth can be estimated with numerical techniques. Accuracy of the result would depend upon the following factors:

- How much the chemistry of the A515 steel tested matched the chemistry of the tank car head pad being analyzed.

- How well the loading of the material tested to develop the crack growth equation matched the loading of the cracked section of the head pad (i.e. the ASTM test is pure crack tip opening loading, which may provide results which differ when opening, bending, and tearing are coupled).

- How appropriate was the ΔK selected; i.e, how closely does the crack geometry for a given ΔK match the actual crack geometry.

11.0 SIMULOADER TEST BEFORE VERTICAL COUPLER FORCE INPUT

11.1 SIMULOADER TEST BEFORE VERTICAL COUPLER FORCE INPUT – PROCEDURES

Preliminary exploratory Simuloader fatigue tests were conducted in November, 1991, to determine the effectiveness of the input profile developed from the OTR test data.

11.1.1 RDL

The Simuloader is located in the RDL, a 55,000 square foot, high-bay building, which also houses other test facilities including the VTU, the Roll Dynamics Unit, the Traction Motor Test Stand, the MSU, and the Container/Package Laboratory. Also located in the RDL are instrumentation, data collection and analysis equipment, and vehicle handling equipment. The systems in the RDL can duplicate, in a controlled environment, the forces and stresses which affect rail vehicles, or other vehicles and structures. This can be done while also taking measurements of response phenomena.

The RDL is served by two rail tracks. Two 100-ton capacity traveling bridge cranes and pneumatic lifting devices are used to position test cars and related equipment for testing.

11.1.2 Simuloader Test Facility

The Simuloader is a hydraulic shaker system that inputs vertical and lateral loads into a truck bolster interface, and longitudinal loads into the couplers. The car tested is supported by the Simuloader truck bolsters with conventional center bowl and side bearing equipment. The fatigue machine, manufactured by MTS Corporation, can excite the test car with input profiles and waveforms that represent the bolster's response to actual railroad environment.

In its original configuration, the Simuloader includes four vertical 110-kip, two lateral 77-kip, and four yaw 22-kip electrohydraulic actuators, which are displacement controlled, and one longitudinal actuator, which is force controlled. The lateral, vertical, and yaw actuators apply loads into a truck bolster interface. The longitudinal actuator, which is controlled with an instrumented load measuring coupler, is capable of applying 750-kip buff and 600-kip draft loads. The yaw actuators are used mainly to support the bolster assembly. The actuators use MTS 256 and 252 servo-valves. The actuators' required hydraulic supply is met by six pumps, each with a 55 gallon-per-minute capacity. The operating pressure is 3,000 psi.

The Simuloader is designed to run efficiently for long periods of time, which makes it particularly well suited for fatigue tests. Thus, the fatigue life of a railcar (average of 30 years) can be determined from data with just a few weeks or months of testing. The resulting fatigue analysis serves as a source of design and safety data.

Figures 61 and 62 illustrates a tank car on the Simuloader.
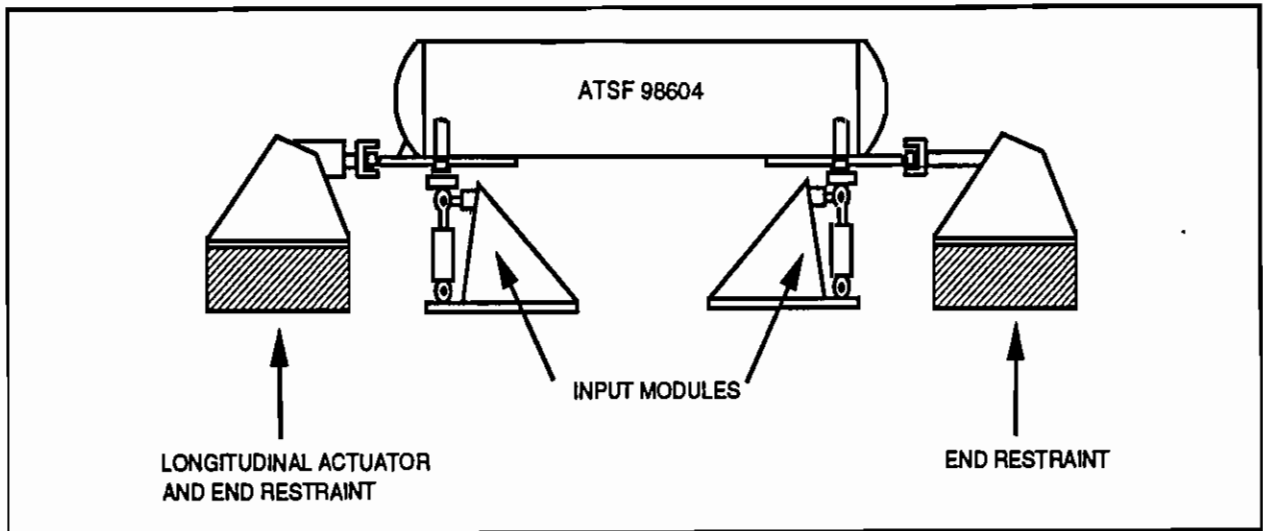
Figure 61. Tank Car on Simuloader
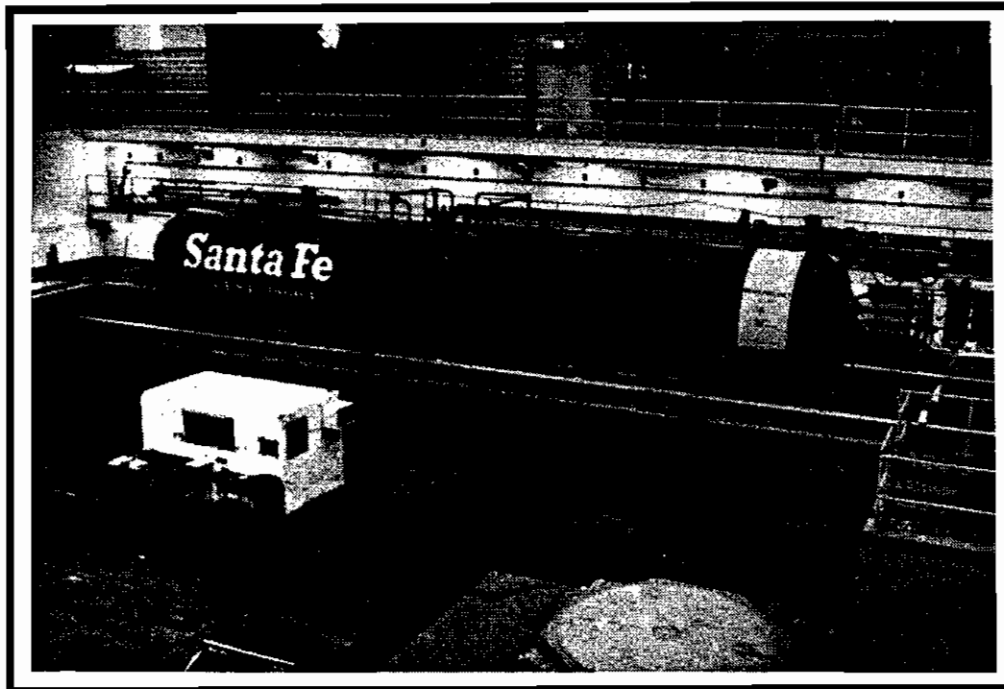
Figure 62. Tank Car on Simuloader

11.1.3 Test Car Preparations

The Simuloader's force-controlled longitudinal actuator requires a significant volume of oil to operate -- particularly for large displacements. For this reason, the test car was equipped with solid draft gears to minimize the displacement travel required for the longitudinal actuator to reproduce the desired loads.

11.1.4 Test Instrumentation

The measurements recorded during the supplemental tests, with the exception of speed, were recorded during the Simuloader tests. Several measurements, listed in Table 23, were added for the Simuloader tests without the vertical coupler load input capability. These additional measurements included actuator displacements and strain gages. TTC's data van was used to house the instrumentation hardware and computer systems for the Simuloader tests. The HP data acquisition systems used for the OTR, and Supplemental tests were also used for the Simuloader test data acquisition.

Table 23. Additional Measurements for Simuloader Tests Without Vertical Coupler Load Input

Name	Description and Location	Type	Est. Range
LAT1	Simuloader Lateral Actuator 1	Displacement	± 3"
LAT2	Simuloader Lateral Actuator 2	Displacement	± 3"
LV1	Simuloader Left Vertical Actuator 1	Displacement	± 3"
RV1	Simuloader Right Vertical Actuator 1	Displacement	± 3"
LV2	Simuloader Left Vertical Actuator 2	Displacement	± 3"
RV2	Simuloader Right Vertical Actuator 2	Displacement	± 3"

The AAR's SPATE system (Stress Pattern Analysis Through Thermal Emissions), was used for one day of Simuloader tests. SPATE is a non-contacting stress measurement system, which operates on the principle that a specimen under cyclic stress loading produces measurable heat energy. SPATE measures the heat energy with a sensitivity of one one-thousandth of a degree in the infrared spectrum, while referencing the input dynamic load to negate the temperature fluctuations associated with the cyclic loading. The result is a color map that is proportional to the stress contours.

11.1.5 Input Profile Development -- OTR Test Data

The 157 fifteen-minute data files of digital information recorded during the OTR test were reduced to 750 seconds of "significant" data. These data were processed into two files; one file included the response measurements, while the second was comprised of the measurements required for development of the Simuloader input profile.

11.1.5.1 Computational Facilities

TTC's VAX 11/780 computer was used for the processing of the Simuloader input profile. This computer runs the CFAS software referred to earlier. This software, in addition to the cutting and editing routines required for condensation of the significant data, provides the LTHD processing algorithms for Simuloader input profile development.

The input profile was converted into analog signals with a DEC 11/23 computer system, which can be used to provide the command signals to several shakers in addition to the Simuloader. The 11/23 can also be used to acquire and analyze up to 64 channels of data (while providing shaker inputs).

11.1.5.2 LTHD Technique

The LTHD system was originally devised to provide an "inexpensive unmanned track geometry measurement capability that can be used by the railroads to detect unsafe track conditions during routine revenue operations."[15] This system was developed further in order to record and process space displacement profiles to excite the VTU. The VTU is a shaker system located at TTC which excites four-axle railroad vehicles at the wheel/rail interface. Subsequently, the LTHD package was modified again in order to provide input signals for the Simuloader.

In the development of Simuloader input profile, the LTHD method requires two vertical accelerometers to be mounted on both ends of each truck bolster. One laterally configured accelerometer is also required for each truck bolster. Longitudinal and vertical coupler forces were also recorded for Simuloader input profile. The LTHD processing software passes these signals along with the processed displacements from the accelerometer measurements. Figure 63 shows the LTHD measurement locations.
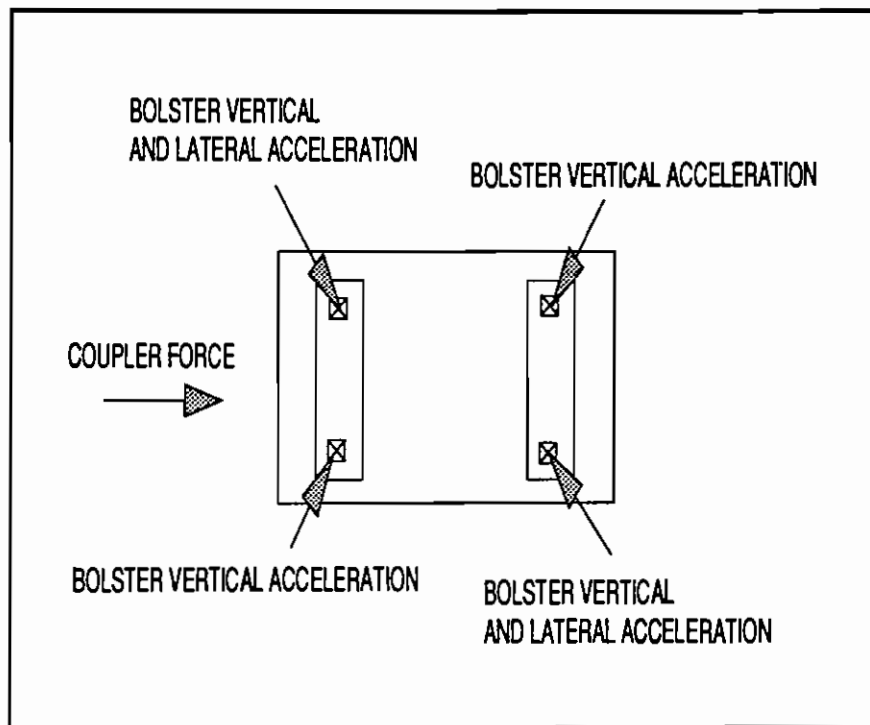
Figure 63. LTHD Accelerometer Locations for Simuloader Input Development

As specified in the system's manual, special filters are used to attenuate the acceleration signals above 1.0 Hz to allow the low frequency track geometry (profile) data to be amplified and accurately recorded. The manual specifies "Upon playback, the filtered data...is treated in the LTHD data processing software via an inverse transform to retrieve the full spectrum of frequencies seen by the axle up to 20 Hz. Then, a double integration technique is employed within the software to convert acceleration to displacement." The resulting signals are corrected for angular and gravitational effects, and for speed sensitivity.[16]

11.1.5.3 Input Profile Development

Initially, the OTR test data was reduced to 750 seconds. After defining two response types, however, it was apparent that additional time could be shaved from the OTR test data to further accelerate the condensed input. This resulted in a 338-second file which was subsequently processed with the LTHD package to generate a Simuloader input profile. Table 24 lists the event number, response type, and time (subslices) used to create the 338-second file of condensed OTR test data.

92

Table 24. Event, Response Type, and Time Subslices

Event No.	Response Type	Portion of 50-Second Slice Used (Time Subslice)
1	Type 1	5 seconds
2	Type 1	4 seconds
3	Type 1	4 seconds
4	Type 1	4 seconds
5	Type 1	4 seconds
6	Type 1	4 seconds
7	Type 1	4 seconds
8	Type 1	4 seconds
9	Type 2	50 seconds
10	Type 2	50 seconds
11	Type 2	50 seconds
12	Type 2	50 seconds
13	Type 2	50 seconds
14	Type 2	50 seconds
15	Type 1	5 seconds

11.1.6 Test Procedure

Before the vertical coupler load actuator system was designed and implemented, the exploratory Simuloader tests began November 6, 1991, and were completed on November 19, 1991. The agenda for these tests was as follows:

(1) Gain precise control of the Simuloader

(2) Determine the effectiveness of the Simuloader to reproduce strains in the critical region

(3) Investigate ways of modifying the Simuloader operating procedures to more accurately reproduce the strains seen during the OTR tests

Table 25 describes the tests conducted. The run numbers designate the HP computer file number.

11.1.7 Test Data Analysis

Statistics, time histories, and rainflow counts shown in histogram format were used to analyze the exploratory Simuloader test data.

Table 25. Exploratory Simuloader Test Matrix

Run	Description
TANC_RN100	Noise background check
TANC_RN101	Quasi-static longitudinal coupler force application
TANC_RN102	50% gain, 130 seconds of 338-second input file
TANC_RN103	100% gain, 130 seconds of 338-second input file
TANC_RN104	100% gain, 130 seconds of 338-second input file, yaw actuators applied for Simuloader stability (used for all runs thereafter)
TANC_RN105	zero coupler force recording
TANC_RN106	5Hz longitudinal coupler cyclic loading, 0-80 kips buff, to support SPATE measurement
TANC_RN107	5Hz longitudinal coupler cyclic loading, ±90 kips (buff and draft), to support SPATE measurement
TANC_RN108	Quasi-static longitudinal coupler force application, ±330 kips at 70-kip steps
TANC_RN109	Same as TANC_RN108 with ±1 inch vertical offset to introduce angles into longitudinal coupler loads
TANC_RN110	100% gain on longitudinal coupler force input, 130-second input file
TANC_RN111	150% gain on longitudinal coupler force input, 130-second input file
TANC_RN112	200% gain on longitudinal coupler force input, 130-second input file
TANC_RN113	200% gain on longitudinal coupler force input, 130-second input file, +1 inch vertical offset (continuous)
TANC_RN114	200% gain on longitudinal coupler force input, 130-second input file, -1 inch vertical offset (continuous)
TANC_RN115 to TANC_RN120	Tests to excite bounce modes in the test car
TANC_RN121	Test to excite rocking modes (rock-and-roll) in the test car
TANC_RN122	Test to excite lateral modes in the test car
TANC_RN123	160 % vertical and lateral input gain, 200% longitudinal coupler load gain
TANC_RN124	160 % vertical and lateral input gain, 200% longitudinal coupler load gain
TANC_RN125	160 % vertical and lateral input gain, 376% longitudinal coupler load gain
TANC_RN126	160 % vertical and lateral input gain, 566% longitudinal coupler load gain
TANC_RN127	160 % vertical and lateral input gain, 566% longitudinal coupler load gain, +1 inch continuous vertical input

11.2 SIMULOADER TEST BEFORE VERTICAL COUPLER FORCE INPUT – RESULTS

11.2.1 OTR Test Simulation Results

Simuloader tests with the 338-second input file showed that the Simuloader, in its standard configuration, was unable to reproduce the magnitude of the significant strain values in the critical region. Specifically, the responses of gages SG08, SG09, and SG10 and the symmetrically placed gages SG28, SG29, and SG30 were not matched.

Figures 64 and 65 show the inability of the Simuloader, in its original configuration, to replicate the responses of gages SG28 and SG29. These channels were chosen for display because it was known that cracks from the MSU test did not exist near these gages when the exploratory Simuloader tests without VCF were conducted. The plots are the result of a cycle counting routine called rainflow counting. This technique counts numbers of cycles in pre-defined ranges, doing so on short and long duration cycles.

The figures show OTR test data and three Simuloader test runs, for Simuloader longitudinal coupler force gains of 1.0, 2.0, and 5.66. For SG28, Figure 64, it can be seen that the nominal Simuloader longitudinal coupler force is significantly less severe than the OTR test data. This is also true for the Simuloader test data when the longitudinal coupler force was amplified by 2.0. Only when the Simuloader longitudinal coupler force was increased to be more than five times greater than the OTR test longitudinal coupler force did the response of SG28 match or exceed the OTR test data response.

Figure 65 shows that the Simuloader test SG29 response did not approach the response achieved during the OTR test even when the Simuloader longitudinal coupler force was five times greater than the OTR test longitudinal coupler force.
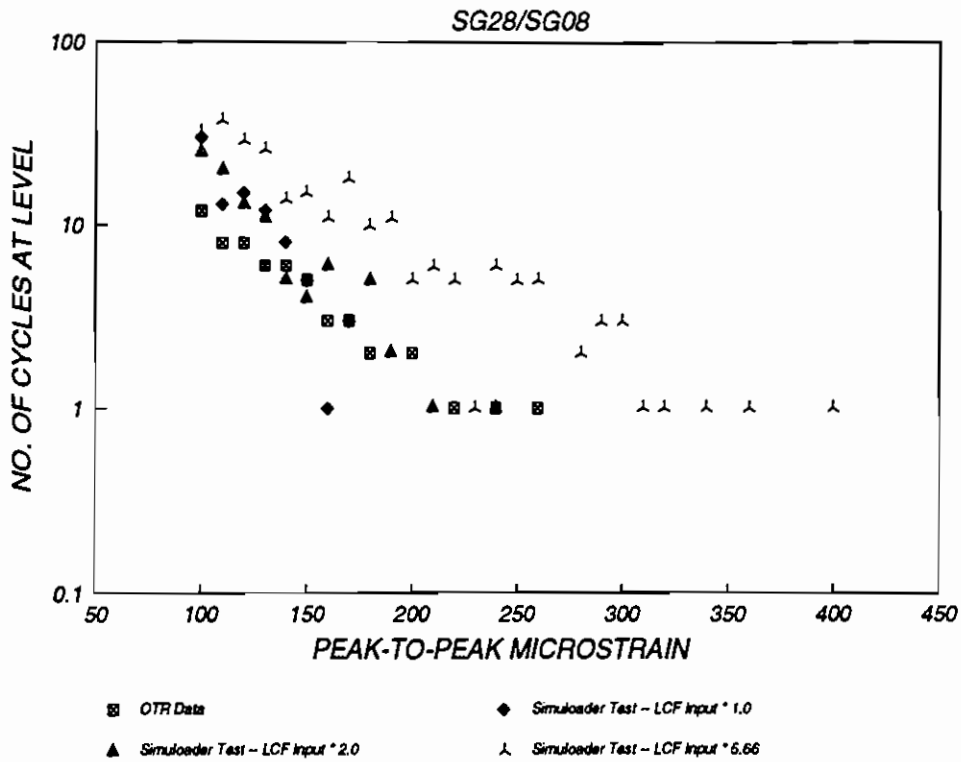
Figure 64. Simuloader Test W/O VCF, SG28 Results
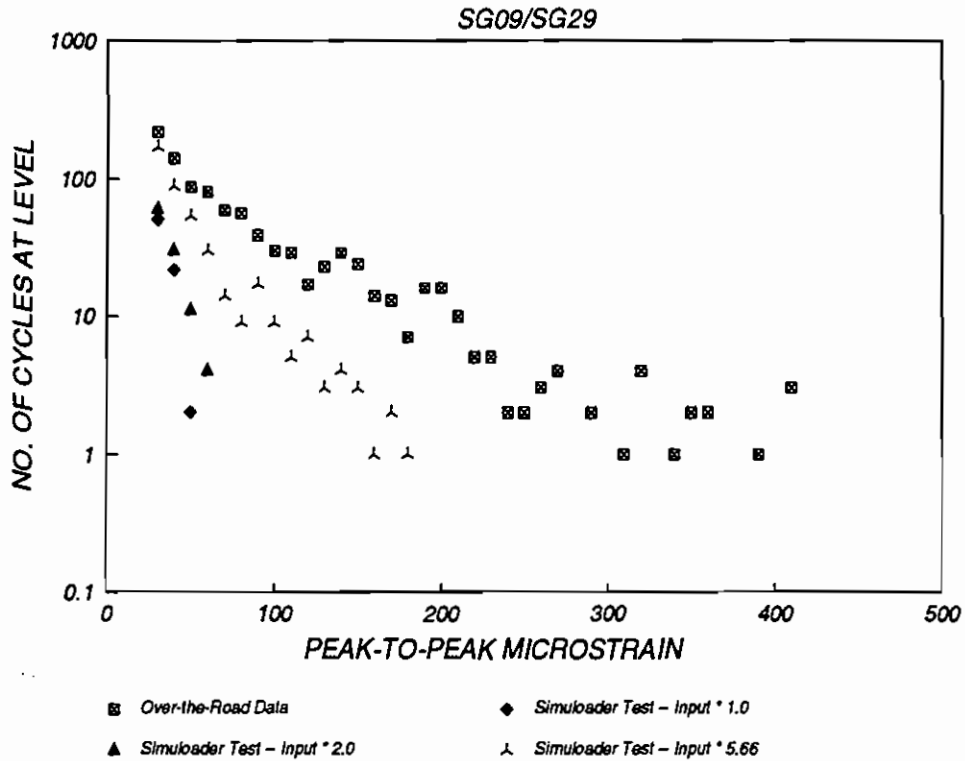
Figure 65. Simüloader Test W/O VCF, SG29 Results

11.2.2 Variations of Simuloader OTR Test Procedures

In addition to increasing the longitudinal coupler force Simuloader input levels, variations in Simuloader operating procedures were attempted. The replication of the vertical component of the longitudinal coupler forces, felt to be the missing ingredient in the Simuloader operation, was the function of these tests. The procedure was to introduce an angle in the longitudinal actuator, thus producing a vertical coupler force component. The tests were unsuccessful due to the lack (by design) of a vertical reaction on the longitudinal actuator.

11.2.3 Sinusoidal Inputs/SPATE Measurement Results

Simuloader tests were conducted with a sinusoidal waveform input profile to further investigate the vibrations encountered during the OTR test. A mode of vibration was noted during these tests and was termed "ballooning." This was a predominant shell flexing mode which seemed to be excited at several frequencies. Figure 66 displays the ballooning tank shell shapes.
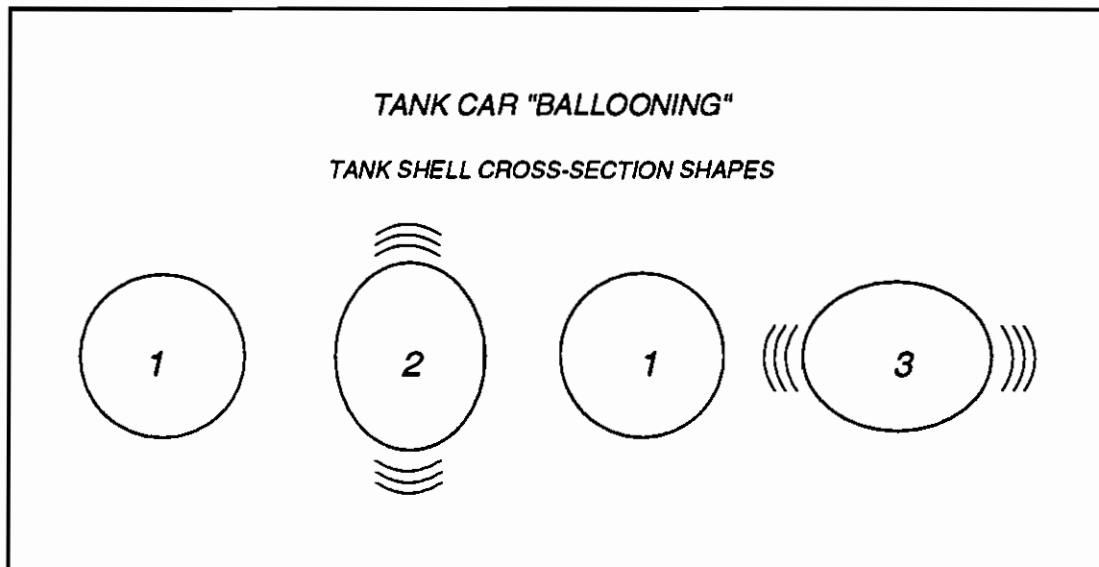
Figure 66. Ballooning Tank Shell Shapes

During some Simuloader testing of the tank car using sinusoidal waveform inputs, SPATE was used to map the stress gradient profiles at two locations. This provided

information on the adequacy of the strain gage measurement locations by showing the stress "hotspots" in the structure locations evaluated when subjected to ±90-kip buff loads with a 110-kip buff preload.

SPATE provides a digitized color map of the stress gradient profiles. Figure 67 shows the profiles for the critical-region head pad to sill corner connection where strain gages SG28 - SG30 are located. Figure 68 shows the stress profile at the tank shell midspan. Both confirmed that the measurement locations chosen were acceptable.
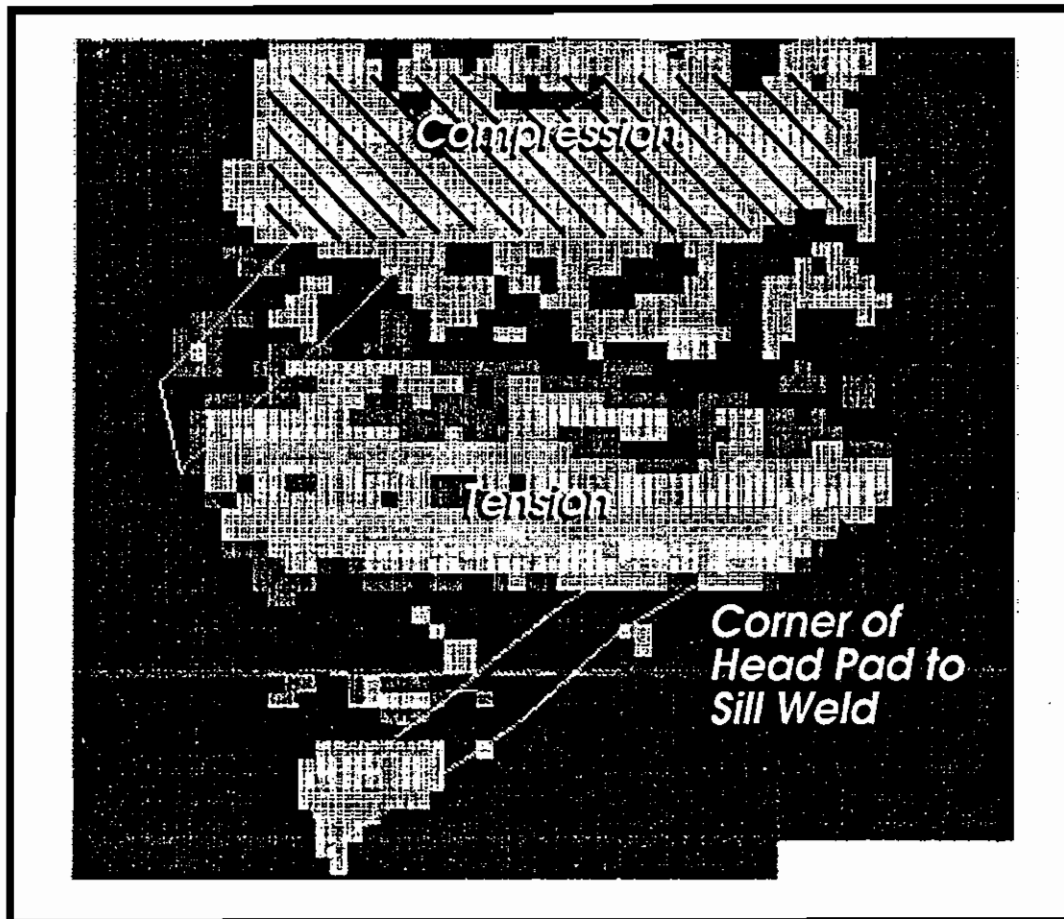
Figure 67. SPATE Stress Map, Stub Sill and Head Pad Area
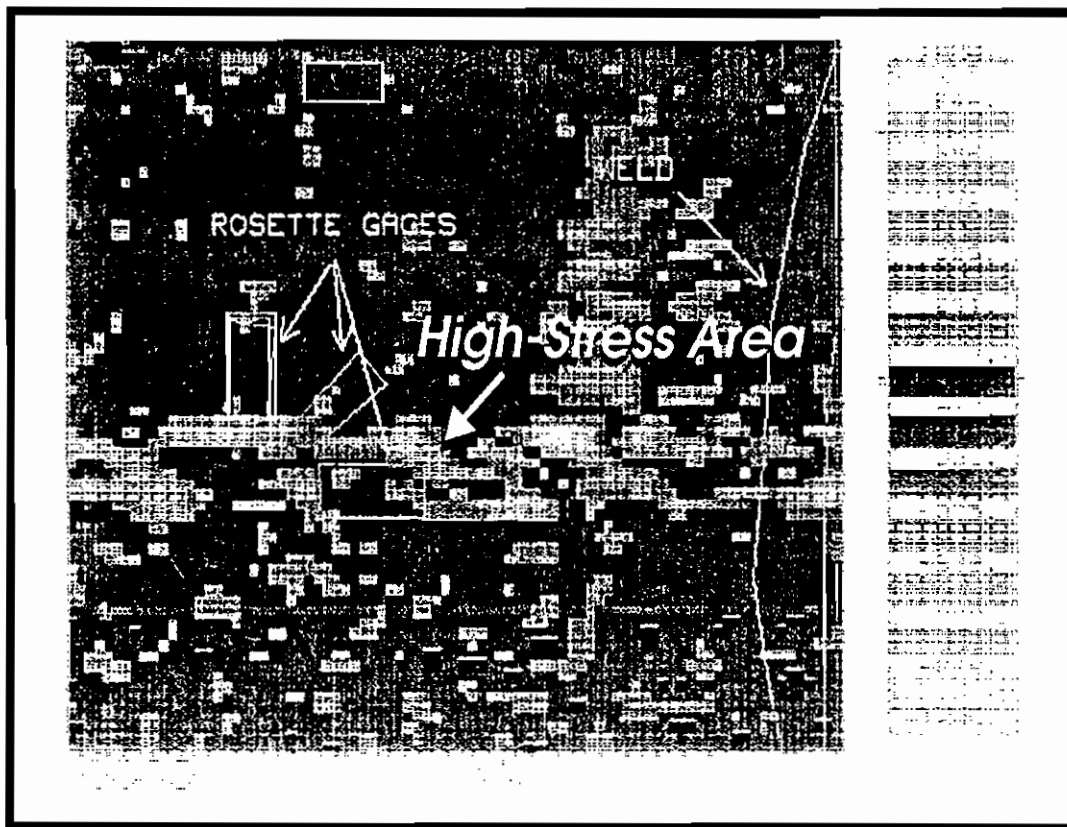
Figure 68. SPATE Stress Map, Tank Car Underside Mid Span

11.3 SIMULOADER TEST BEFORE VERTICAL COUPLER FORCE INPUT — CONCLUSIONS

The Simuloader tests conducted with the 338-second input profile developed from the OTR test data showed the Simuloader's inability to reproduce the vertical coupler force component of the longitudinal coupler loads. The vertical coupler forces, necessary to induce the significant strains at the head pad to stub sill connection, inspired the discussions for adding a vertical coupler load actuator system to the Simuloader.

12.0 SIMULOADER TEST WITH VERTICAL COUPLER FORCE INPUT

12.1 SIMULOADER TEST WITH VERTICAL COUPLER FORCE INPUT — PROCEDURES

During the preliminary exploratory Simuloader fatigue tests, the ability of the Simuloader to re-create the vertical component of coupler loading was closely scrutinized. The criteria

for evaluating the performance of the Simuloader were strain ranges and strain cycle counts. Comparisons of critical-region strain ranges for the OTR, impact, MSU, and exploratory Simuloader tests showed that the Simuloader was unable to reproduce many of the OTR strain ranges due to vertical coupler loading; whereas, the MSU was able to do so. In addition, AAR consultant Samuel Halcomb developed free-body diagrams, shown in Appendix C, which support the need for vertical coupler force.

A hypothesis which may explain this and the vertical coupler load phenomenon, developed by Moyar, is presented below.[17]

> A hypothetical scenario of "explanation" is offered under the assumption that the vertical coupler loading behavior in question is "real." The stub sill will respond to the eccentric buff load such as might occur during severe run-ins by bending downward.... This downward deflection will be resisted at some point when the internal vertical clearance is closed by contact of the sill striker bar with the coupler shank (unless the car is coupled to an identical stub sill car). It is further speculated that the buff/draft vertical deflection response is nonlinear... so that significant deflection only occurs under buff loading above a high longitudinal compression load when a local shell elastic buckling or "oil canning" type response is induced. When such a hypothetical buckling event occurs, the vertical reaction force between the sill and coupler to oppose sill rotation or deflection may be large.

> Such behavior may not, or need not, be symmetrical; that is, the same magnitude of draft may not cause the same magnitude of up deflection. If the B-end instrumented coupler has less vertical clearance for up/down motion or angling within the stub sill than the other end, the vertical reaction at the coupler friction interface with the adjacent (presumably through sill) car may occur and be greater for the B-end. Such a vertical reaction at this end would not occur until a critical buff load is reached and then the reaction force would be much greater than would be expected from the vertical component of the coupler force derived from the coupler inclined angle.

For the reasons above, vertical coupler loading was discussed at a meeting held December 10, 1991, with Oscar Orringer and Jeff Gordon of the VNTSC, Jose Pena and Gunars Spons of the FRA, and AAR representatives. At this meeting it was agreed that vertical coupler loading capabilities be added to one end of the Simuloader. This technique

increased the effectiveness of the Simuloader for reproducing the fatigue environment of stub sill tank cars, especially when combined with the longitudinal coupler loads and vertical displacements currently replicated by the Simuloader.

The improvement did not affect the overall cost of the program because hole drilling measurements and mid-Simuloader test impacts were not conducted. This was addressed at the meeting, and all agreed that the benefits lost from these tasks were minimal compared to the benefit gained by the addition of the vertical coupler loading capability to the Simuloader.

At the meeting, it was also decided to use FEEST load levels, which are published in the AAR *Manual of Standards and Recommended Practices*,[18] as a measure to increase the OTR test data used for Simuloader testing. Specifically, the input longitudinal and vertical coupler loads were scaled up, while the existing OTR test phase relationships remained unchanged. This was done because the OTR test loads, which contain the necessary phase relationships required to operate the Simuloader, were not as severe as the published FEEST design data. Also the FEEST data, plotted in this report in counts of load cycles, is commonly used for fatigue life predictions of new car designs. Thus, the fatigue input loads used became hybrid version of the OTR test data. The techniques developed for doing this work were dubbed the "Enhanced Input Profile Development Methodology." Figures 69 and 70 are comparisons of vertical and longitudinal coupler force occurrences at level for the 338-second OTR test data and the FEEST vertical coupler forces measured for a loaded tank car over 22,994 miles. From these figures, the motivation to utilize the FEEST load levels is clearly evident.

COMPARISON OF 338 SECOND (OTR) VCF TO FEEST VCF

NO. OF CYCLES AT LEVEL

P-P VERTICAL COUPLER FORCE (KIPS)

■ "SIGNIFICANT" OTR DATA   ◆ FEEST DATA
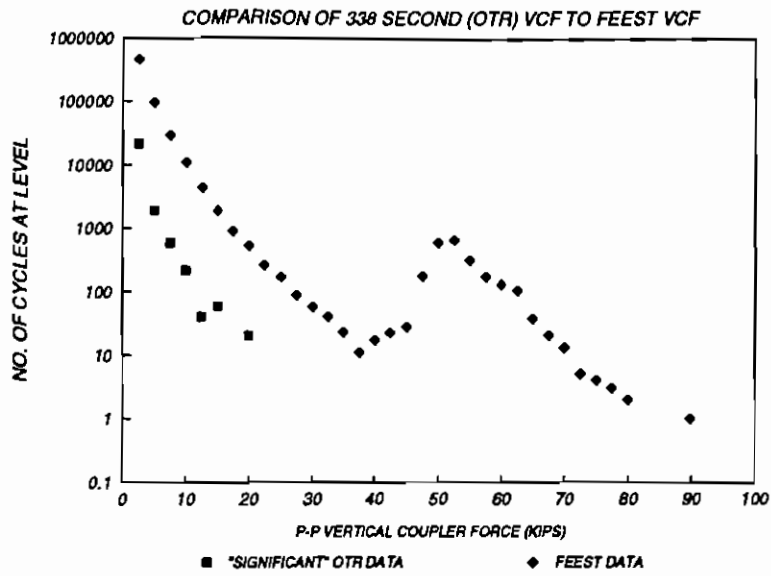
Figure 69. Comparison of FEEST Data to OTR Test Data --
Vertical Coupler Force

COMPARISON OF 338 SECOND (OTR) LCF TO FEEST LCF

NO. OF CYCLES AT LEVEL

P-P LONGITUDINAL COUPLER FORCE (KIPS)

■ "SIGNIFICANT" OTR DATA   ◆ FEEST DATA
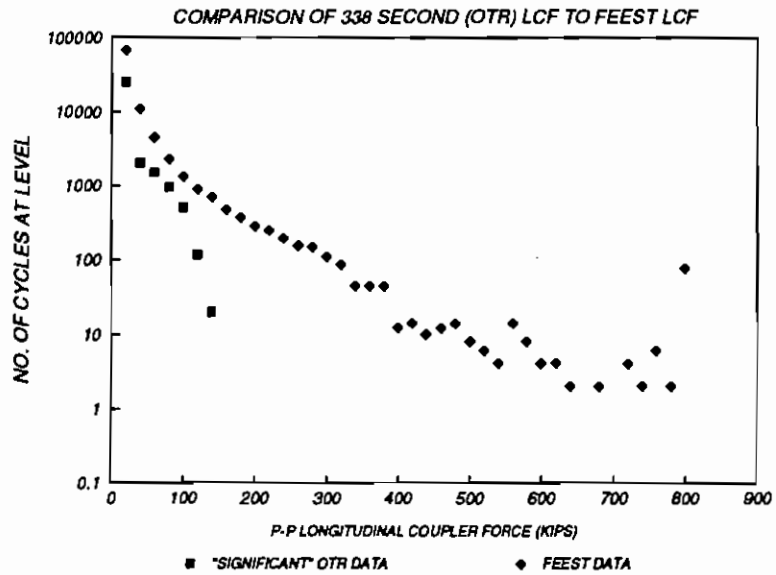
Figure 70. Comparison of FEEST Data to OTR Test Data --
Longitudinal Coupler Force

12.1.1 Vertical Coupler Addition to Simuloader Test Facility

A 110-kip actuator with a MTS 256 servo valve was used to apply the vertical coupler loads. A fixture was designed to allow vertical coupler loads to be introduced through the underside of the B-end of the tank car. Figure 71 shows the overall schematic drawing of the fixture and actuator system.

Figure 71. Vertical Coupler Load Fixture

12.1.2 Vertical Coupler Force Signal Generation

The calibration data of SG01 response versus vertical coupler load, presented in Section 8.2.1.1, was the main component for the synthetic generation of a vertical coupler force signal. A linear-regression fit of the data resulted in the following equation:

$$VCF(kips) = -\frac{SG01 - 50.2}{15.22}$$

where: Positive = upward force
          Negative = downward force

Strain gage SG01, on top of the sill between the front and rear draft stops, could not record structural strain due to buff forces because it was located in front of the rear draft gear reaction points. Therefore, in buff loading, strains recorded by SG01 were only associated with sill bending. In draft loading situations, however, the longitudinal strain component was backed out. Thus, the synthetic generation of the vertical coupler force input signal was as follows:

$$\text{BUFF} \quad VCF(kips) = -\frac{SG01 - 50.2}{15.22}$$

$$\text{DRAFT} \quad VCF(kips) = -\frac{SG01 - 50.2}{15.22} - \frac{LCF_{Draft}}{Area_{Sill}E}$$

### 12.1.3 Enhanced Input Profile Development Methodology

The enhanced input profile development methodology involves synthetic matching of the number and magnitude of published vertical and longitudinal coupler load cycles. The published data were obtained from a tank car subjected to a variety of environmental conditions during revenue service. The data, published in AAR's *Manual of Standards and Recommended Practices*,[19] are commonly used for fatigue life calculations for freight cars and were acquired under the AAR FEEST test program.

Use of the AAR's published fatigue coupler-loads data for Simuloader inputs in itself is not possible because the data exists only in histogram form, whereas the Simuloader requires time history signals to operate. Therefore, the published coupler loads were incorporated with actual representative time histories of coupler forces and bolster motions from the OTR test.

The vertical coupler force cycles, deemed most important, were the main concentration of this technique. The corresponding longitudinal coupler load cycles were also considered extremely important. However, the best re-creation of the published loads

was for the vertical coupler forces. The first step in this technique was to select approximately 60 seconds of representative data from the 750 seconds of OTR test data. Next, the vertical and longitudinal coupler load cycles from this time slice were counted by a rainflow counting routine to obtain a histogram of the load cycles, then compared to the AAR's published data histogram for severe loaded tank car service. The final step was to multiply the short time slice vertical coupler loads with several amplification factors, then repeat and append the various 60-second amplified time histories, with the addition of several individual makeup cycles, into three long duration files. The resulting vertical and longitudinal coupler force cycles were subsequently compared in histogram format to the published data to ensure a reasonable match.

Figure 72 displays cycle counts of vertical coupler force for the FEEST data, the 60-second section of the OTR data selected, and of the final input file created from the OTR data. Figures 73 and 74 present similar results for the buff and draft longitudinal coupler loads.
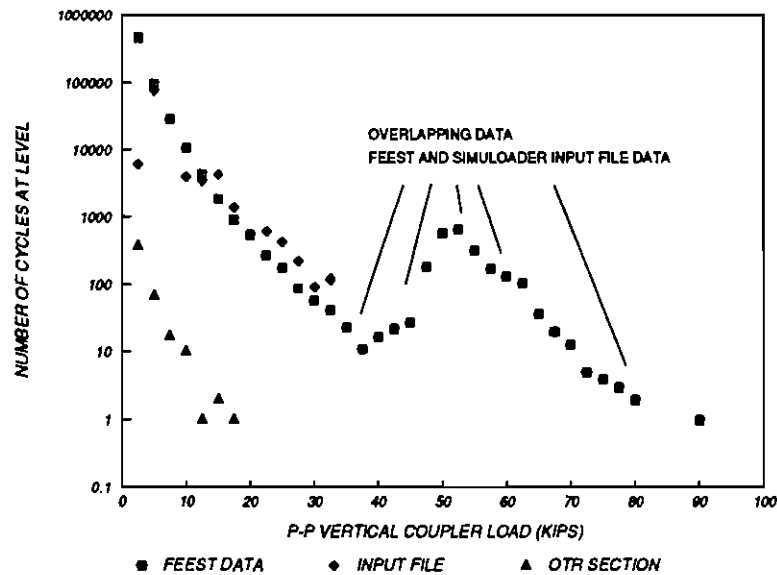
Figure 72. FEEST Data, 60-second OTR, and Final Input Data --
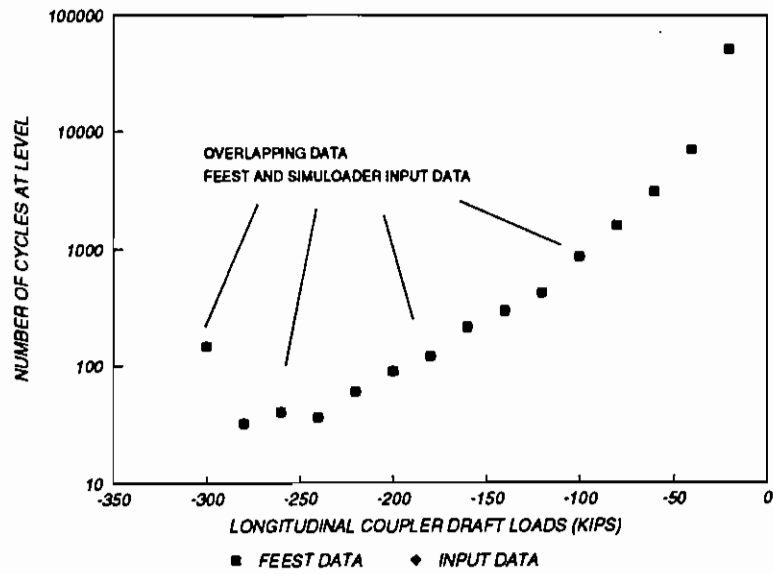**Vertical Coupler Force**

**Figure 73. FEEST Data, 60-second OTR, and Final Input Data --
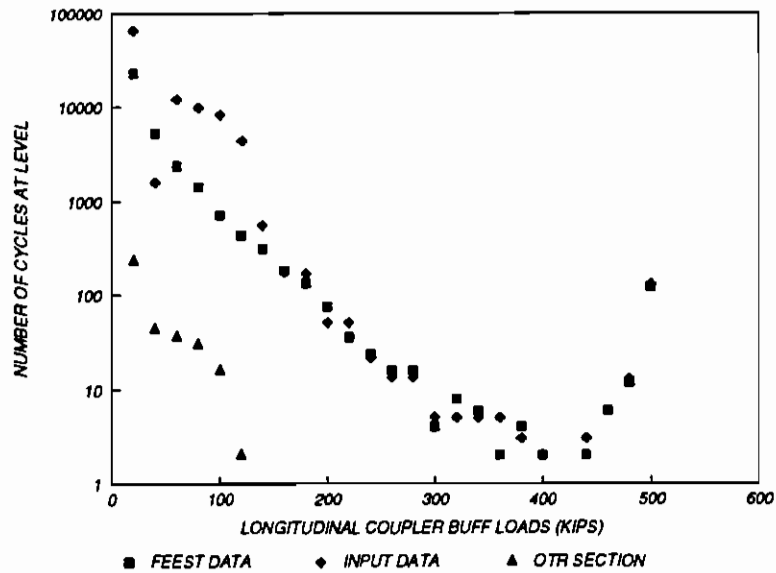Longitudinal Coupler Force Buff**

**Figure 74. FEEST Data, 60-second OTR, and Final Input Data --
Longitudinal Coupler Force Draft**

In terms of fatigue crack growth, median value of input loads may be important in addition to the peak-to-peak cycle value shown thus far. Thus, a peak-to-peak cycle load of 0 to 100 kips might have a different effect on fatigue if input on a structure at 500 to 600 kips.

Three-dimensional charts can be used to display this term with the load ranges shown previously. However, unless the data are extremely simplistic, these representations can be confusing. Therefore, the maximum, minimum, and average median value of the input load peak-to-peak cycles are displayed separately, as shown in Figures 75 and 76. A difference does exist between the synthetic input load median values and the FEEST median values. However, given the method of extrapolation of the input loads, these differences are quite reasonable.
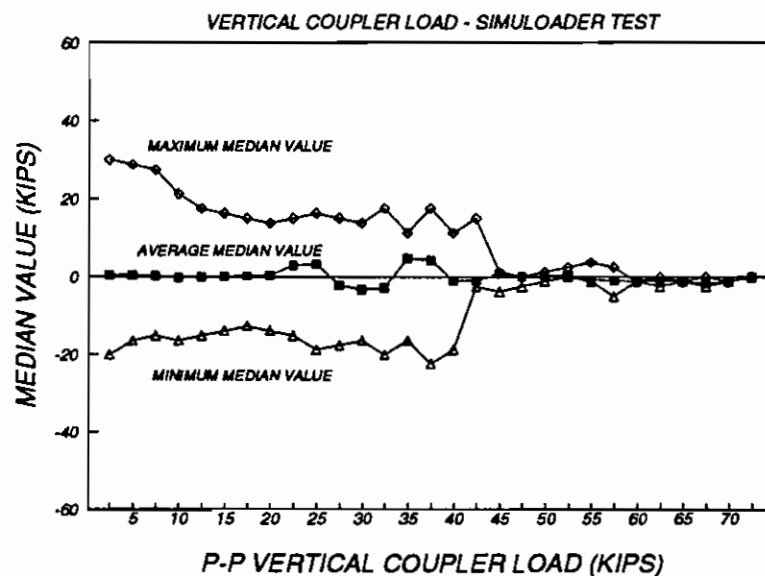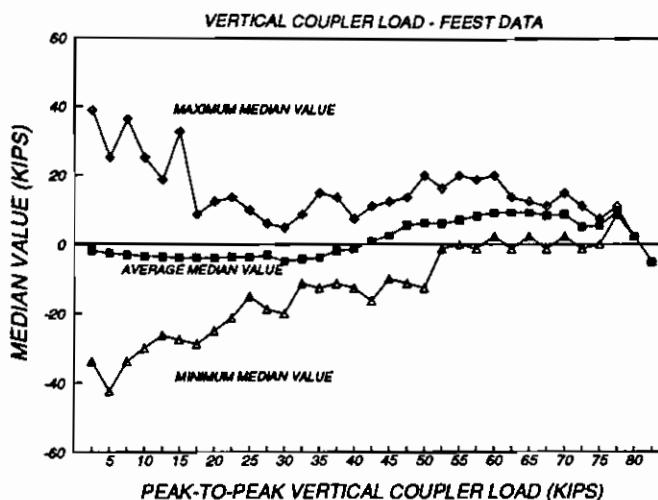

Figure 75. Median Value for FEEST Vertical Coupler Force Data

Figure 76. Median Value for Final Simuloader Input
Vertical Coupler Force Data

12.1.3.1 Final Simuloader Excitation Input Profile

The FEEST loads replicated, containing 22,994 loaded-car miles of significant loads, encompassed nearly five hours of input data, for an accelerated-test rate of 4,400 miles of simulated loaded-car service in one hour of test operation. This history, broken into four files (FILE1.RCF, FILE2.RCF, FILE3.RCF and FILE4.RCF), was repeated 13 times to complete the 300,000 mile fatigue test. In addition, the 338 second OTR test data inputs were run each 22,994 mile load cycle. The resulting data from the 338-second test, short in duration compared to files 1 through 4 (allowing quick analysis to be done), was used to ensure consistent Simuloader operation. Table 26 describes the input files.

Table 26. Simuloader Test With Vertical Coupler Force -- Input Files

Input File	Approx. Seconds	Comment
TFILE.RCF	338	OTR Test Input Data
FILE1.RCF	3260	First of four files containing 22,994 loaded-car miles of FEEST level inputs
FILE2.RCF	2941	Second of four files containing 22,994 loaded-car miles of FEEST level inputs
FILE3.RCF	4080	Third of four files containing 22,994 loaded-car miles of FEEST level inputs -- to be run twice per cycle
FILE4.RCF	3480	Fourth of four files containing 22,994 loaded-car miles of FEEST level inputs

12.1.3.2 FEEST Test Procedures

A detailed account of the AAR FEEST program was presented by Sharma and Punwani in 1984.[20]

12.1.4 Test Instrumentation

The measurements recorded during the Simuloader tests without the vertical coupler load capability were recorded during the Simuloader tests with vertical coupler load. In addition, several measurements, listed in Table 27, were added. The additional measurements were strain gages positioned in an attempt to determine the effect of stress concentration in the critical region. The data van was used again to house the instrumentation hardware and computer systems for the Simuloader tests. The HP data acquisition systems were also continued to be used.

Table 27. Additional Measurements for Simuloader Tests with
Vertical Coupler Load Input

Name	Description and Location	Type	Est. Range
SG45	B-End Head Pad Left Corner Vertical Strain, Chevron Inside SG28-30	Strain-Gage	±4000 µε
SG46	B-End Head Pad Left Corner Diagonal Strain, Chevron Inside SG28-30	Strain-Gage	±4000 µε
SG47	B-End Head Pad Left Corner Lateral Strain, Chevron Inside SG28-30	Strain-Gage	±4000 µε
SG48	B-End Head Pad Left Corner Vertical Strain, Chevron Inside SG28-30	Strain-Gage	±4000 µε
SG49	B-End Head Pad Left Corner Diagonal Strain, Chevron Inside SG28-30	Strain-Gage	±4000 µε
SG50	B-End Head Pad Left Corner Lateral Strain, Chevron Inside SG28-30	Strain-Gage	±4000 µε

12.1.5 Test Procedure

Simuloader vertical coupler load input development testing and the 300,000 mile fatigue testing, with the vertical coupler load actuator system, began on February 5, 1992, and was completed on April 2, 1992.

The development tests included static calibrations of vertical coupler force and longitudinal coupler force, checkout runs to ensure proper control of the new vertical

coupler load force input, sinusoidal input profile tests to evaluate the ability to excite car body midspan responses, and tests with the OTR input profile summed with sinusoidal "dither" in an attempt to better excite the mid-span responses.

Thirteen load cycles, comprised of TFILE and the FILE1-4 input profiles, were performed. Thus, a total of 298,922 loaded-car miles of FEEST replicated input profiles were run. The OTR test data (TFILE), was not used in the mileage calculation. Table 28 lists the tests conducted. The run numbers designate the HP computer file number.

NDE inspections with dye penetrant were done at 22,994 mile intervals (for each load cycle) to monitor crack growth.

Table 28. Simuloader Test With Vertical Coupler Force -- Test Matrix

Run	Description
TANK_RN500	Static vertical coupler force calibration, ±20 kips VCF
TANK_RN501	Static longitudinal coupler force calibration, ±300 kips LCF
TANK_RN502 - TANK_RN504	TFILE.RCF input, 50% vertical coupler force signal -- to determine responsiveness and control of vertical coupler force input system with dynamic inputs.
TANK_RN505 - TANK_RN508	TFILE.RCF input, 100% vertical coupler force signal -- to determine responsiveness and control of vertical coupler force input system with dynamic inputs.
TANK_RN509 - TANK_RN510	TFILE.RCF input, 100% vertical coupler force signal. Increase vertical bolster displacements to 150% to improve the accuracy of the level of the side bearing strikes.
TANK_RN511	TFILE.RCF input, 100% vertical coupler force signal. Add shims to side bearings. Run with vertical bolster displacements at 100%.
TANK_RN512	TFILE.RCF input, 100% vertical coupler force signal. With side bearing shims added, increase vertical bolster displacements to 150% to improve the accuracy of the level of the side bearing strikes.
TANK_RN513 - TANK_RN515	Sinusoidal testing to obtain "dither" levels to improve tank midspan response during Simuloader testing.
TANK_RN516 - TANK_RN519	TFILE.RCF input summed with various levels of dither to determine if midspan responses are improved.
TANK_RN520 - TANK_RN550	Fatigue cycle 1, 22,994 miles, all data recorded. TFILE input = RN520. Inputs FILE1-4 correspond to runs 521 - 550.
TANK_RN551 - TANK_RN576	Fatigue cycle 2, 45,988 miles, all data recorded. TFILE input = RN551. Inputs FILE1-4 correspond to runs 552 - 576. Vertical coupler force input gains adjusted slightly to improve fatigue simulation (based on fatigue analysis of cycle 1).
TANK_RN577	Fatigue cycle 3, 68,982 miles. Only TFILE input recorded.
TANK_RN578	Fatigue cycle 4, 91,976 miles. Only TFILE input recorded.
TANK_RN579	Fatigue cycle 5, 114,970 miles. Only TFILE input recorded.
TANK_RN580 - TANK_RN590	Fatigue cycle 6, 137,964 miles, all data recorded. TFILE input = RN580. Inputs FILE1-4 correspond to runs 581 - 590.
TANK_RN591	Fatigue cycle 7, 160,958 miles. Only TFILE input recorded.

Table 28. Simuloader Test With Vertical Coupler Force -- Test Matrix -- continued

TANK_RN592 - TANK_RN593	Fatigue cycle 8, 183,952 miles. Only TFILE input recorded.
TANK_RN594	Fatigue cycle 9, 206,946 miles. Only TFILE input recorded.
TANK_RN595	Fatigue cycle 10, 229,940 miles. Only TFILE input recorded.
TANK_RN596	Fatigue cycle 11, 252,934 miles. Only TFILE input recorded.
TANK_RN597	Fatigue cycle 12, 275,928 miles. Only TFILE input recorded.
TANK_RN601	Fatigue cycle 13, 298,922 miles. Only TFILE input recorded. HP runs 598 - 600 were aborted.
TANK_RN602	Post fatigue cycle 13, 298,922 miles. Only TFILE input recorded.

12.1.6 Test Documentation

Photographs and video were taken during the conduct of the Simuloader test with the vertical coupler load actuator.

12.1.7 Test Validation

Comparisons of histograms and computed fatigue lives using the FEEST data and the loads produced by the Simuloader were done to validate the simulation.

12.1.8 Test Data Analysis

Statistics and time histories were used for data analysis to ensure proper simulation throughout the fatigue test and to indicate changes in tank car structure integrity.

12.1.9 Fatigue Analysis

AAR's Fatigue Life Analysis Program (FLAP) was used to compute fatigue life with the FEEST data and with Simuloader test data.

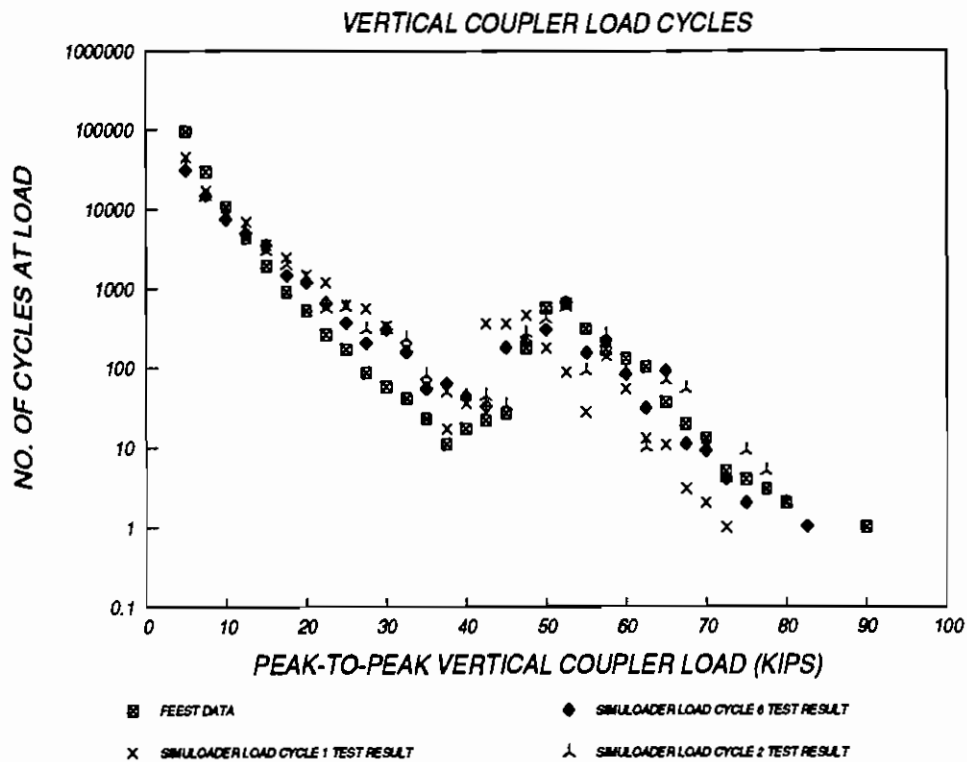## 12.2 SIMULOADER TEST WITH VERTICAL COUPLER FORCE INPUT -- RESULTS

12.2.1 Input Development Results/Input Validation

Sections 12.2.1 through 12.2.3 illustrate the validity of the final input profile with comparative plots of input load and response cycles, time histories, and autospectral densities. Section 12.2.4 shows comparisons of the computed fatigue life for the desired FEEST loads and the actual loads produced by the Simuloader. Section 12.2.4 also shows the computed critical region fatigue life based on the calculated principal stress.

The validation results given in Sections 12.2.1 through 12.2.4 also demonstrate the improvement of the tank car critical region strain responses on the Simuloader by the additon of the Simuloader vertical coupler force capability. Results shown for critical region strain gage SG08 illustrate the improvement. Not shown are critical region strain gages SG09 and SG10, with SG10 getting the most improvement and SG09 seeing some improvement. The computed fatigue life based on principal stress values, given in Table 29 in Section 12.2.4, shows that the critical region is subjected to the proper fatigue loading with the addition of the vertical coupler force capability in combination with the FEEST loads.

12.2.1.1 Cycle Counting

Figure 77 illustrates the comparison of the AAR published vertical coupler load cycles to the loads introduced as Simuloader inputs. Similar results, though not as precise, were obtained for the longitudinal coupler force inputs.

VERTICAL COUPLER LOAD CYCLES

Figure 77. Simuloader Test and FEEST Vertical Coupler Force Cycles

Side bearing loading is not a direct Simuloader input. However, this response can be modified by adjusting side bearing clearance and increasing or decreasing the gain on the vertical actuator bolster displacements. Figure 78 compares the cycle counts for the FEEST right and left side bearing loads to side bearing loads recorded during the Simuloader test input load cycles 1 and 2. The difference is characteristic to the rocking motions encountered in transit for the FEEST test and the OTR test conducted under this program. The load cycle 2 data shows the effect of adjusting side bearing clearance.

113
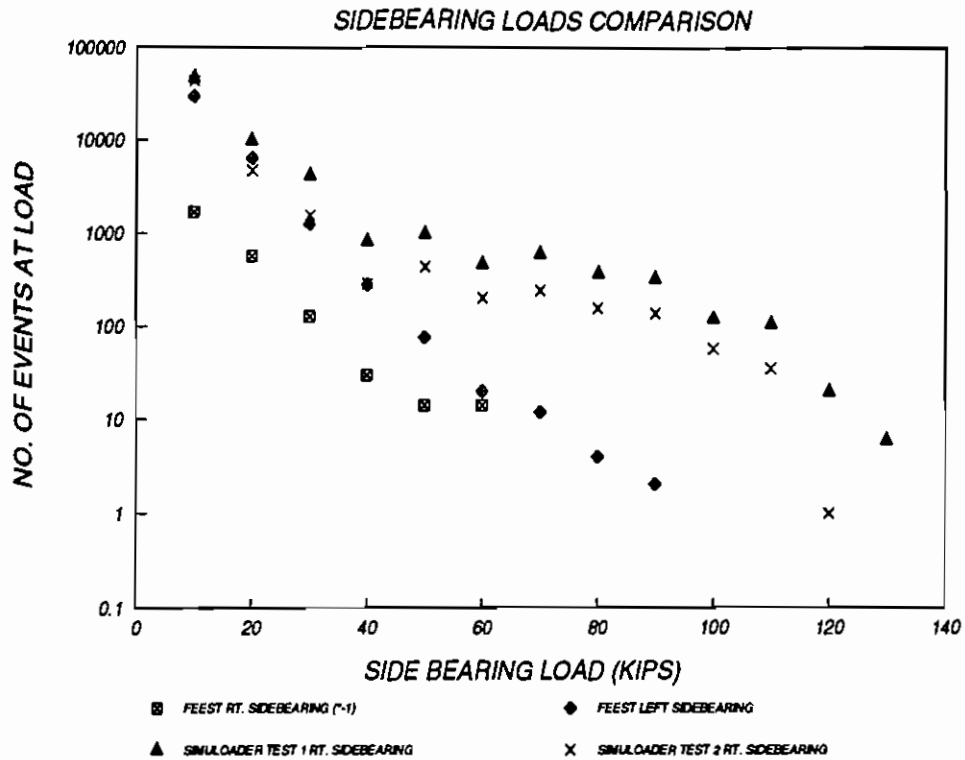
Figure 78. Simuloader Test and FEEST Side Bearing Loads
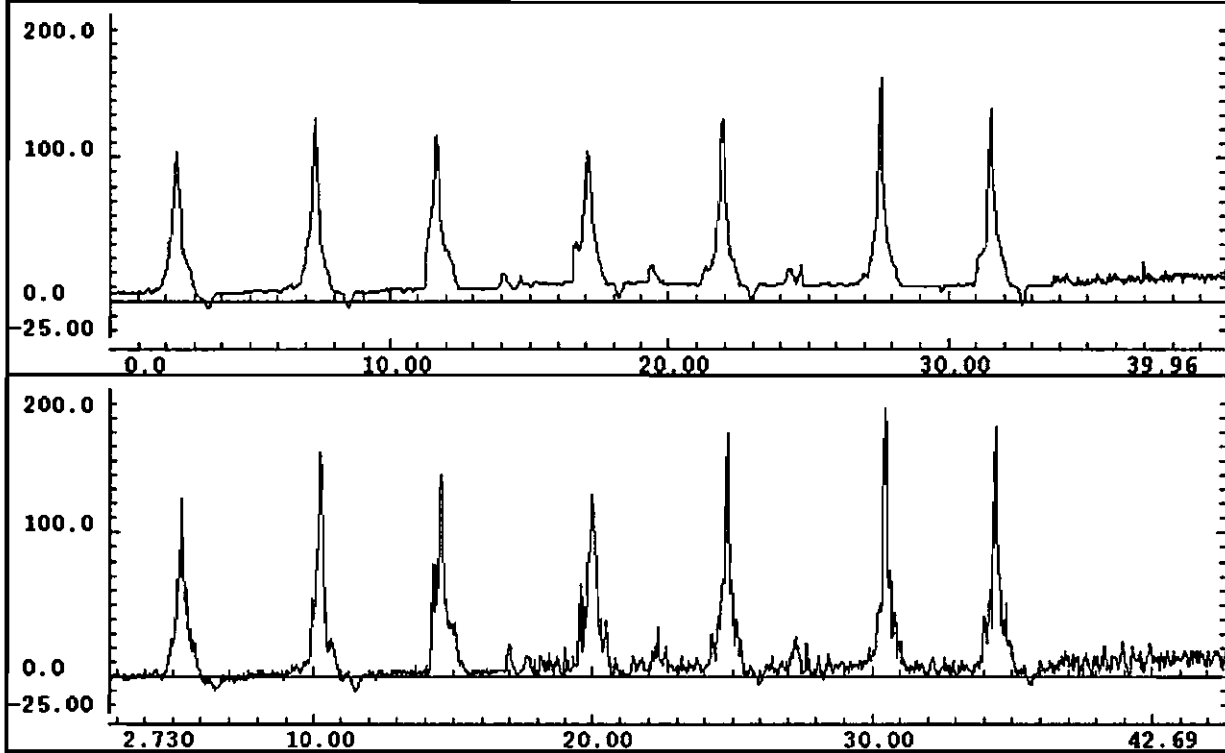
12.2.1.2 Time Histories

Figures 79-81 contain selected time histories which demonstrate the quality of the Simulation by showing OTR test longitudinal and vertical coupler force data with corresponding Simuloader test data. Figures 79 and 80 display the longitudinal coupler force signal from the OTR test and the Simuloader test with vertical coupler force.

Figure 81 displays an example of the vertical coupler force signal from the OTR test and Simuloader test with vertical coupler force input. This data was digitally low-pass filtered at 10 Hz to show the similarity of the motions.

LONGITUDINAL COUPLER FORCE COMPARISON
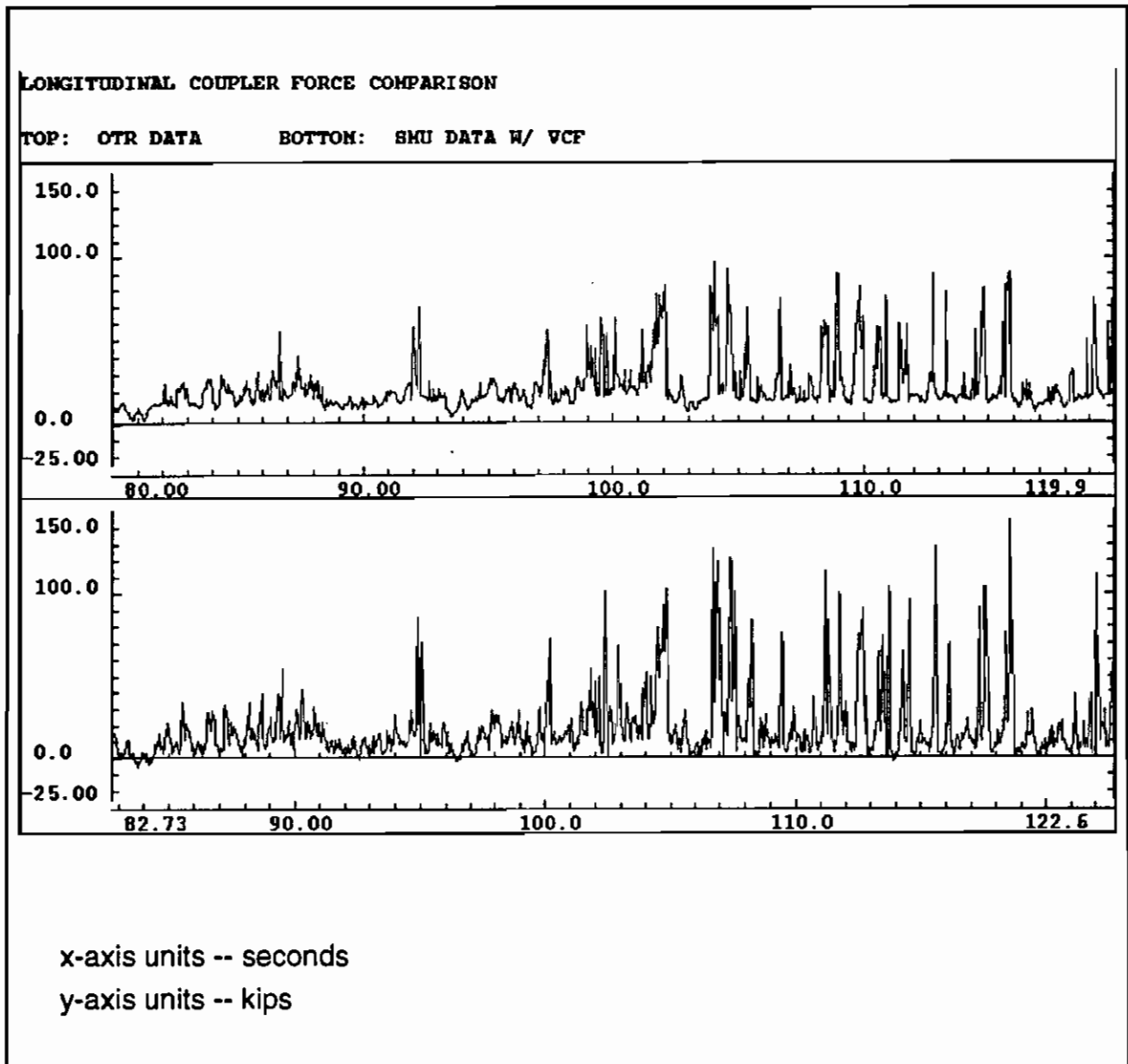
TOP: OTR DATA   BOTTOM: SMU DATA W/ VCF

x-axis units -- seconds
y-axis units -- kips

Figure 79. OTR and Simuloader Test Time Histories --
Longitudinal Coupler Force

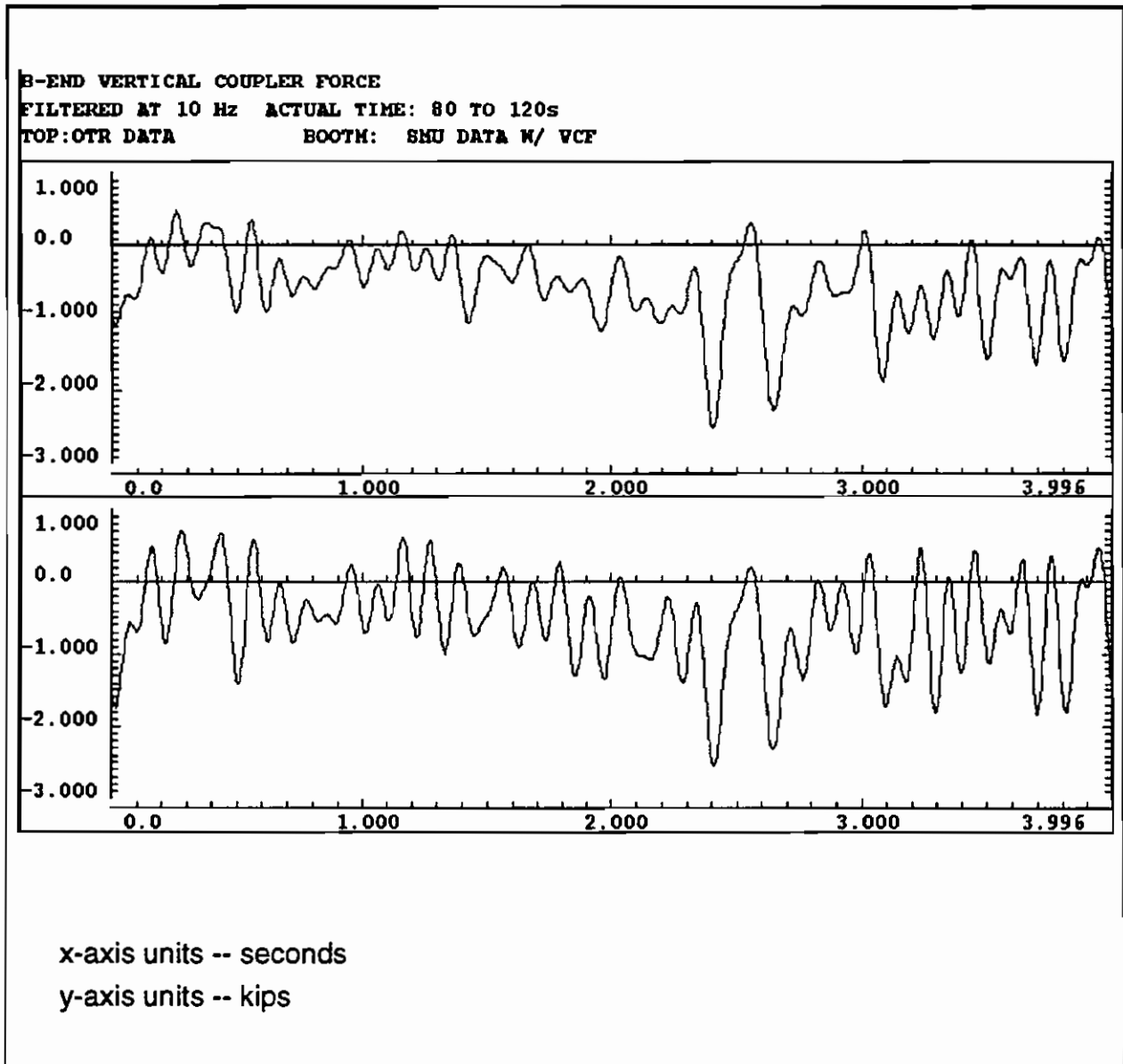Figure 80. OTR and Simuloader Test Time Histories --
Longitudinal Coupler Force

B-END VERTICAL COUPLER FORCE
FILTERED AT 10 Hz   ACTUAL TIME: 80 TO 120s
TOP:OTR DATA   BOOTM: SMU DATA W/ VCF

x-axis units -- seconds
y-axis units -- kips

Figure 81. OTR and Simuloader Test Time Histories --
Vertical Coupler Force

12.2.1.3 Autospectral Densities

Autospectral density plots, also known as power spectral density (PSD) plots, illustrate the frequency content of data. Figures 82 through 89 display PSD plots of longitudinal and vertical coupler forces, critical-region strain gage measurement SG08 response, and car body lateral acceleration measurement AX3 response replicated by the Simuloader. For each measurement, the top spectrum is the OTR test result, and the bottom is the Simuloader test result.

Two time histories are given for each of the measurements presented. The first given for each measurement is scaled from 0 to 30 Hz. The second time history is scaled from 0 to 5 Hz. In each case, the PSD plot shows evidence of the Simuloader, with vertical coupler force ability, to re-create the environment below 5 Hz. Although some anomalies occur on the Simuloader spectrum above 5 Hz, the Simuloader was generally able to re-create desired response. This accuracy of the Simuloader responses below 5 Hz is more notable when it is realized that the gross motions experienced by a railcar are below 5 Hz.
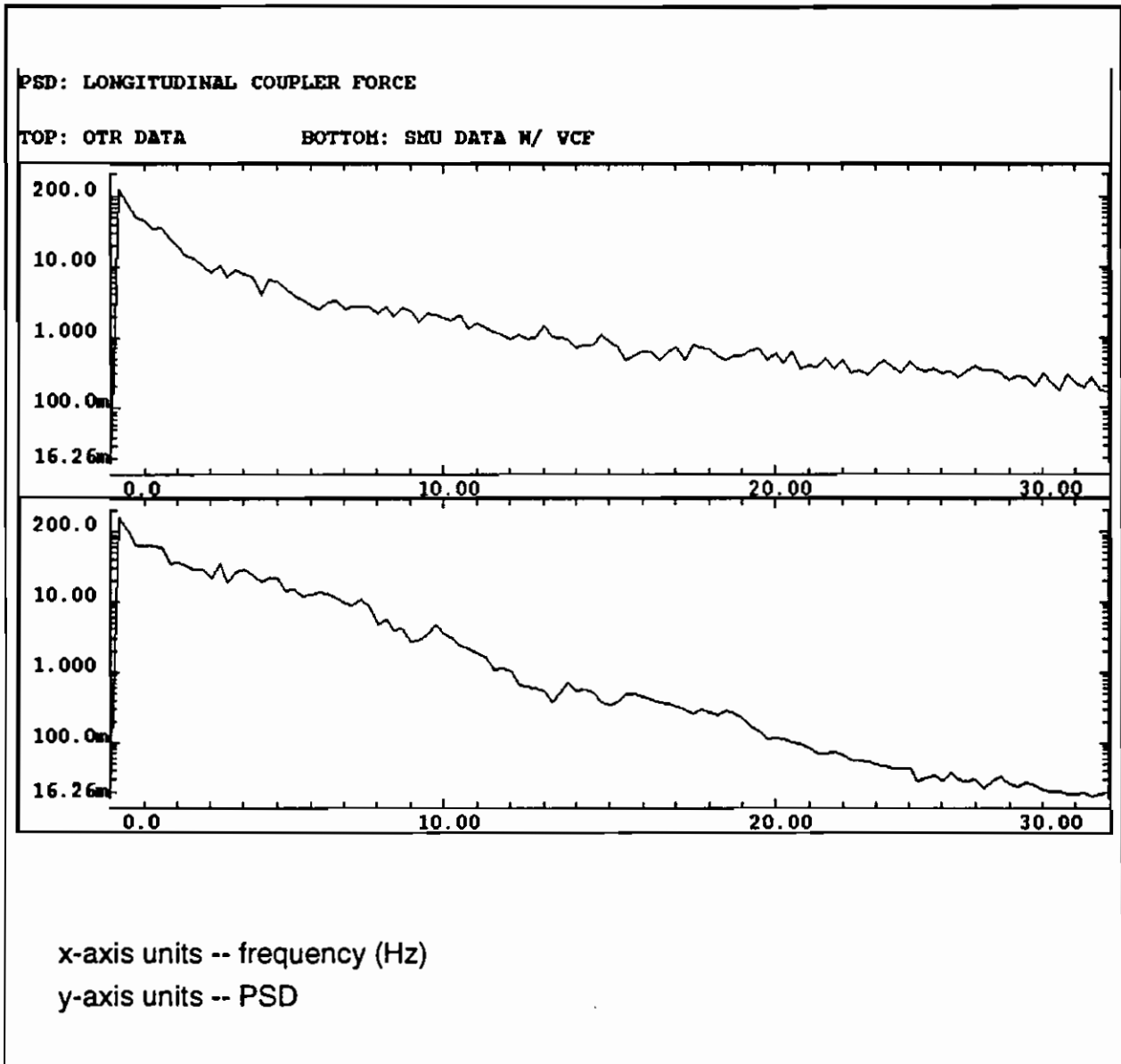
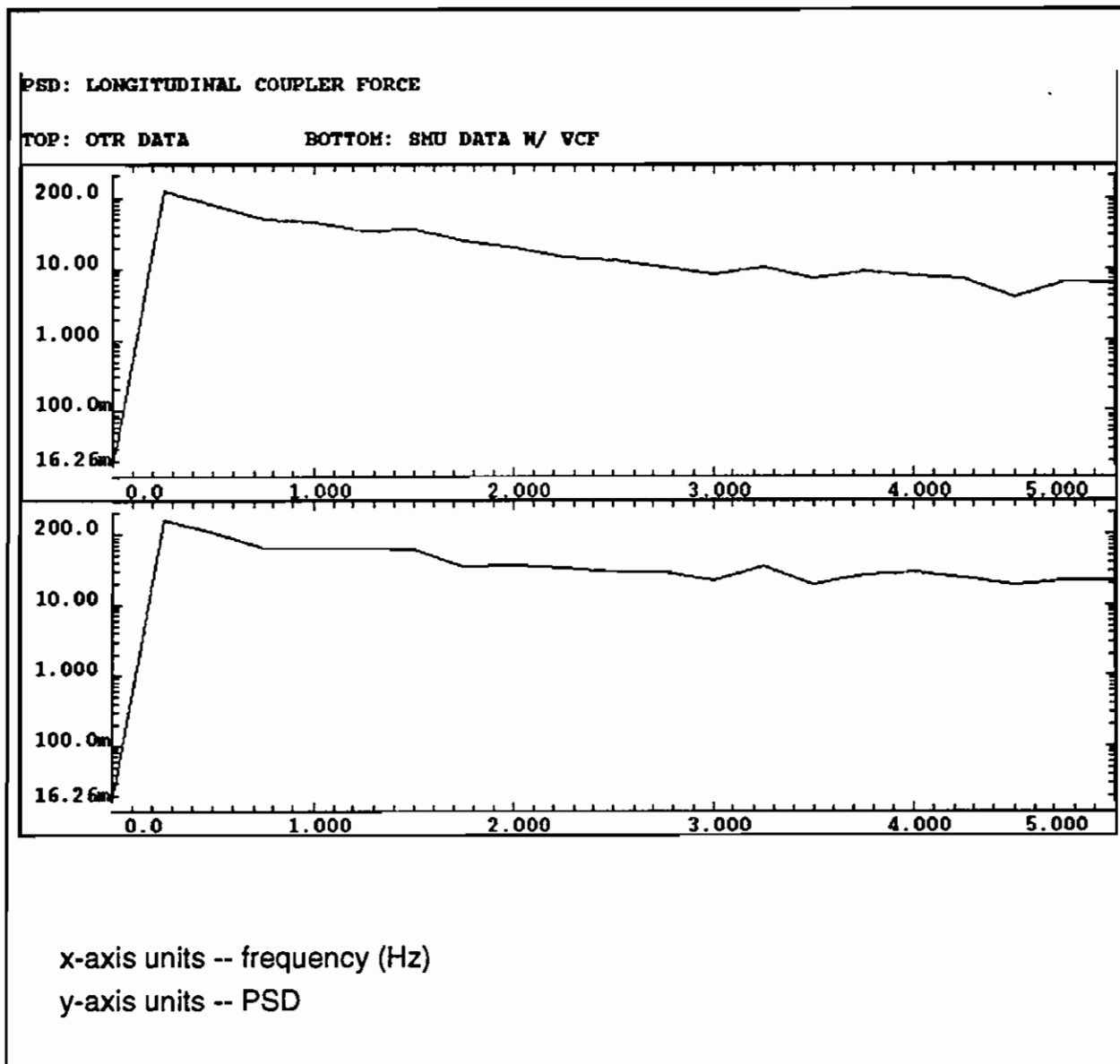Figure 82. OTR and Simuloader Test 30Hz PSD Plots --
Longitudinal Coupler Force

PSD: LONGITUDINAL COUPLER FORCE

TOP: OTR DATA   BOTTOM: SMU DATA W/ VCF

x-axis units -- frequency (Hz)

y-axis units -- PSD

Figure 83. OTR and Simuloader Test 5 Hz PSD Plots --
Longitudinal Coupler Force

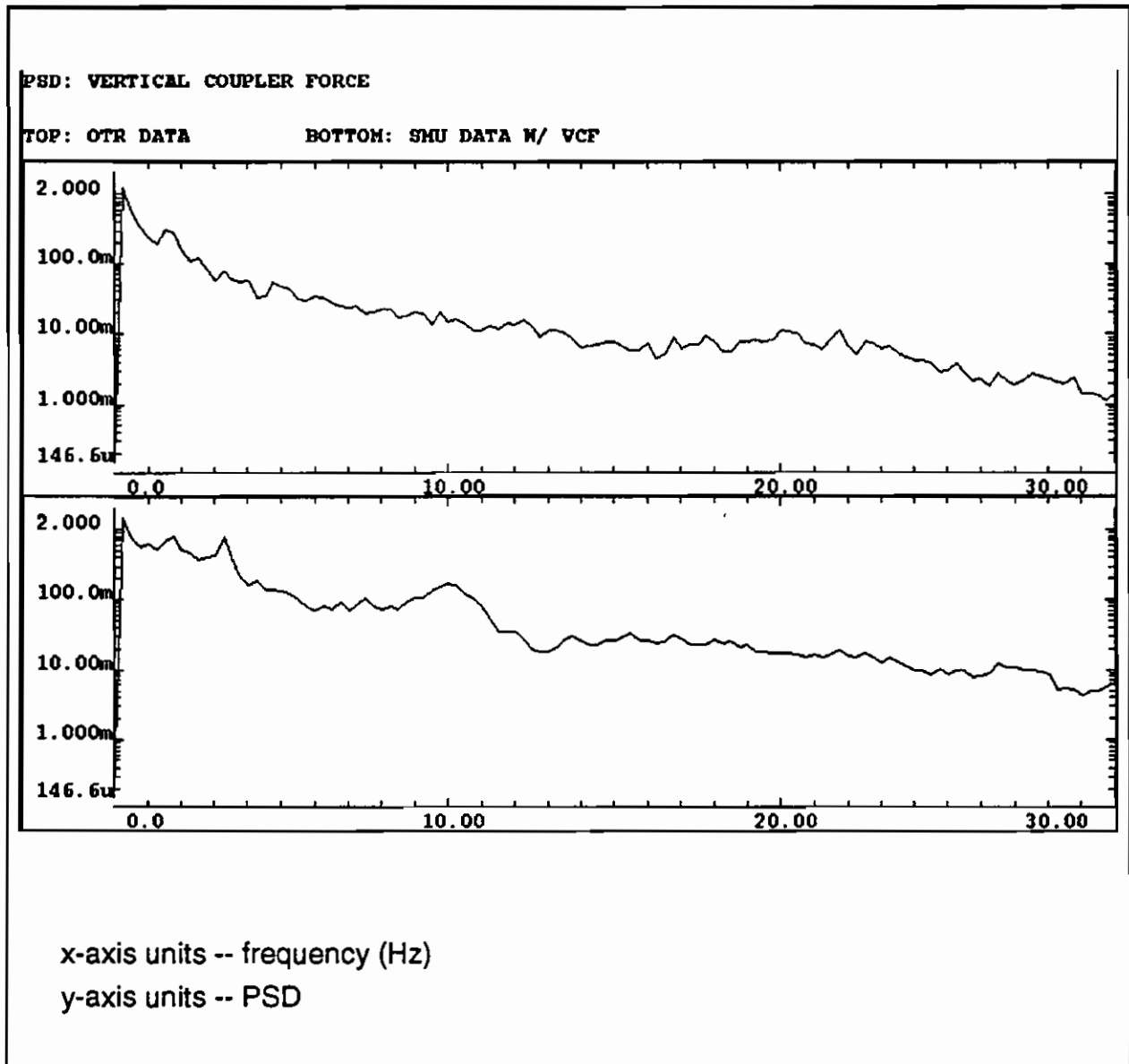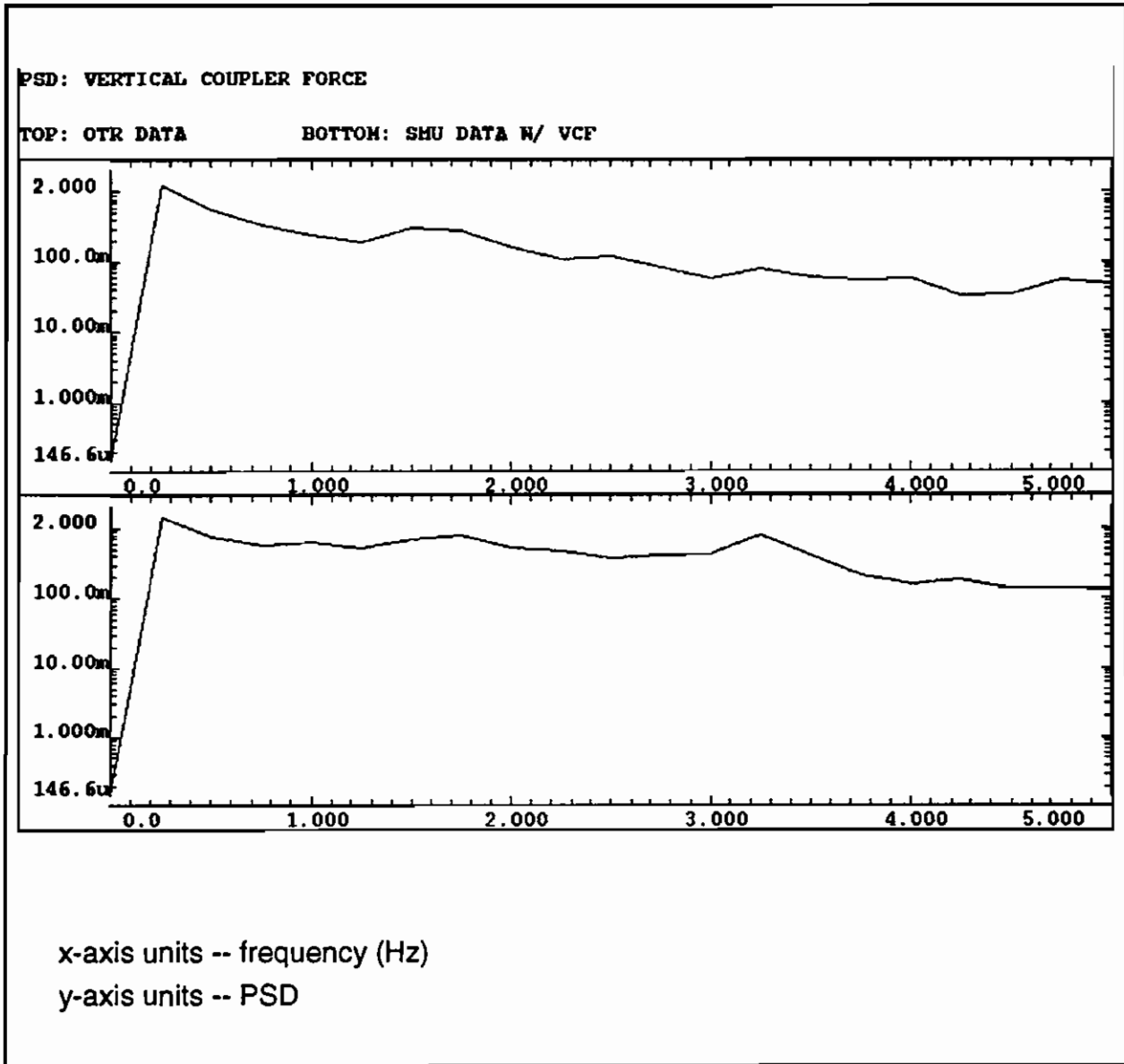Figure 84. OTR and Simuloader Test 30 Hz PSD Plots --
Vertical Coupler Force

PSD: VERTICAL COUPLER FORCE

TOP: OTR DATA   BOTTOM: SMU DATA W/ VCF

x-axis units -- frequency (Hz)

y-axis units -- PSD

Figure 85. OTR and Simuloader Test 5 Hz PSD Plots --
Vertical Coupler Force

PSD: SG08, B-END HEAD PAD CORNER, VERTICAL

TOP: OTR DATA   BOTTOM: SMU DATA W/ VCF

x-axis units -- frequency (Hz)
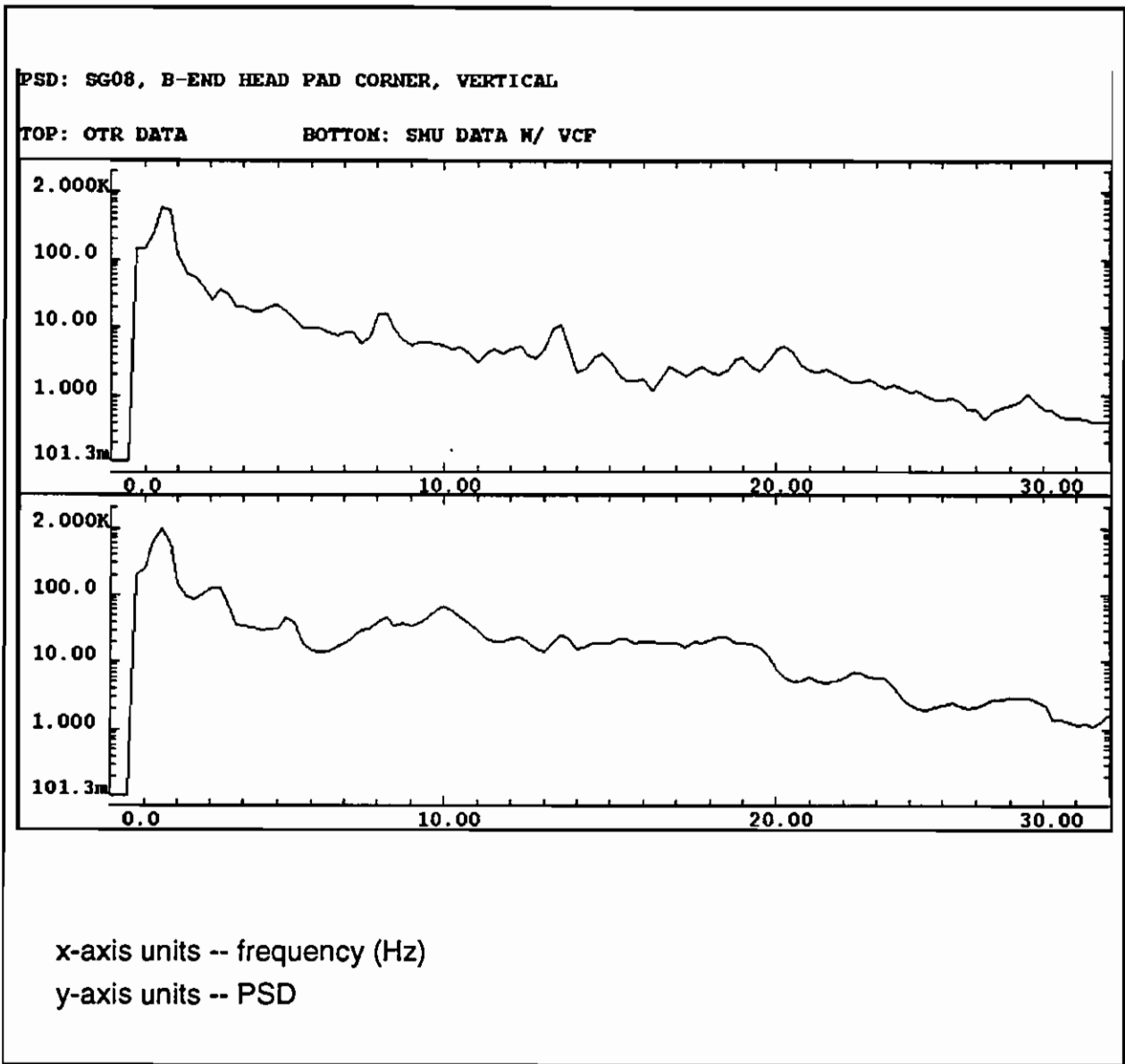y-axis units -- PSD

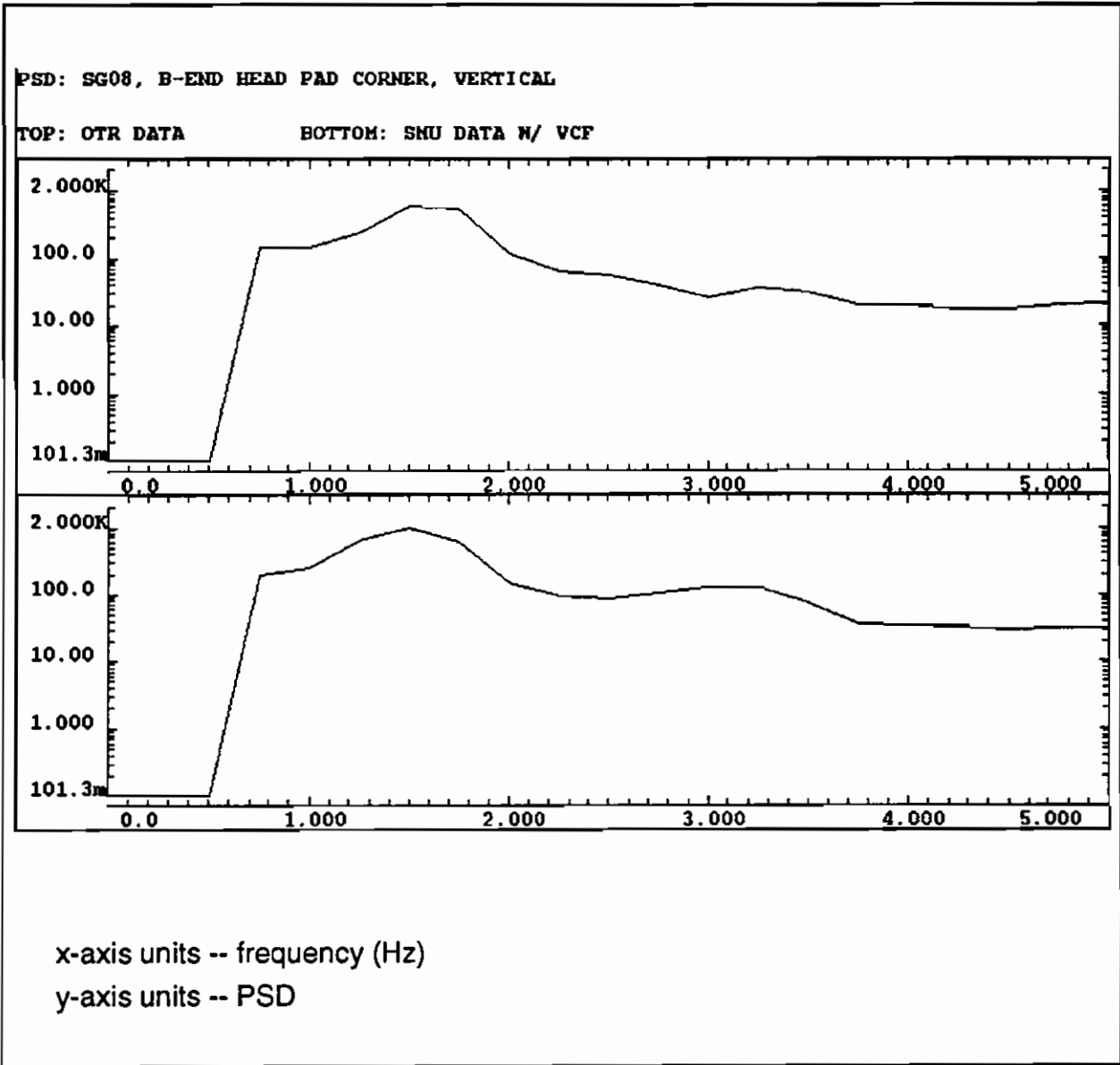**Figure 86. OTR and Simuloader Test 30 Hz PSD Plots -- SG08**

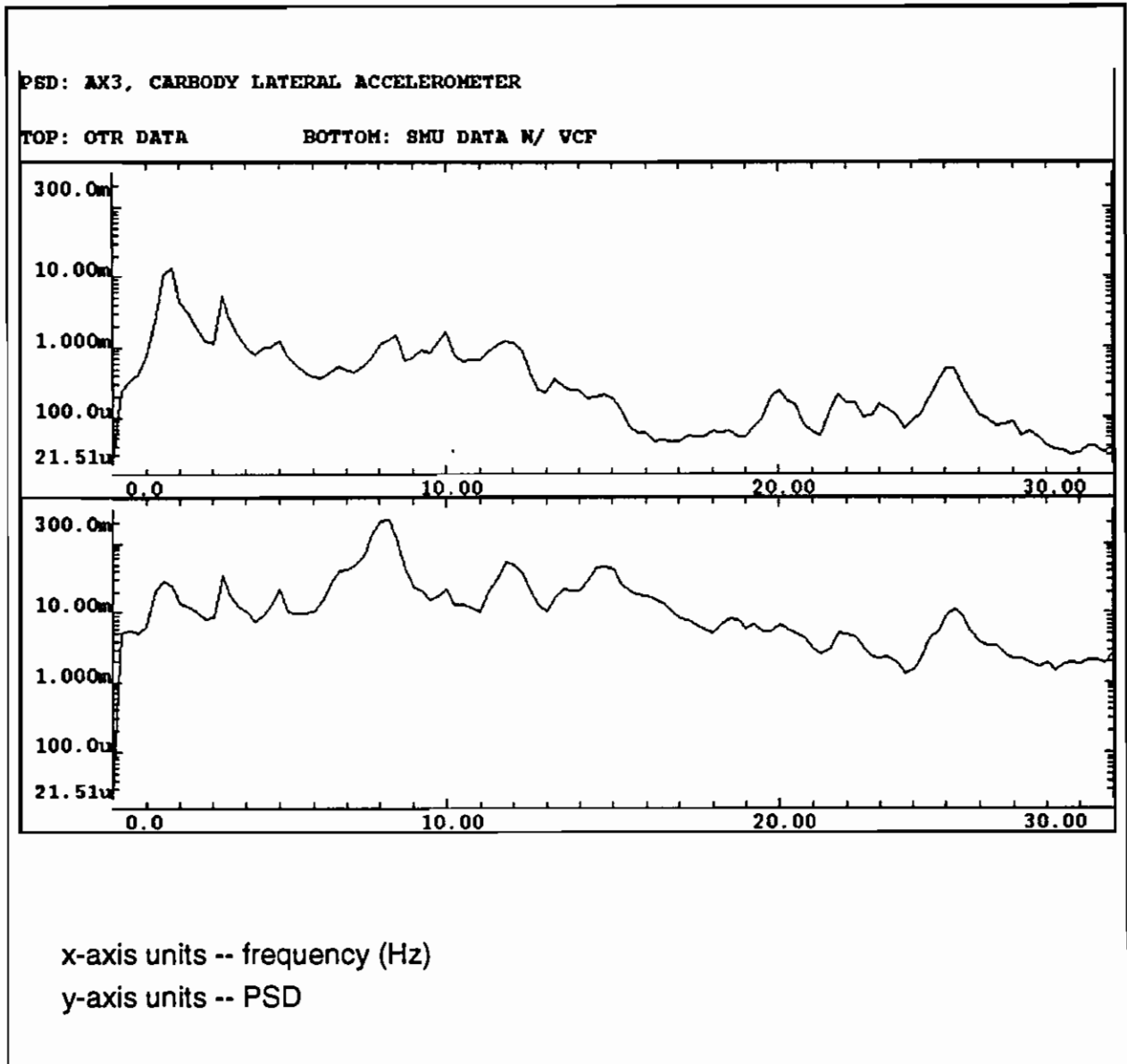Figure 87. OTR and Simuloader Test 5 Hz PSD Plots -- SG08

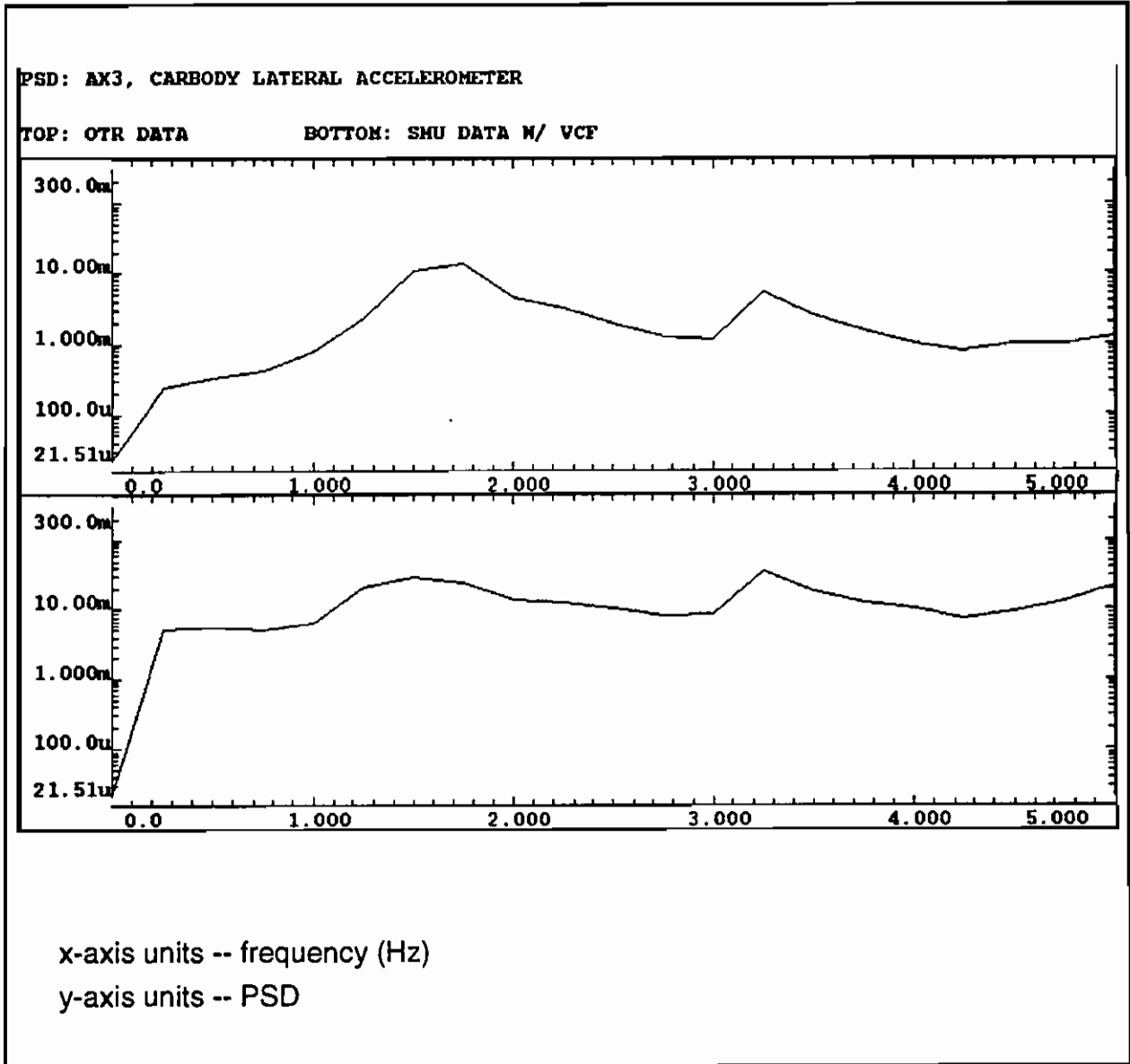Figure 88. OTR and Simuloader Test 30 Hz PSD Plots -- AX3

Figure 89. OTR and Simuloader Test 5 Hz PSD Plots -- AX3

12.2.1.4 Fatigue Life Computations

Computing the fatigue life was the final method of ensuring proper simulation. The technique was to take results of rainflow counting, as shown in the plots in Section 12.2.1.1, and compute the resulting fatigue life with the technique discussed in Section 8.2.2.1. The calculated result was then compared to the results obtained with the FEEST results. All calculations were done for a 90 percent survival rate.

The fatigue life was computed using AAR's FLAP program. The MGD selected for analysis during the MSU test, discussed and illustrated in Section 8.2.2.1, was also used for this analysis.

Fatigue life was computed using the input loads and FEEST loads, as well as with response of strain gages at the critical region. A rainflow counting routine was used to process the input loads and strain responses to allow fatigue analysis to be done.

FATIGUE LIFE COMPUTED USING THE INPUT LOADS AND FEEST LOADS

Critical-region load sensitivities, obtained from quasi-static Simuloader calibration tests, were 8.45 ksi per 100 kips coupler force, -22.75 ksi per 25 kips vertical coupler force, and -5.3 ksi per 50 kips side bearing load. The longitudinal and vertical coupler force sensitivities were more refined than used previously, a result of the control the Simuloader allows when introducing these loads statically. The individual fatigue lives were combined to a single life value as follows:

$$LIFE = \frac{1}{\frac{1}{LIFE_{LCF}} + \frac{1}{LIFE_{VCF}} + \frac{1}{LIFE_{SideBearing}}}$$

FATIGUE LIFE COMPUTED USING RESPONSE OF CRITICAL-REGION STRAIN MEASUREMENTS

Critical-region load strain histories were converted to maximum and minimum stress histories, then rainflow counted.

Table 29 shows the computed fatigue life for Simuloader testing and the OTR test in actual miles. Simuloader test input load cycles 2 and 6 show improvement over input load cycle 1, a result of a refinement of the Simuloader actuator gains after analysis of the first 22,994 loaded-car miles of simulation conducted under input load cycle 1.

Table 29. Computed Fatigue Life, Simuloader Test and FEEST Data

Description	Computed Life
Fatigue Calculation with Rainflow Counts of Vertical, Longitudinal, and Side bearing Loads and Sensitivity at Critical Region to Loads	
Theoretical using published AAR FEEST data	21,000 miles
Simuloader loads measured during the first load cycle (first 22,994 miles)	30,000 miles
Simuloader load inputs measured during the second load cycle (after correction to Simuloader gain)	23,300 miles
Simuloader load inputs measured during the sixth load cycle	23,900 miles
Fatigue Calculation with Rainflow Counts of Principal Stress Values	
Maximum principal stress, critical region, load cycle 1	21,000 miles
Minimum principal stress, critical region, load cycle 1	16,000 miles
Maximum principal stress, critical region, load cycle 2 (shows effect of cracking on strain measurement)	47,400 miles
Minimum principal stress, critical region, load cycle 2 (shows effect of cracking on strain measurement)	86,900 miles

12.2.2 Simuloader Fatigue Test Consistency

Figure 90 shows peak-to-peak values of vertical coupler force and longitudinal coupler force recorded while inputting the 338-second Simuloader input file for each 22,994-mile load cycle. These plots were created to ensure Simuloader operation consistency from load cycle to load cycle.
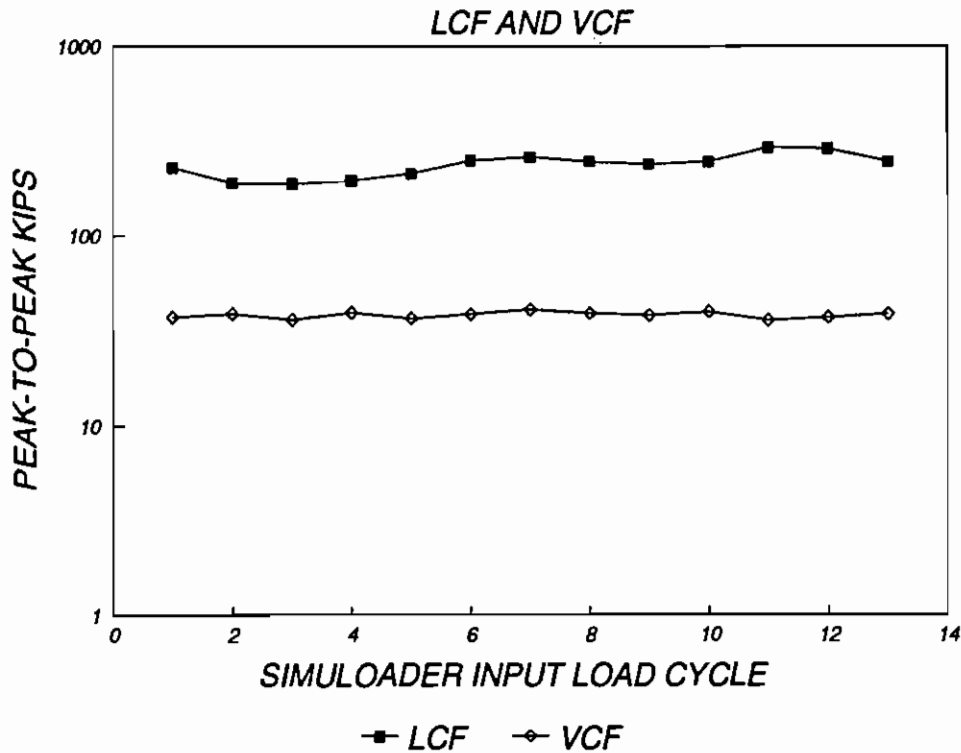
Figure 90. Peak-to-Peak Vertical Coupler Force and Longitudinal Coupler Force Values, Load Cycles 1-13

12.2.3 300,000 Mile Fatigue Test Results -- Crack Growth

The cracks monitored during the 300,000 mile fatigue test were all in the stub sill to head pad connection area, on the B-end (end without the retrofit). The cracks found, similar to cracks observed in 2 of the 10 sample head pads, followed for the most part the stub sill to head pad welds. The specific crack locations prohibited the use of crack growth gages; thus, dye penetrant, calipers, and a ruler were used to measure crack growth. For consistency, one technician was responsible for this measurement.

After the first few load cycles, it was determined that the crack measurements could be taken safely with the vertical coupler force actuator system applying a downward force of 10 kips. This allowed an intuitive feel for change in crack depth to be developed by squeezing excess dye out of the crack when removing the load. The cracks monitored are defined in Table 30.

Table 30. Crack Descriptions

Crack No.	Description
1	Right side, longitudinal weld toe to pad
2	Right side, transverse weld toe to pad
3	Right side, longitudinal weld toe to sill
4	Right side, transverse weld toe to sill
5T	Left side, longitudinal and transverse weld toe to pad (measured as one crack due to wide radius of corner). Measured with tape, thus the 5T notation.
6	Left side, transverse weld toe to sill.
7	Left side, longitudinal weld toe to sill.

Table 31 is a tabulation of the crack growth results after each of thirteen 22,994-mile Simuloader input load cycles. This table shows that the fatigue cracks propagated for the first 161,000 miles of the 300,000 mile fatigue test.

What cannot be shown is the depth of the cracks. It was noted that the crack depths increased through the duration of the 300,000 mile test. Unfortunately, the dye excretion method described above used to make this determination does not lend itself to exact values for depth.

Table 31. Crack Growth Results

Crack No.	Tank Car Fatigue 22,994-Mile Simuloader Input Load Cycle												
	1	2	3	4	5	6	7	8	9	10	11	12	13
	Crack Length (inches)												
1	3 3/32	3 27/32	4 1/32	n/c	n/c	4 6/32	n/c	n/c	n/c	n/c	n/c	n/c	n/c
2	2	--	1 22/32	n/c	n/c	2 5/32	n/c	n/c	n/c	n/c	n/c	n/c	n/c
3	--	9/32	14/32	18/32	n/c	n/c	n/c	n/c	n/c	n/c	n/c	n/c	n/c
4	--	--	--	1 35/64	n/c	2 19/32	n/c	n/c	n/c	n/c	n/c	n/c	n/c
5T	--	3 1/4	n/c	4 2/32	n/c	4 17/32	4 20/32	n/c	n/c	n/c	n/c	n/c	n/c
6	--	--	--	--	--	1 10/32	n/c	n/c	n/c	n/c	n/c	n/c	n/c
7	--	--	--	--	--	--	1/8	n/c	n/c	n/c	n/c	n/c	n/c

n/c = no change in crack   -- = before crack was found

Figure 91 illustrates the dye penetrant method exhibiting cracks 1 and 3 at the stub sill to head pad connection.

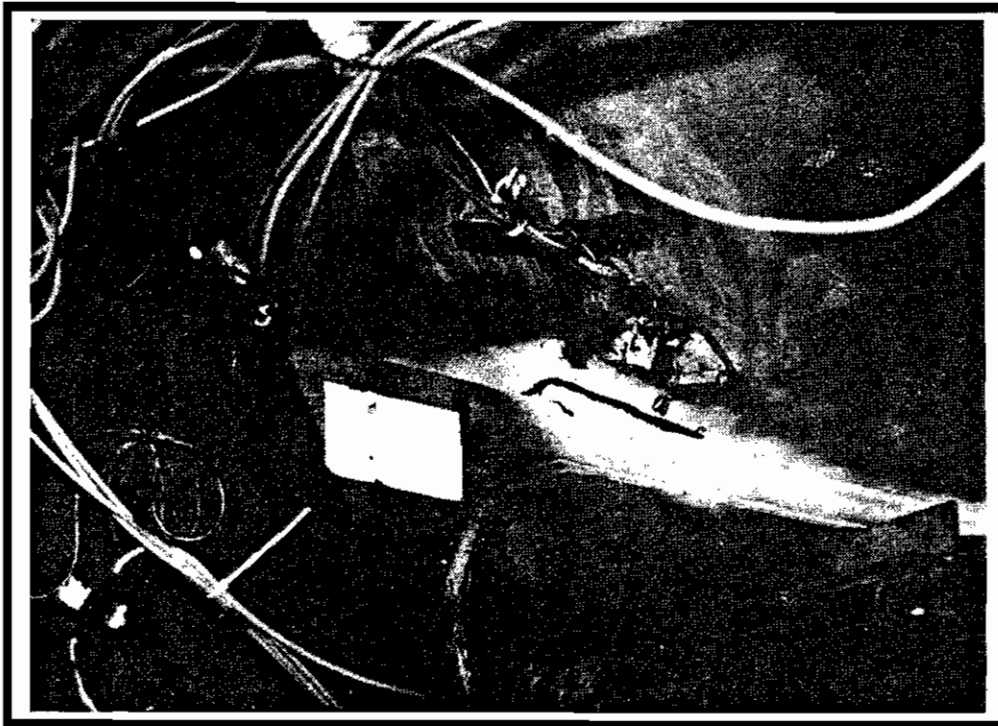Figures 92 and 93 illustrate the seven crack locations.
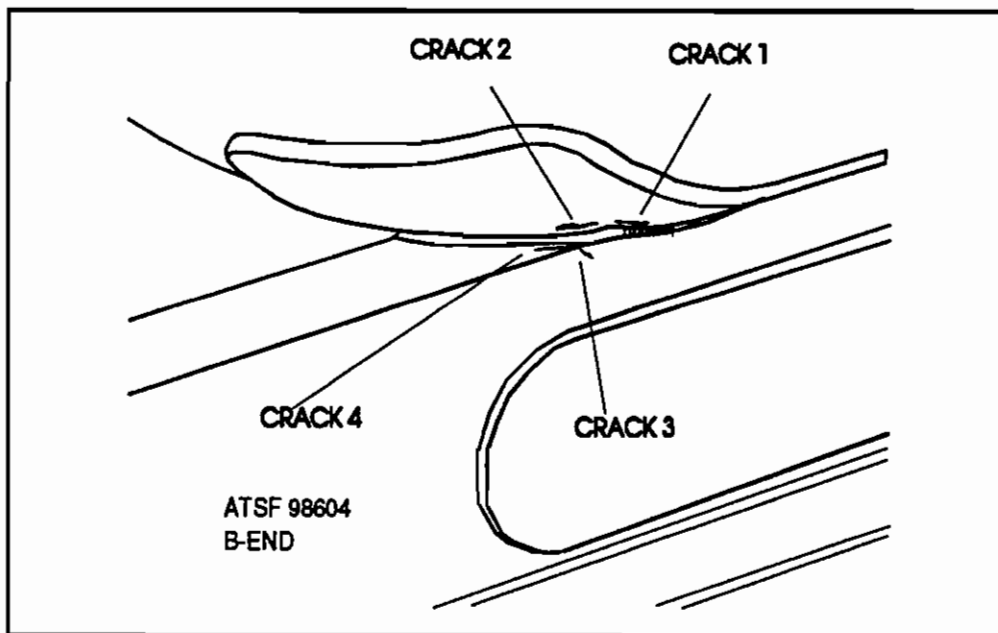

Figure 91. Cracks 1 and 3 Propagated on Simuloader

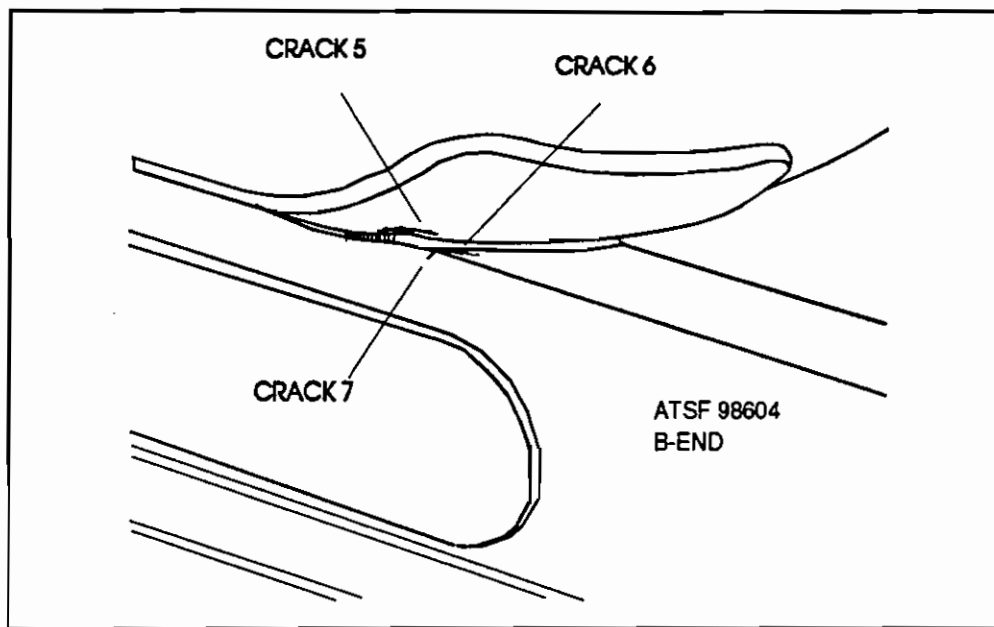**Figure 92. B-end, Right Side Cracks at Head Pad to Sill Connection**

Figure 93. B-end, Left Side Cracks at Head Pad to Sill Connection

12.3 SIMULOADER TEST WITH VERTICAL COUPLER FORCE INPUT – CONCLUSIONS

The Simuloader 300,000 mile fatigue test was accomplished effectively with the addition of the vertical coupler force actuator. The tests resulted in the following accomplishments and realizations:

- The addition of the vertical coupler force actuator made possible the completion of an accurate and successful 300,000 mile fatigue test.

- Time histories, PSD plots, and fatigue life computations validated the simulation and fatigue loading.

- Fatigue life computations were found to be useful for fatigue test validation and corresponded well with the fatigue test results.

- Vertical coupler forces were found to be the most significant fatigue causing loads in the ATSF 98604 stub sill tank car.

- Seven fatigue cracks, only one of which existed before the Simuloader test began, propagated during the 300,000 mile fatigue test.

- The fatigue cracks were similar to cracks found in head pads removed in the field.

- The fatigue cracks stopped propagating lengthwise after significant mileage was accrued. This happenstance possibly resulted from the lack of cold-weather testing conditions and the high-quality welding. However, significant increases in crack depth were noted throughout the entire 300,000 mile fatigue test.

13.0 ERROR ANALYSIS

The overwhelming amount of data presented in this report precludes the calculation of and use of error bars for each data value. For example, each time history in Figures 79 through 81 may contain 1024 or more points, making it impossible to provide error bands for each point. However, "common-sense" measurement error analysis was done to ensure adequate measurement accuracy. Detailed error analysis, of which an example is given in this section, was done for selected measurements.

Table 16, presented in Section 6.2.1, is repeated in Table 32. Error analysis will be shown for the highlighted maximum principal stress value of 29.7 ksi, which is an average of results for runs 19 and 20.

Table 32. Impact Test Result Summary, Tests at Approx. 6.5 mph
(Repeat of Table 16)

Configuration, Run	Speed (mph)	Coupler Force (kips)	Max. Stress Computed from Rosette 2 — Max (ksi)
88% Outage, Coupler Centered, Average of Runs 7, 15, and 27	6.67	520	20.8
88% Outage, Coupler Up, Average of Runs 19 and 20	6.55	565	29.7
88% Outage, Coupler Down, Average of Runs 13 and 14	6.5	515	23.3

The associated strain gage values and computed stress values are listed individually in Table 33 for impact test runs 19 and 20.

Table 33. Rosette 2 Strain Gage Values, Impact Test Runs 19 and 20

| Run | Speed (mph) | Coupler Force (kips) | Rosette 2 | | | Max. Stress Computed from Rosette 2 |
			SG31 $\varepsilon_1(\mu\varepsilon)$	SG32 $\varepsilon_2(\mu\varepsilon)$	SG33 $\varepsilon_3(\mu\varepsilon)$	Max (ksi)
Run 19	6.5	540	680	833	462	25.6
Run 20	6.6	590	756	927	496	33.8

The method used to estimate uncertainty, presented by Kline and McClintock,[21] is defined by the relationship:

$$w_R = \left[\left(\frac{\partial R}{\partial x_1} w_1 \right)^2 + \left(\frac{\partial R}{\partial x_2} w_2 \right)^2 + \ldots + \left(\frac{\partial R}{\partial x_n} w_n \right)^2 \right]^{1/2}$$

where: w_R = uncertainty of the result

R = result

$x_1, x_2, \ldots x_n$ = independent variables

$w_1, w_2, \ldots w_n$ = uncertainties in the independent variables

The first step in this analysis was to evaluate the three strain gages in the rosette. An error of 1.02 percent was computed with the uncertainty equation for each gage, combining gage factor error (1%), shunt calibration resistor error (0.1%), amplifier error (0.16%), and digitizer error (0.15%).

The maximum principal stress calculation gives the maximum possible stress value at the juncture of the three strain gages. Therefore, the error of the principal stress calculation is a combination of the individual 1.02 percent errors for each strain gage. The method for solving for the computed principal stress error involved the determination of the partial derivative of the result as a function of $\varepsilon_1, \varepsilon_2$, and ε_3 from the principal stress equation given below.

$$\sigma_{max} = \frac{E(\varepsilon_1 + \varepsilon_3)}{2(1-\mu)} + \frac{E}{\sqrt{2}(1+\mu)} [(\varepsilon_1 - \varepsilon_2)^2 + (\varepsilon_2 - \varepsilon_3)^2]^{1/2}$$

where: E = Young's modulus

μ = Poisson's ratio

The partial derivatives, along with the independent variable uncertainties, were input into the uncertainty equation. The resulting error in the principal stress calculation was found to be 0.68 percent. This was very tolerable, especially when compared to the error obtained by determining the partial derivatives with respect to Young's modulus E and Poisson's ratio μ, arbitrarily selecting one percent uncertainties for each and combining them with the strain gage errors. The resulting error was computed to be 3.41 percent.

Finally, because the average stress was computed, the final error (using the 0.68 values) was determined to be 0.96 percent for the average principal stress. Table 34 shows the value analyzed with the computed tolerance included.

Table 34.   Impact Test Result Summary, Tests at Approx. 6.5 mph
(Repeat of Table 16, With Tolerance)

Configuration, Run	Speed (mph)	Coupler Force (kips)	Max. Stress Computed from Rosette 2 — Max (ksi)
88% Outage, Coupler Centered, Average of Runs 7, 15, and 27	6.67	520	20.8
88% Outage, Coupler Up, Average of Runs 19 and 20	6.55	565	29.7±0.29
88% Outage, Coupler Down, Average of Runs 13 and 14	6.5	515	23.3

14.0 RECOMMENDATIONS

Recommendations, based on the findings of the Tank Car Fatigue Crack Growth Test, are as follows:

- This program showed, on a better than average car, that fatigue cracking at the stub sill to head pad connection of stub sill tank cars can occur. It is recommended that other typical cars, of similar and dissimilar design, be tested to validate and increase the information base.

- Vertical coupler force was added only to one end of the Simuloader. It is recommended that this capability be added to the other end of the Simuloader for future testing of stub sill tank cars.

- The mechanism for which the vertical coupler loads are introduced into the stub sill; that is, how vertical loads enter the coupler joint and their transmission into the sill, is not understood. Such information would prove valuable to the future design of stub sill tanks and potential exists for better environmental replication through the Simuloader.

  The Railway Progress Institute recently funded a study by Dr. Gerald Moyar, with the objective of investigating the reliability of known vertical coupler loads and the mechanism in which these loads are introduced. This work, though useful, did not benefit from testing and modeling designed to expose the vertical coupler loading mechanism. For these reasons, AAR/TTC recommends a research and test program, involving industry, and utilizing dynamic modeling and testing to determine the mechanism.

- Vertical coupler loading should be taken into consideration during the design stage for new generation stub sill tank cars. The tank car designers should perform fatigue analysis of their stub sill designs by including vertical coupler loads in conjunction with other loading requirements.

References

1. Walsh, W. J., R. C. Rice and D. R. Ahlbeck. "Stub sills on Tank Cars," Department of Transportation, Federal Railroad Administration, Office of Research and Development. Report No. 89-01, March 1989. NTIS PB 90 161456, Springfield, VA.

2. Department of Transportation, Transportation Systems Center. Task Force Report, DOT-111A/100W Tank Cars Special Retrofit Stiffener Integrity Assessment, Cambridge, MA, April 1987.

3. Larson, R. K. Jr and B. R. Rajkumar. "Stub Sill Tank Car Compression Test," Department of Transportation, Federal Railroad Administration, Office of Research and Development, Washington, D.C., April 1989.

4. "Monsanto Company's Procedure for Acoustic Emission Evaluation of Railroad Tank Cars and Intermodal Tanks," Issue J, Monsanto Company, February 1990.

5. Task Force Report. DOT-105/111/112/114 Tank Cars, Steel Cracking and Structural Integrity Assessment, DOT Transportation Systems Center, Cambridge, MA 02142, November, 1986.

6. Walsh, W. J., et al. Report No. 89-01, March 1989.

7. Rolfe, S.T. and J. M. Barsom. *Fatigue and Fracture Control in Structures*, Prentice-Hall, Englewood Cliffs, NJ, 1977.

8. Moyar, G. "Critical Evaluation of AAR Fatigue Methodology for Stub Sill Tank Cars," Railway Progress Institute, Association of American Railroads, Chicago Technical Center, September 15, 1992, Illinois.

9. Association of American Railroads, Operations and Maintenance Department Mechanical Division. *Manual of Standards and Recommended Practices*, Section C - Part II, Section 7.4, 1988.

10. Ibid

11. Brave, Glenn H. "Failure Analysis of Cracked Stub Sill Head Pads," Transportation Test Center, Pueblo, Colorado, internal document, July 1992.

12. Tada, H., Paris, P.C. and G.R. Irwin. *Stress Analysis of Cracks Handbook*, Del Research Corporation, Hellertown, PA, 1973.

13. Sih, G. C. *Handbook of Stress Intensity Factors*, Institute of Fracture and Solid Mechanics, LeHigh University, Bethlehem, PA, 1973.

14. Rooke, D. P. and D. J. Cartwright. *Compendium of Stress Intensity Factors*, H. M. Stationery, London, 1976.

15. Corbin, J., Lazzaro, J. and C. Peterson. "Locomotive Track Hazard Detector Program (LTHD) Interim Report," August, 1981. The MITRE Corporation for the U.S. Department of Transportation

16. *Operations Manual for Track Geometry Acquisition - LTHD Operations*, Transportation Test Center, Pueblo, CO, Systems Manual SMO-8200.1.

17. Moyar, G., Railway Progress Institute, September 15, 1992

18. Association of American Railroads. Operations and Maintenance Department Mechanical Division. *Manual of Standards and Recommended Practices*, Section C - Part II, Chapt. VII p. 174, 1988.

19. Ibid

20. Sharma, V. and S. K. Punwani. "Freight Equipment Environmental Sampling Test Description and Results." Paper presented at the ASME Rail Transportation Division Spring Conference, Chicago, IL, April 4-6, 1984.

21. Kline, S. J. and F. A. McClintock. "Describing Uncertainties in Single-Sample Experiments," *Mechanical Engineering*, p. 3, January 1953.

APPENDIX A

STRAIN MEASUREMENTS FOR OVER-THE-ROAD TESTS

B - END
TANK

Location of
Strain Gage SG01

2 IN.

27 IN.

STRIKER PLATE
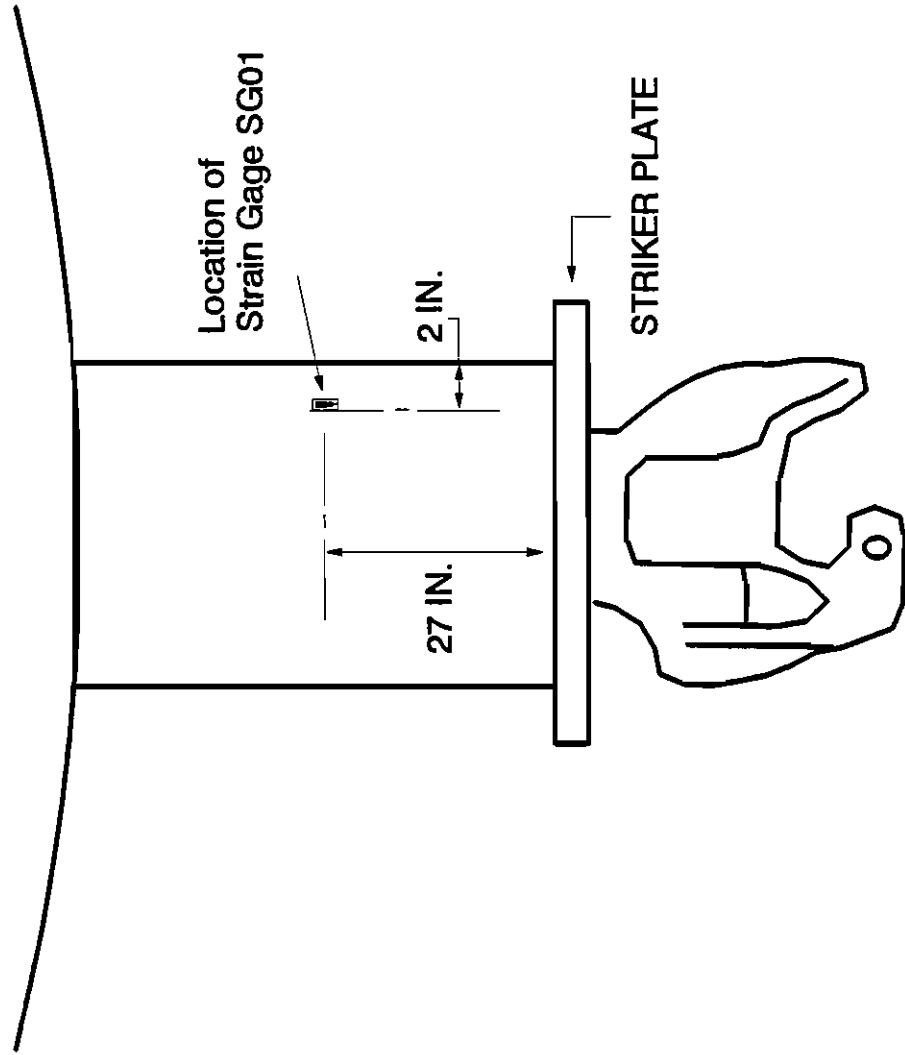
LOCATION OF STRAIN GAGES SG02
ON TRUCK BOLSTER AS VIEWED
FROM BELOW
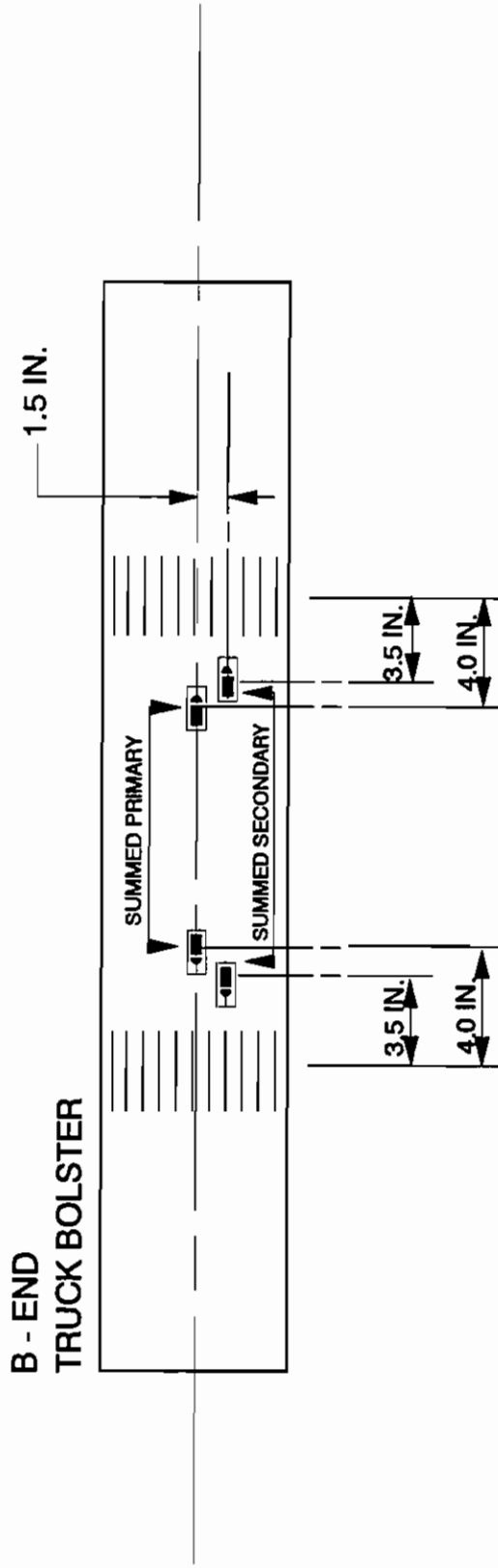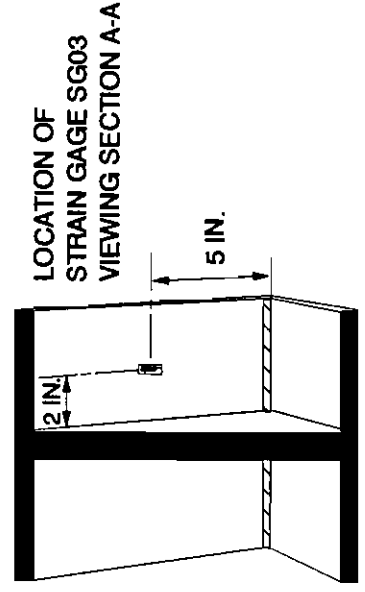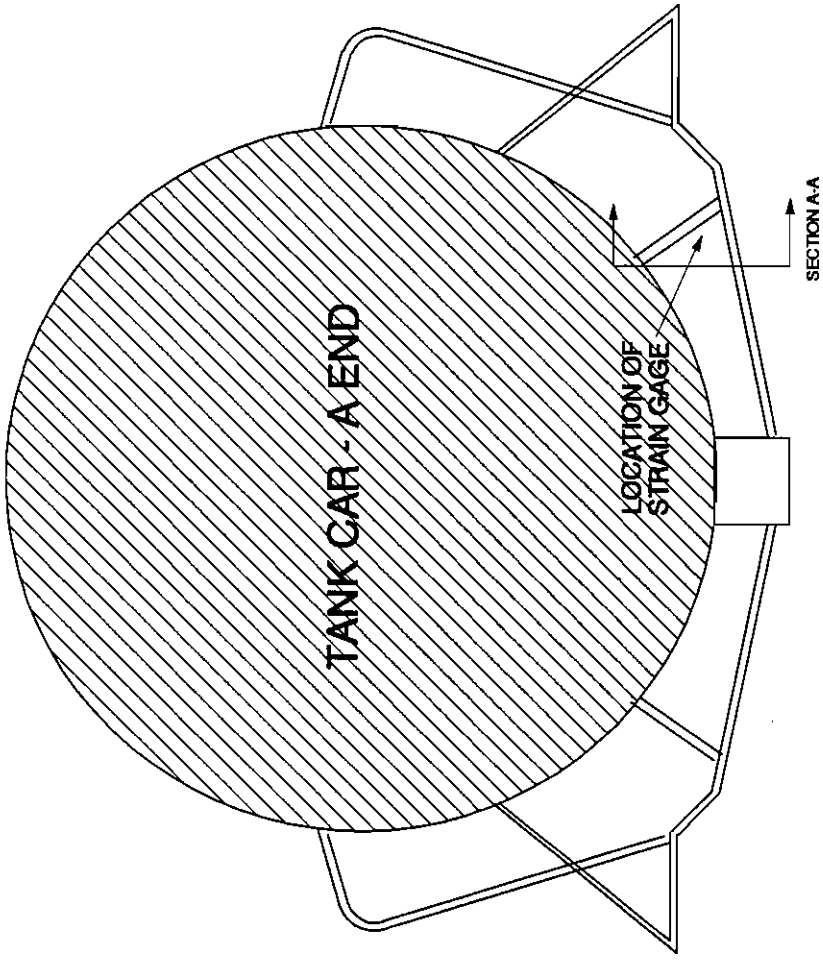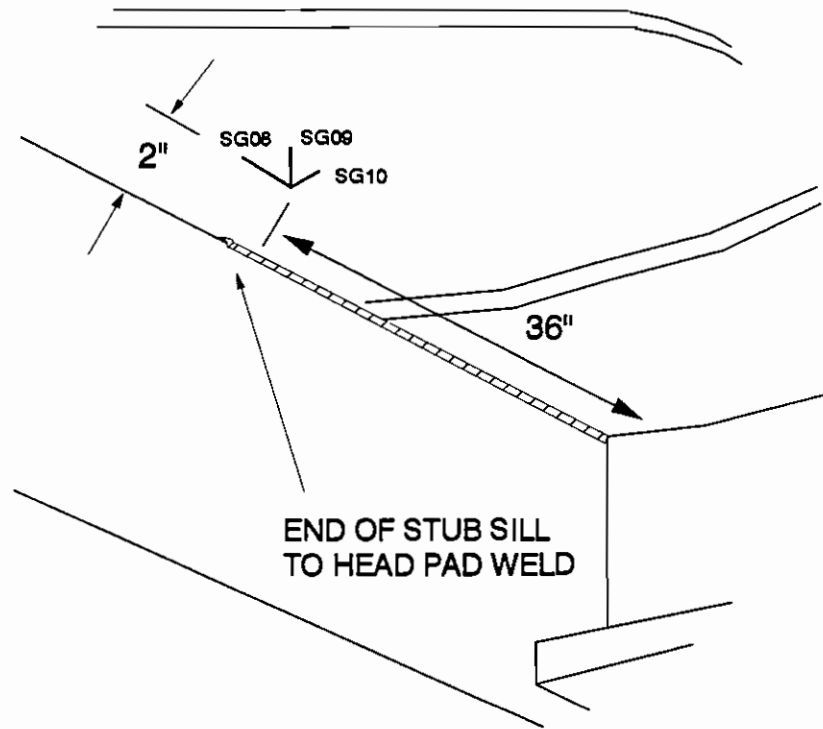
B - END
TRUCK BOLSTER

1.5 IN.

SUMMED PRIMARY

SUMMED SECONDARY

3.5 IN.

4.0 IN.

3.5 IN.

4.0 IN.

TANK CAR - A END

LOCATION OF
STRAIN GAGE

SECTION A-A

LOCATION OF
STRAIN GAGE SG03
VIEWING SECTION A-A

5 IN.

2 IN.

2"

SG08   SG09
       SG10

36"

END OF STUB SILL
TO HEAD PAD WELD

LOCATIONS OF STRAIN GAGES
ON TANK CAR END
WITHOUT RETROFIT

B - END OF TANK CAR

SG04

1.5 IN.

SG05   2.5 IN.

SG06   SG07   SG08   SG09

                                    SG10

2.0 IN.

(36 IN. FORWARD
FROM CRADLE
VERTICAL MEMBER.)

Center
Line
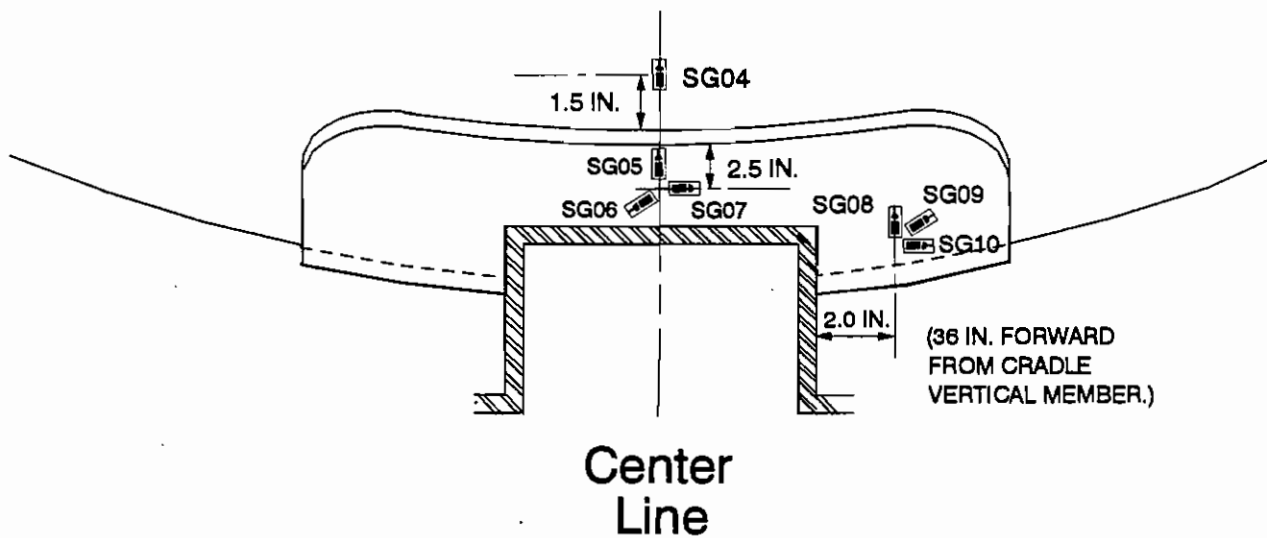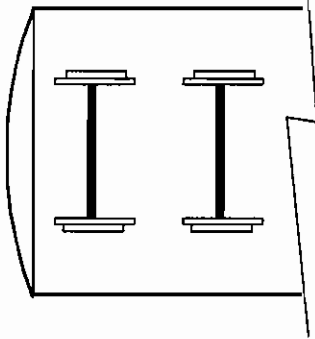
A - END

B - END

Orientation of
Strain Gages
as seen from
underneath
Tank Car

SG11 SG12

SG13
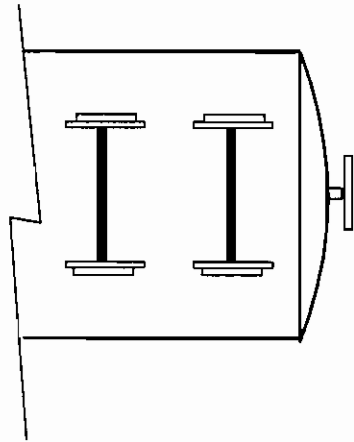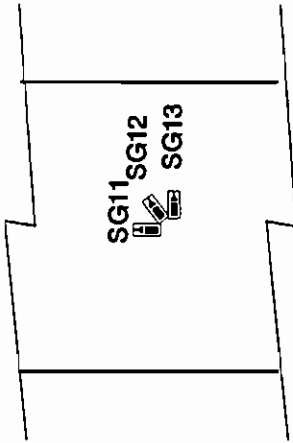
LOCATIONS OF STRAIN GAGES
ON END OF TANK CAR
WITH RETROFIT

A - END

SG14

1.5 IN.

SG15 2.5 IN.

SG16 SG17

0.75 IN.

SG44

SG18 SG19

SG20

2.0 IN.

(36 IN. FORWARD
FROM CRADLE
VERTICAL MEMBER.)

CENTER LINE OF
CENTER SILL
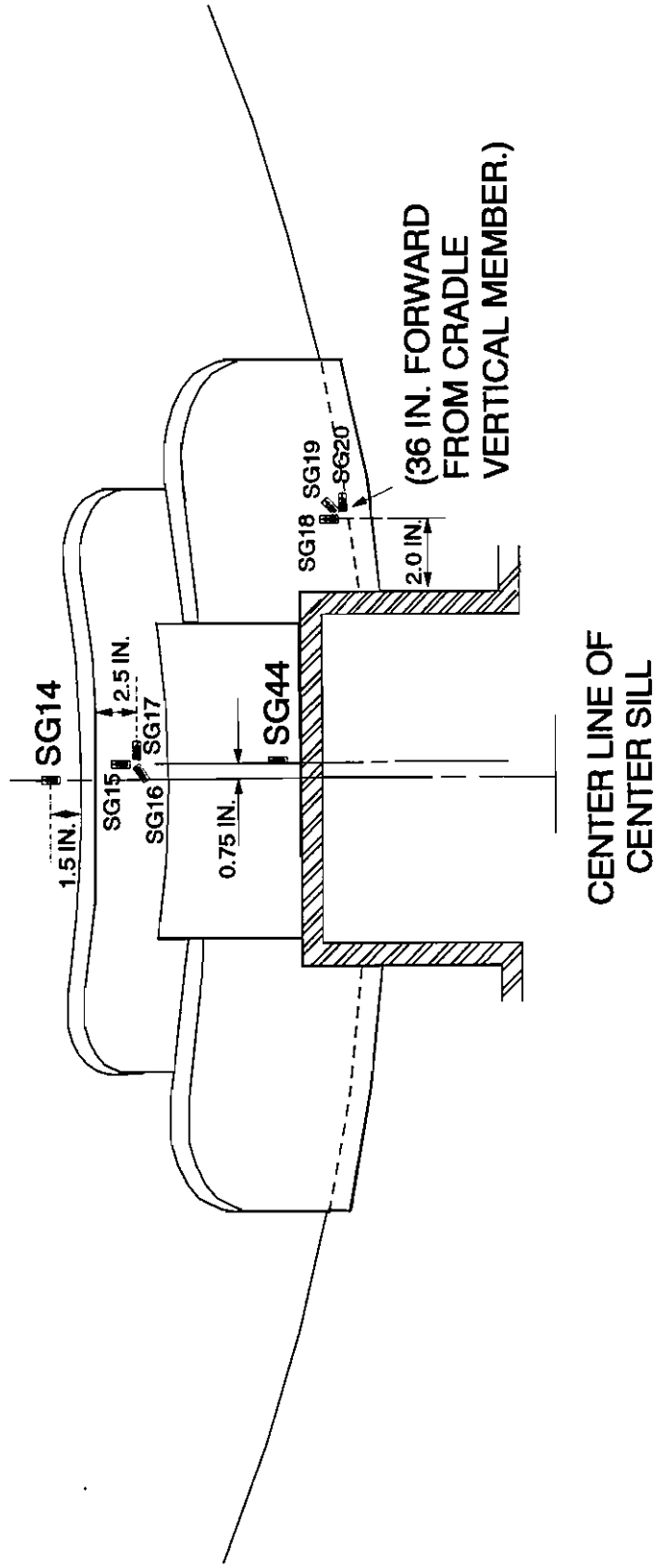
APPENDIX B

ADDITIONAL STRAIN MEASUREMENTS FOR SUPPLEMENTAL TESTS
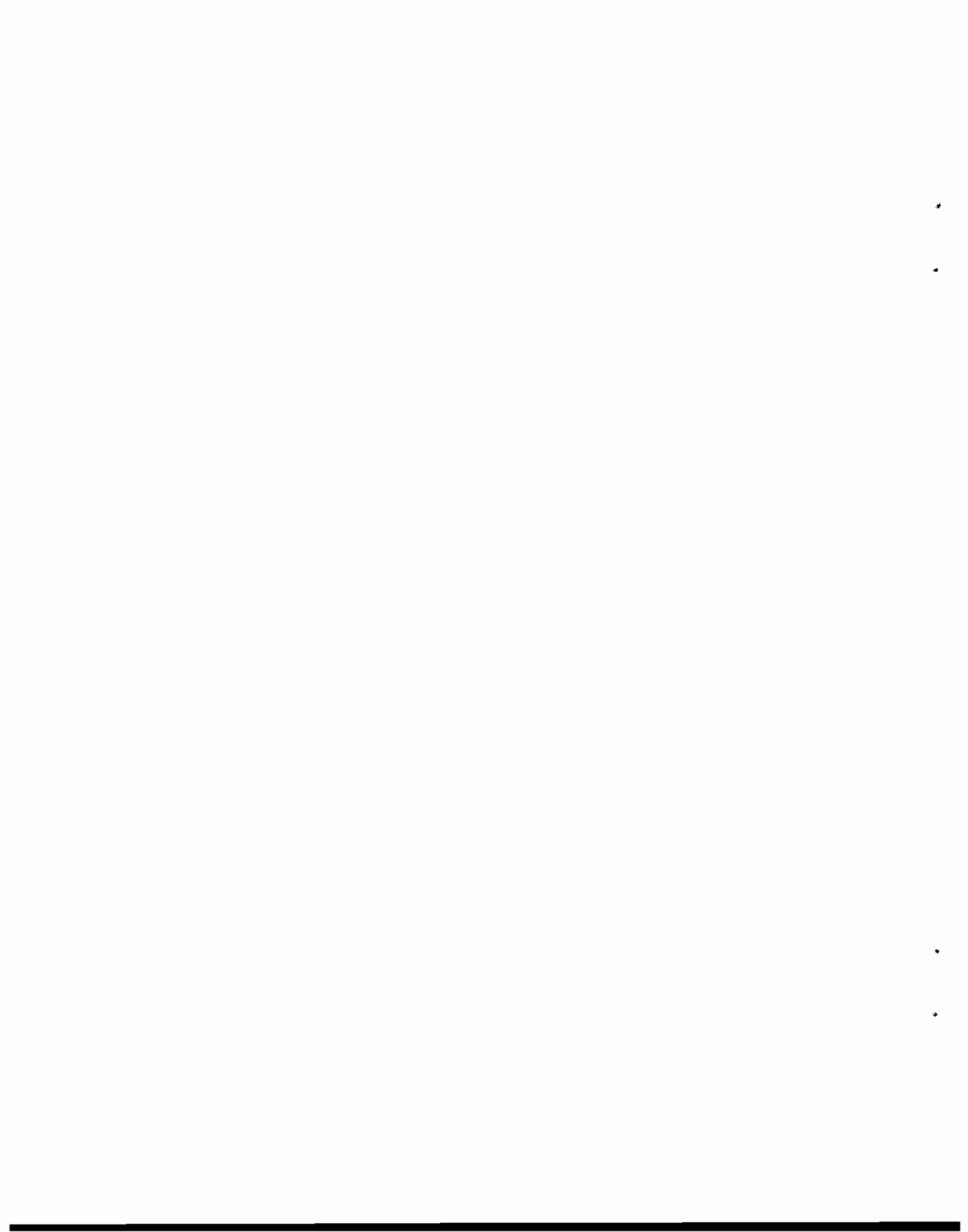
LOCATIONS OF STRAIN GAGES
ON TANK CAR END
WITHOUT RETROFIT

B - END OF TANK CAR

Center Line

Original Measurements

Additional Measurements

SG09
SG10
SG08
SG25
SG26
SG27

BONDABLE GAGES (ROSETTE)
WITHIN 1/2" OF WELD
- INSIDE PREVIOUS ROSETTE

SG26
SG27
SG25

(37.5 IN. FORWARD
FROM CRADLE
VERTICAL MEMBER.)

1/2 IN.
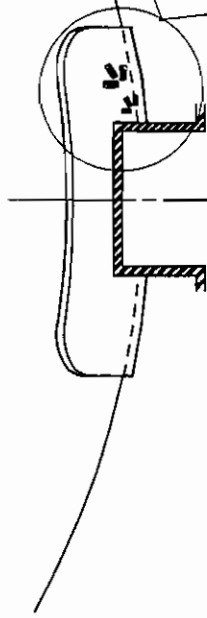
Center
Line
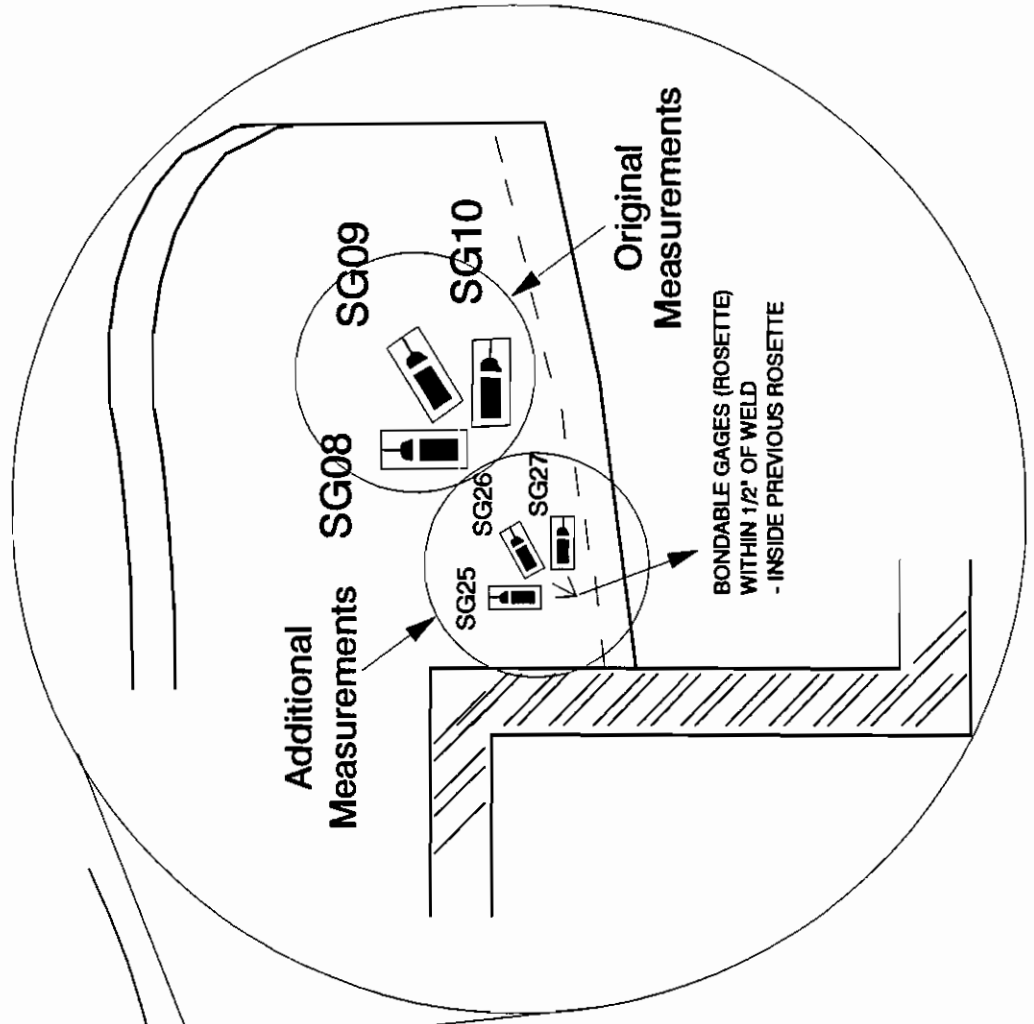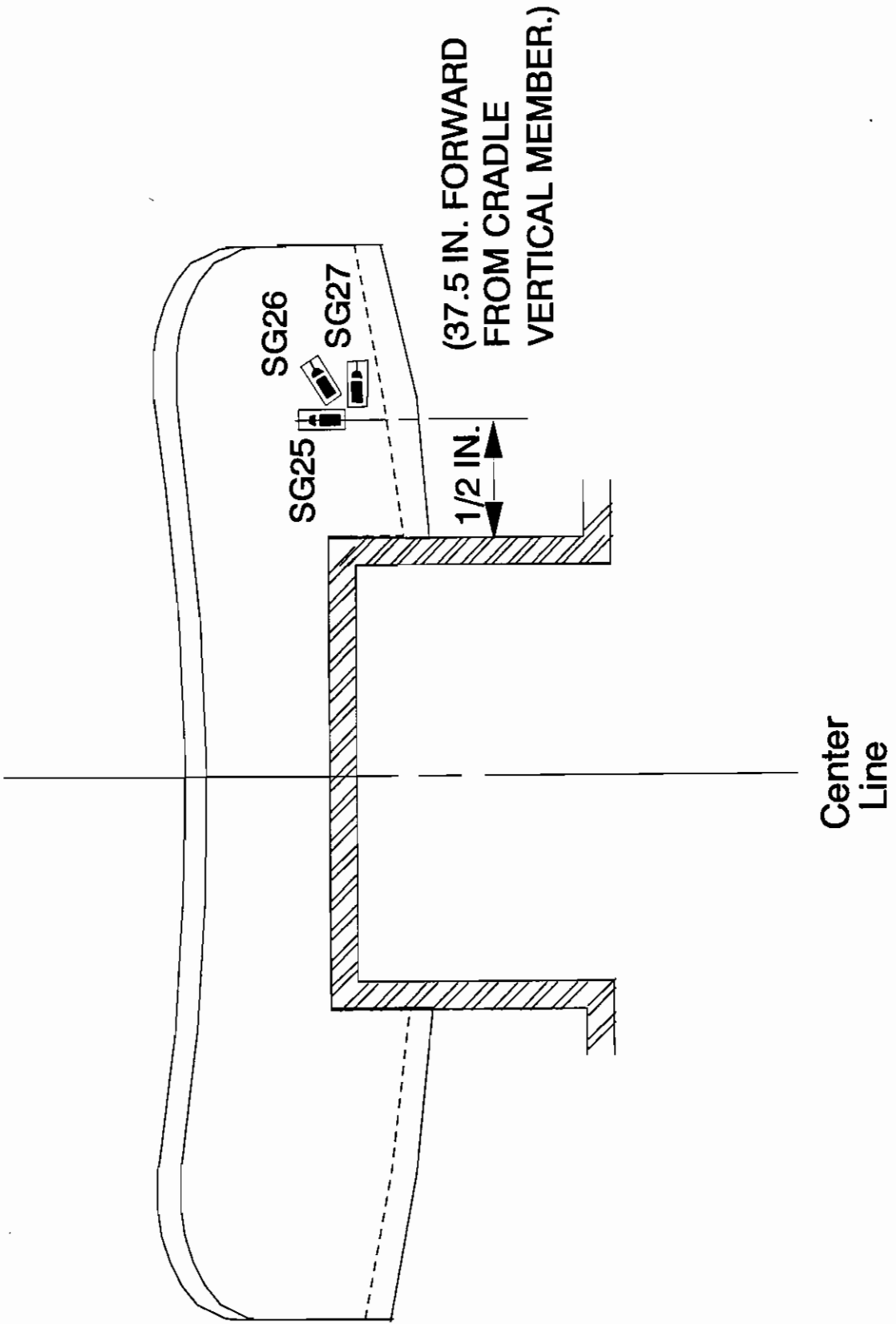
B-END, RIGHT SIDE STUB SILL TO PAD CONNECTION

WELDABLE GAGES (USED ALL TESTS): SG08 - SG10
BONDABLE GAGES (SUPPLEMENTAL, SIMULOADER TESTS ONLY): SG25 - SG27
37 1/4" FROM CRADLE VERTICAL MEMBER

EDGE OF HEAD PAD

Original
Measurement

SG09
SG10
SG08 ○

Additional
Measurement

SG26
SG25 ○ SG27

5/8"

CORNER, PAD TO
SILL CONNECTION
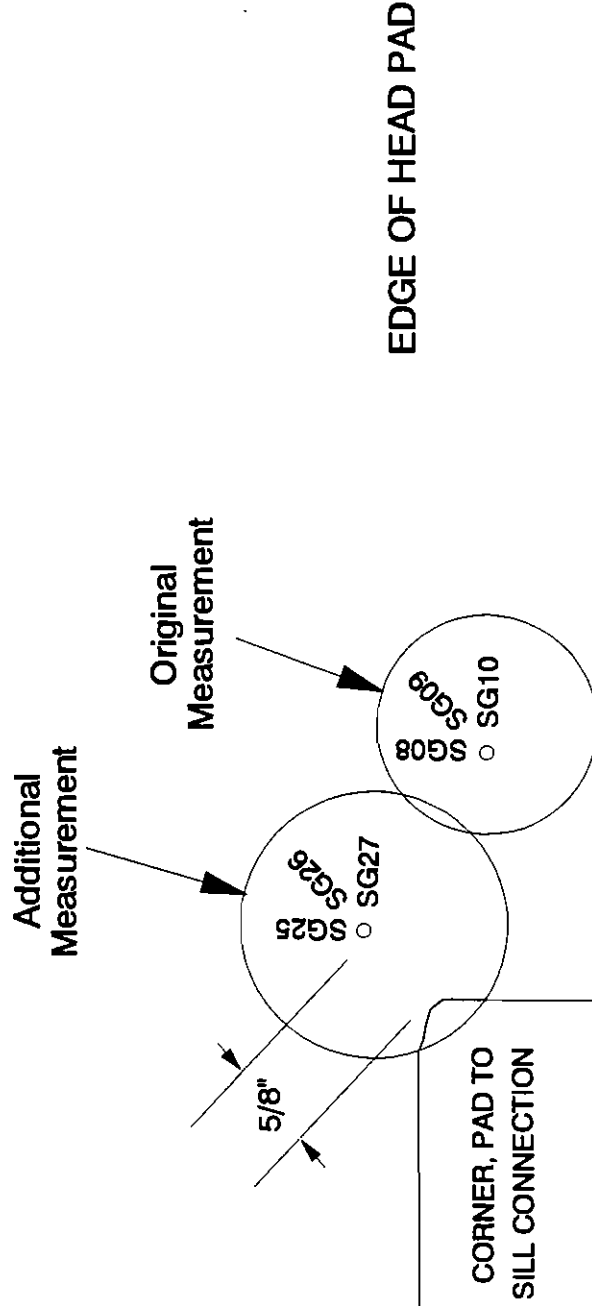
B-END, LEFT SIDE STUB SILL TO PAD CONNECTION

WELDABLE GAGES (SUPPLEMENTAL, SIMULOADER TESTS ONLY):   SG28 - SG30

BONDABLE GAGES (SUPPLEMENTAL, SIMULOADER TESTS ONLY):   SG31 - SG33
37 1/4" FROM CRADLE VERTICAL MEMBER

BONDABLE CHEVRON GAGES (SIMULOADER TEST ONLY):   SG45 - SG50

CORNER, PAD TO
SILL CONNECTION

5/8"

3/4"

3/4"

SG31

SG32

SG45   SG33

SG46

SG47

SG48

SG49   SG50

SG28

SG29

SG30

Additional
Measurements

Original
Measurement

EDGE OF HEAD PAD

B - END
TANK

Original
Measurement

Location of
Strain Gage SG01

2 IN.

SG34

27 IN.

STRIKER PLATE

Additional
Measurement

SG25 SG26 SG27

1/2"

37.25"

END OF STUB SILL
TO HEAD PAD WELD

VIEW FROM BOTTOM

SG22

SG35

SG21

SG36

ON CENTER LINE

STRIKER PLATE

27"

50"

Orientation of
Strain Gages
as seen from
Underneath
Tank Car

A - END

B - END

Original
Measurements

SG11 SG12
SG13

SG40

3"

Additional
Measurement

CRADLE BRACE

WEBBING

END OF TANK CAR

HEAD BRACE

STUB SILL

SG43
SG41
SG42
SG38
SG39
SG37
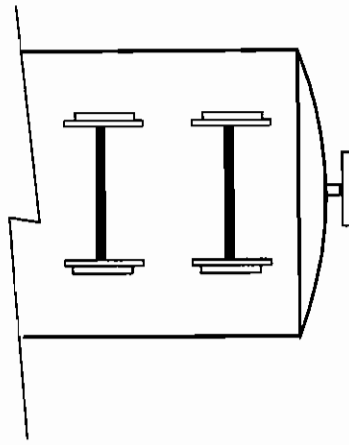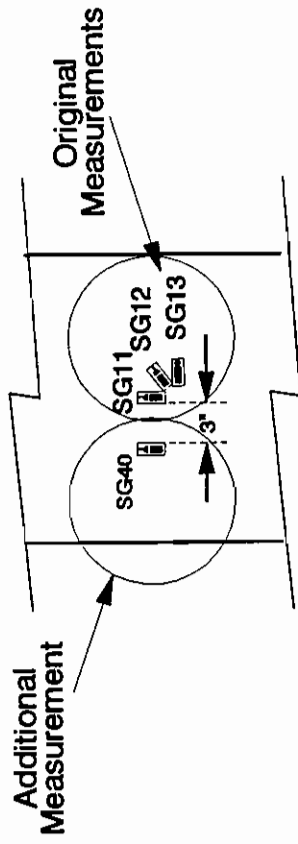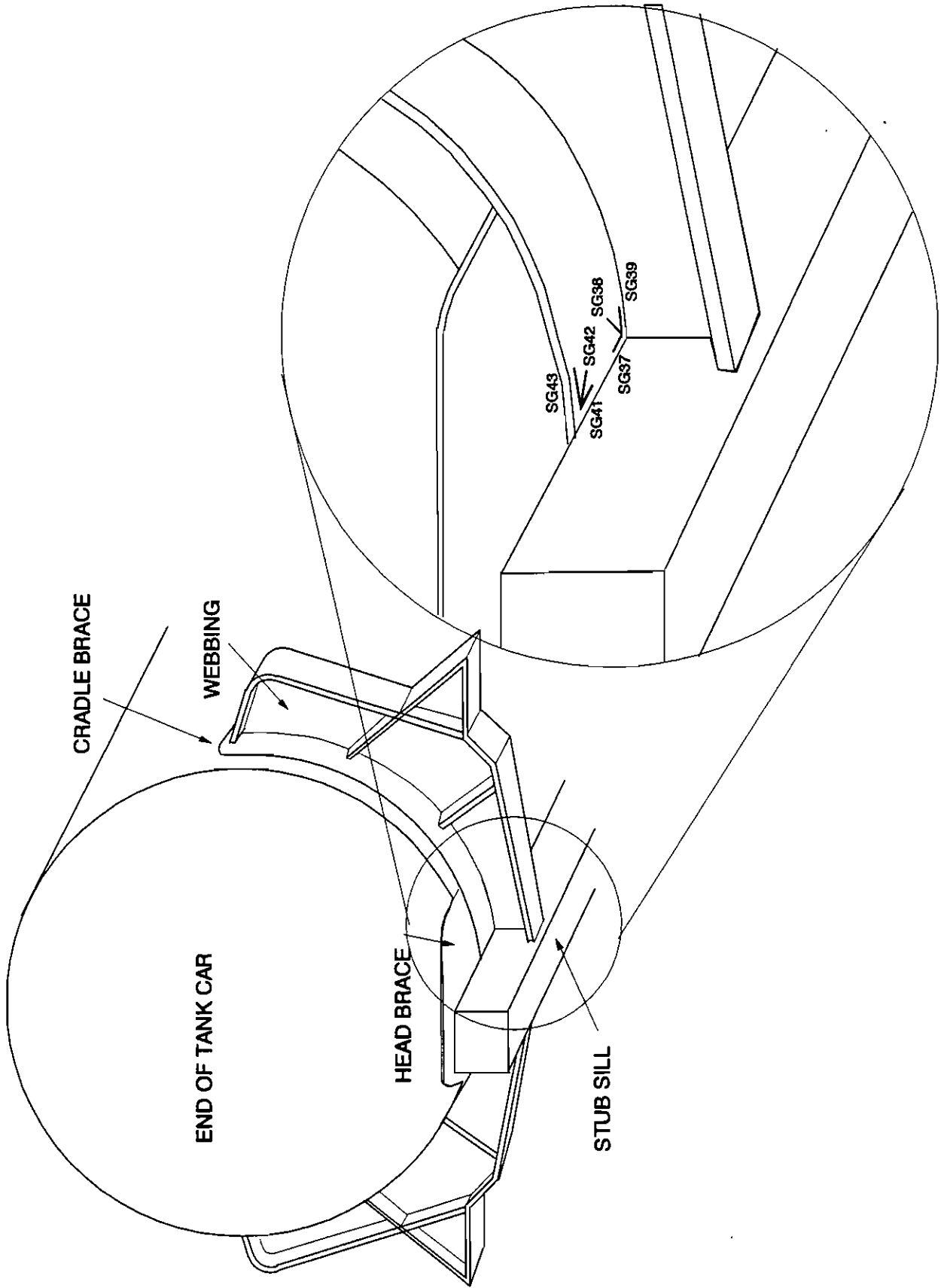
APPENDIX C

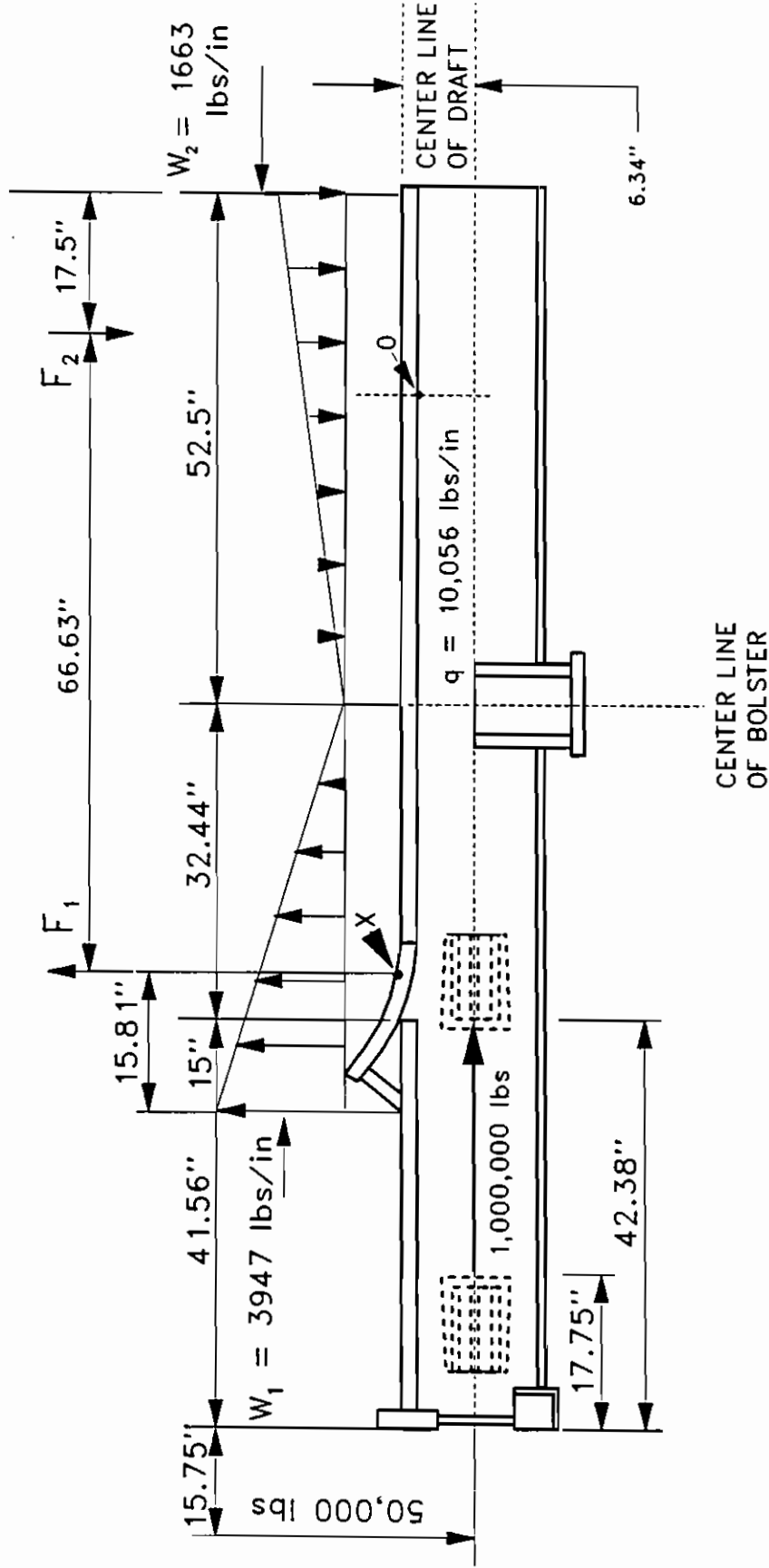## FORCE DIAGRAMS ON TANK SILL WITH AND WITHOUT HEAD BRACE
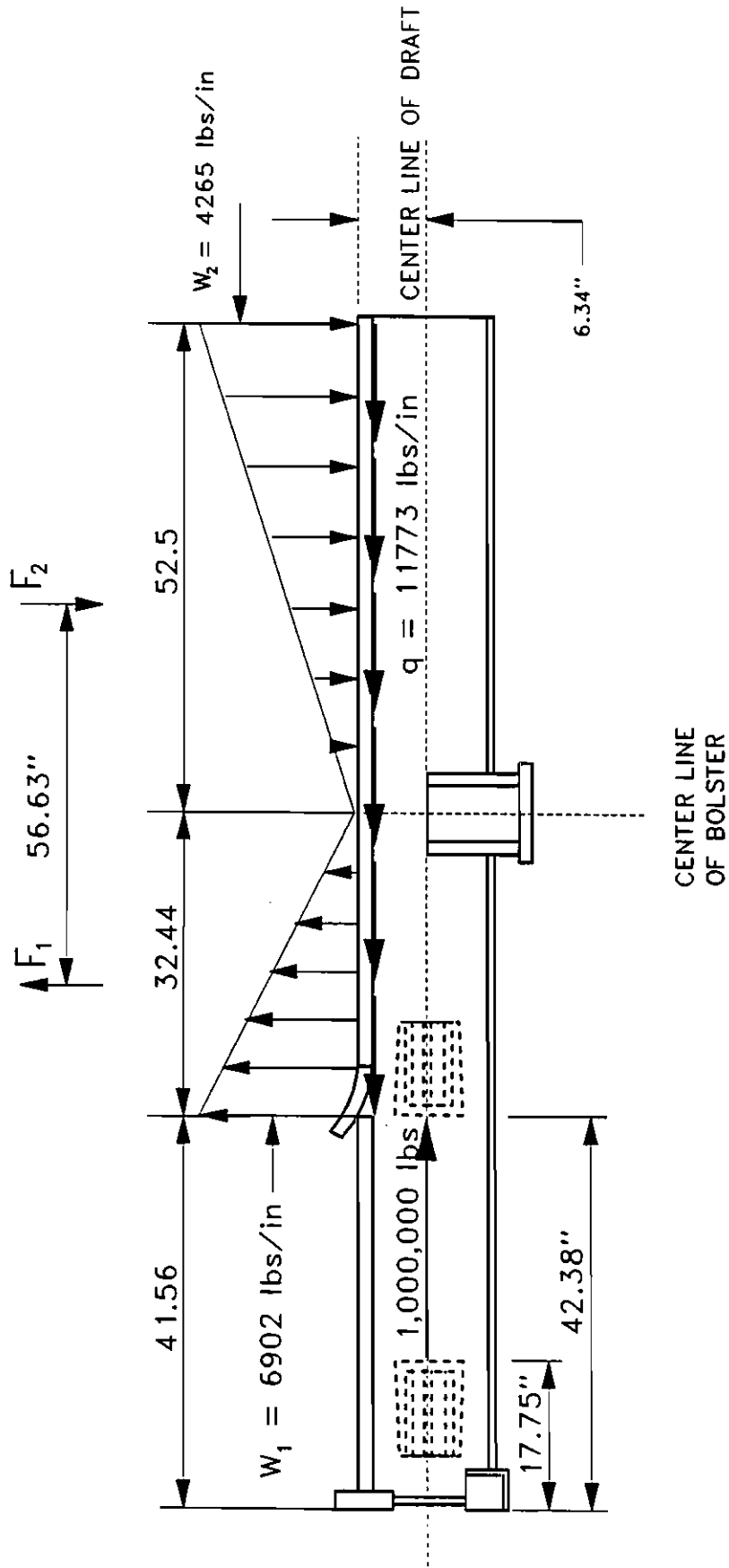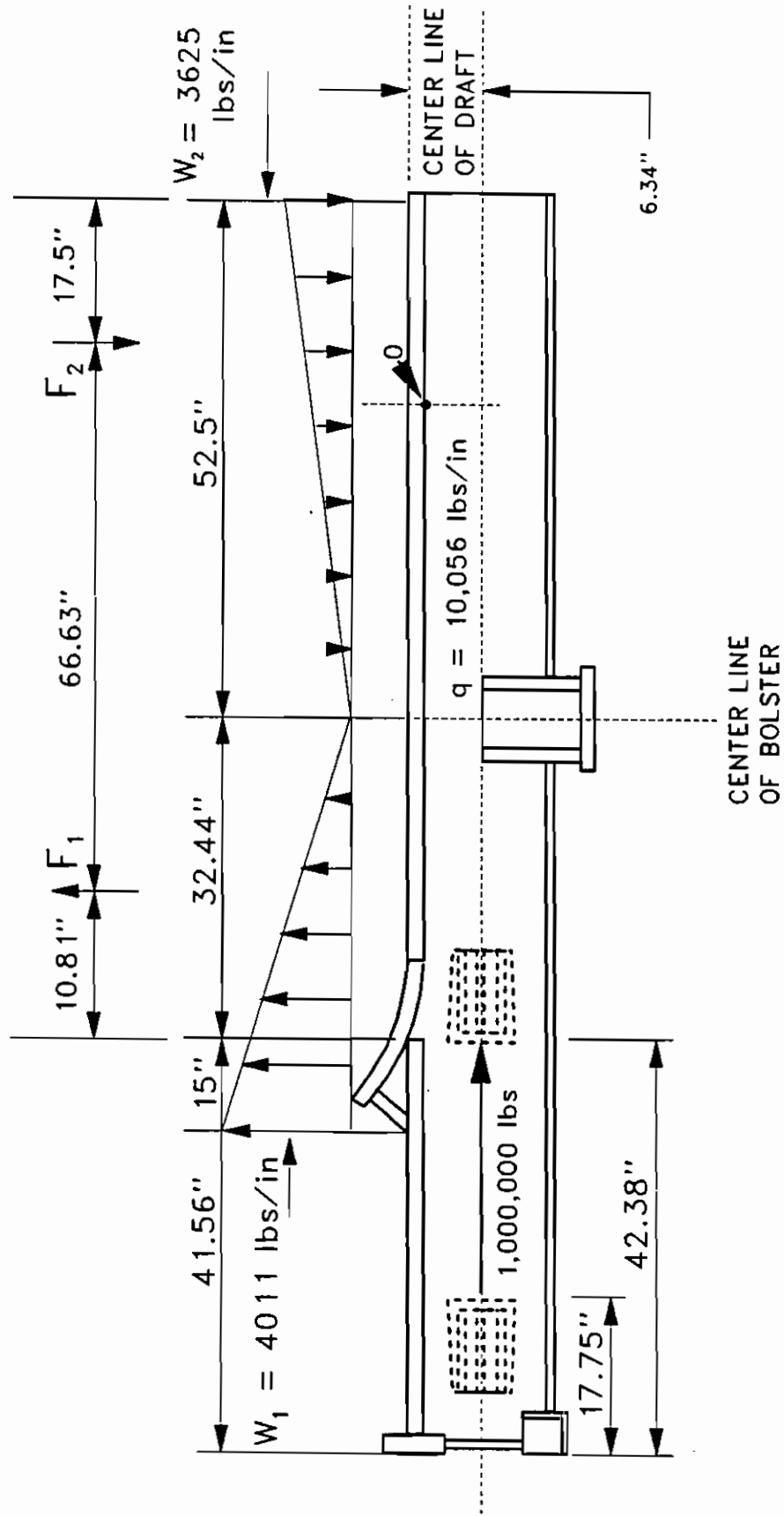
WITHOUT HEAD BRACE

WITH HEAD BRACE

$W_2 = 2291$ lbs/in

CENTER LINE
OF DRAFT

6.34"

F_2 17.5"

52.5"

0

56.63"

CENTER LINE
OF BOLSTER

32.44"

10.81"

X

41.56"

42.38"

$W_1 = 6791$ lbs/in

17.75"

15.75"

50,000 lbs

WITHOUT HEAD BRACE

WITH HEAD BRACE